

Armed Services Technical Information Agency

Because of our limited supply, you are requested to return this copy **WHEN IT HAS SERVED YOUR PURPOSE** so that it may be made available to other requesters. Your cooperation will be appreciated.

AD

36005

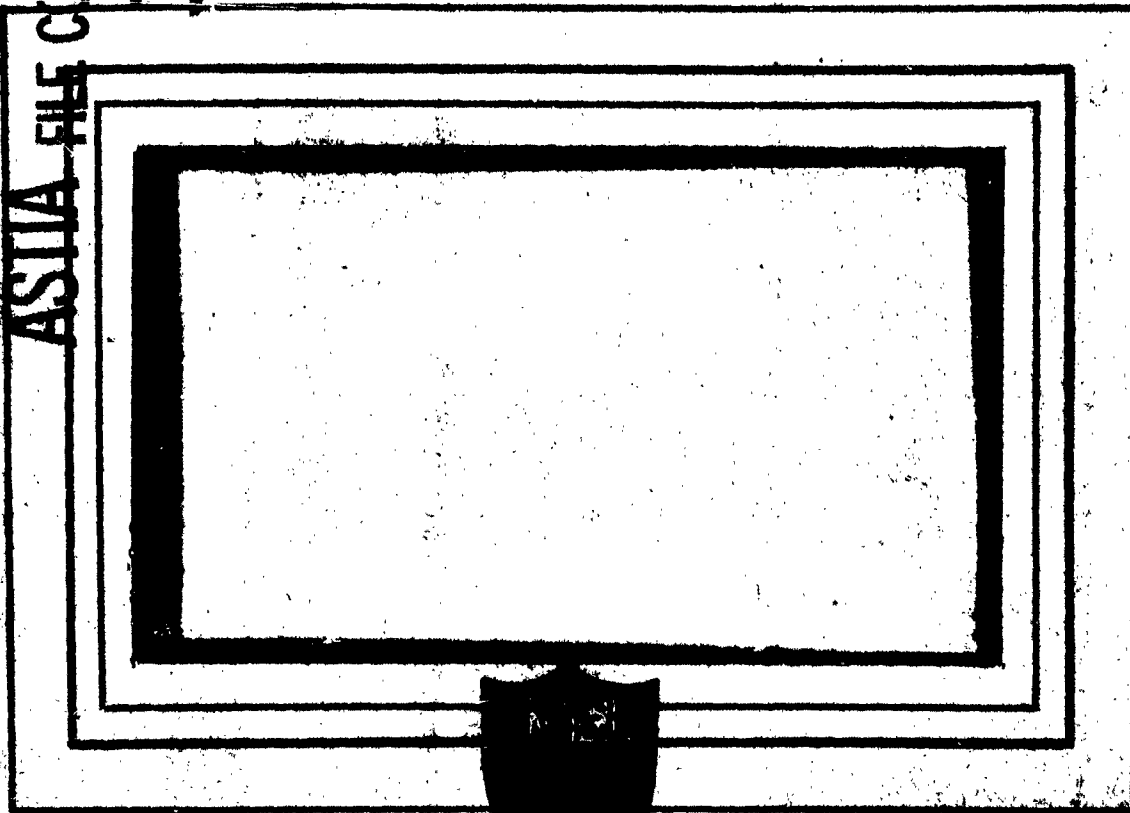
NOTICE: WHEN GOVERNMENT OR OTHER DRAWINGS, SPECIFICATIONS OR OTHER DATA ARE USED FOR ANY PURPOSE OTHER THAN IN CONNECTION WITH A DEFINITELY RELATED GOVERNMENT PROCUREMENT OPERATION, THE U. S. GOVERNMENT THEREBY INCURS NO RESPONSIBILITY, NOR ANY OBLIGATION WHATSOEVER; AND THE FACT THAT THE GOVERNMENT MAY HAVE FORMULATED, FURNISHED, OR IN ANY WAY SUPPLIED THE SAID DRAWINGS, SPECIFICATIONS, OR OTHER DATA IS NOT TO BE REGARDED BY IMPLICATION OR OTHERWISE AS IN ANY MANNER LICENSING THE HOLDER OR ANY OTHER PERSON OR CORPORATION, OR CONVEYING ANY RIGHTS OR PERMISSION TO MANUFACTURE, USE OR SELL ANY PATENTED INVENTION THAT MAY IN ANY WAY BE RELATED THERETO.

Reproduced by
DOCUMENT SERVICE CENTER
KNOTT BUILDING, DAYTON, 2, OHIO

UNCLASSIFIED

AD No. 36 205

ASTIA FILE COPY card
-A Draw
-C



PRINCETON UNIVERSITY

DEPARTMENT OF AERONAUTICAL ENGINEERING

**Best
Available
Copy**

DEPARTMENT OF THE NAVY
BUREAU OF AERONAUTICS

Contract N0as 53-817-c

COMBUSTION INSTABILITY
IN
LIQUID PROPELLANT ROCKET MOTORS
Sixth Quarterly Progress Report
For the Period 1 August 1953 to 31 October 1953
Aeronautical Engineering Report No. 216f

Prepared by:

J. Grey
J. Grey, Research Engineer

Approved by:

L. Gross
L. Gross, Professor in Charge

1 December 1953

PRINCETON UNIVERSITY
Department of Aeronautical Engineering

Reproduced
FROM LOW CONTRAST COPY.

CONTENTS

TITLE PAGE	-
CONTENTS	1
LIST OF FIGURES	11
I. SUMMARY	1.
II. INTRODUCTION	2.
A. Object	2.
B. History	2.
III. APPARATUS	6.
A. Monopropellant Rocket Motor	6.
B. Bipropellant Rocket Motor	6.
C. Instrumentation	8.
IV. INFORMATION AND DATA	11.
V. DISCUSSION	11.
APPENDIX	
A. Concepts and Theory of Combustion Instability	
B. Combustion Time-Lag Measurements - Phase I	
C. Development of the Li-Liu Pressure Pickup	

LIST OF FIGURES -Report 216f

Figure Number

- | | |
|---|-----|
| 1. Installation of Liquid Oxygen Tank | 12. |
| 2. Installation of Alcohol Tank | 13. |
| 3. Bipropellant Thrust Stand | 14. |
| 4. Bipropellant Rocket Motor | 15. |
| 5. Bipropellant Flow Modulating Unit | 16. |
| 6. Bipropellant Feed System Components | 17. |
| 7. Bipropellant Control Panels | 18. |
| 8. Four-Channel Ampex FM Magnetic Tape Recorder | 19. |

I. SUMMARY

Analysis of the recent series of test runs on the monopropellant rocket motor has been completed, illustrating the suitability of the techniques employed to make measurements, and providing a rough check on the pressure-time lag relationship used in Crocco's original theoretical treatment. Accuracy of the measurements was not adequate to provide a detailed check of the theory, however, so that further refinement and development of the instrumentation has been initiated. Results are reported in detail in Appendix B of the present report.

Dynamic flow calibrations were delayed both by the instrumentation refinement program and by a failure of the flow modulating unit, evidently due to malfunctioning of the gas-pressurized lubrication system. Repair of the unit, which included construction of a new connecting rod, piston, and cylinder assembly, is nearing completion as of this date. The hot-wire flow phasemeter has been modified and refined, and is now available for dynamic calibrations. The Li mass flow meter has again been returned to the vendor due to failure of the main drive shaft while being calibrated under low-pressure steady flow conditions.

Operation of the improved Li-Liu pressure pickups has been satisfactory on all tests to date, and it is planned to use these pickups in their present configuration on the bipropellant system. A detailed history of their development up to this stage appears in Appendix C of the present report.

Construction of the bipropellant test stand is complete. Flow and pressure calibrations of both propellant systems have begun. Testing of the bipropellant flow modulating unit will be performed at the conclusion of the steady-state flow checks. Photographs of the various components appear in the present report.

II. INTRODUCTION

A. Object

BuAer Contract Noas 52-713-c was undertaken as a part of the jet propulsion research program of the Department of Aeronautical Engineering at Princeton to "conduct an investigation of the general problem of combustion instability in liquid propellant rocket engines." This program shall consist of theoretical analyses and experimental verification of theory. The ultimate objective shall be the collection of sufficient data that shall permit the rocket engine to produce power plants which are relatively free of the phenomena of instability. Interest shall center in that form of unstable operation which is characterized by high frequency vibrations and is commonly known as "screaming".

B. History

Interest at Princeton in the problem of combustion instability in liquid propellant rocket motors was given impetus by a Bureau of Aeronautics symposium held at the Naval Research Laboratory on the 7th and 8th of December 1950. This interest resulted in theoretical analyses by Professors M. Summerfield and L. Crocco of this Center.

Professor Summerfield's work, "Theory of Unstable Combustion in Liquid Propellant Rocket Systems" (JARS, September 1951), considers the effects of both inertia in the liquid propellant feed lines and combustion chamber capacitance with a constant combustion time lag, and applies to the case of low (up to about 200 cycles per second) frequency oscillations sometimes called "chugging".

Professor Crocco advanced the concept of the pressure dependence of time lag in mid-1951; his paper "Aspects of Combustion Stability in Liquid Propellant Rocket Motors" (JARS, November 1951 and Jan-Feb. 1952), presents the fundamentals resulting from this concept, and analyzes the cases of

low frequency instability with monopropellants, low frequency instability with bipropellants and high frequency instability, with combustion concentrated at the end of the combustion chamber.

Desiring to submit the concept of a pressure dependent time lag to experimental test, a preliminary proposal was made by the University to the Bureau of Aeronautics in the summer of 1951, and following a formal request, a revised proposal was submitted which resulted in Contract No. 52-713-c.

Analytical studies with concentrated and distributed combustion had been carried on in the meantime under Professor Crocco's direction and within the sponsorship of the Guggenheim Jet Propulsion Center by S. I. Cheng and were issued as his Ph.D. thesis, "Intrinsic High Frequency Combustion Instability in a Liquid Propellant Rocket Motor", dated April 1952.

Time was devoted, in anticipation of the contract, during the first third of 1952, to constructing facilities, securing personnel, and planning the experimental approach.

During the first three month period of the contract year, personnel and facilities at the new James Forrestal Research Center were assigned, and the initial phases of the experimental program were planned in some detail.

A constant rate monopropellant feed system was designed and preliminary designs of the ethylene oxide rocket motor and the instrumentation systems were worked out. Special features of the projected systems included a pulsing unit to cause oscillations in propellant flow rate, a water-cooled strain-gage pressure pickup designed for flush mounting in

the rocket chamber and several possible methods for dynamic measurements of an oscillating propellant flow rate.

Searches were made of the literature for sources of information on combustion instability and ethylene oxide, and visits to a number of activities working on liquid propellant rocket combustion instability problems were made for purposes of familiarization with equipment and results.

The basic precepts of Crocco's theory for combustion instability were reviewed, and detailed analyses made for specific patterns of combustion distribution.

Operational tests and calibration of the Princeton-I.I.T. pressure pickup proved the value of the design, although failure of the pickup under "screaming" rocket conditions showed the necessity for modification of the cooling system.

Construction of the monopropellant test stand and rocket motor was completed. Modifications were made to the Princeton-I.I.T. pressure pickup to provide for higher permissible heat-transfer rates in order that it be satisfactory for use under "screaming" conditions in a bi-propellant rocket motor. Construction and preliminary testing of the hot-wire flow phasemeter and its associated equipment were completed.

A new contract, NOas 53-817-c, dated 1 March 1953, was granted by the Bureau of Aeronautics to continue the program originally started under NOas 52-713-c. Operation of the monopropellant rocket motor was begun under this new contract, and shakedown operations were completed. It was found that decomposition of ethylene oxide could not be attained

with the original motor design despite many simple configuration changes, and it was decided to avoid a long and costly development program by operating the "monopropellant" motor with small amounts of gaseous oxygen. The required limits of oxygen flow rate were determined at several chamber pressures, and it was demonstrated that the oxygen would probably have a negligible effect on performance when compared to the effect of ethylene oxide flow rate modulation. Preliminary tests with flow rate modulation up to 100 cps were performed for the purposes of system checkout, using interim AC amplifiers in lieu of the necessary DC instruments.

The time constant of the hot wire liquid flow phasemeter was found to be 0.15 milliseconds and preparations for instantaneous flow calibrations were made. A test rig was constructed for this purpose.

A bipropellant rocket system using liquid oxygen and 100% ethyl alcohol was designed on the basis of monopropellant operational experience, incorporating an adjustable phase flow modulating unit operating on both propellants. Injector design was based on a configuration used extensively by Reaction Motors, Inc.

Operation of the monopropellant system was performed with flow modulation at frequencies up to 200 cps, using a composite instrumentation system to measure mean values, amplitudes of oscillation, and phase difference between injector and chamber pressures.

The Mittelman electromagnetic flowmeter proved unsatisfactory due to equipment malfunctions, and had to be abandoned as a possible means of measuring instantaneous flow rates.

Subsequent efforts are presented in detail in this report.

III. APPARATUS:

A. Monopropellant Rocket Motor:

After completion of a series of monopropellant test runs, the results of which are included as Appendix E to the present report, it was intended to obtain dynamic calibrations of the flow through the injector orifices. However, it was found after termination of the previous series of monopropellant tests that the speed of the flow modulating unit could not be increased beyond 100 cycles per second, even with the propellant feed line empty. All components were carefully checked and found to be satisfactory, so the flywheels, which has been removed for the entire series of test runs, were reinstalled to determine whether the difficulty lay in an unbalance of the unit. Unfortunately, improper lubrication caused seizure of the connecting-rod needle bearing during the first check run, resulting in failure of the connecting rod. No conclusion as to effect of unbalance could be drawn. Repair of the unit has been initiated and installation of a pump-pressurized lubricating system will prevent reoccurrence of the failure.

F. Bipropellant Rocket Motor:

Construction of the test stand is essentially complete, and water flow checks of the system have been initiated. Layouts of the flow and control systems, the rocket motor, and the bipropellant flow modulating unit were included in the previous Quarterly Progress Report. Construction went rapidly and smoothly, primarily due to experience gained during design and construction of the monopropellant stand. The only major delay occurred when pressure-check of the 40 gallon surplus liquid oxygen tank revealed a number of leaks, which were difficult to seal due to its vacuum-jacketed, all-monel construction. Hydrostatic tests up to 1500 psi were finally com-

pleted; however, procurement of an additional surplus tank is now being attempted for use at the higher chamber pressures. Installation of the vessel in the liquid oxygen system is shown in Figure 1. A surplus Navy storage tank and vacuum pump for use with liquid oxygen have been located and will be procured.

Figure 2 illustrates the alcohol pressure-tank, which is of stainless steel, has a capacity of 20 gallons and was also procured from surplus stores. This is the type of tank now being sought for permanent use in the oxidant system, since it is suitable for acid oxidizers as well as for liquid oxygen.

The bipropellant thrust stand with rocket motor and flow modulating unit installed is shown in Figure 3. The stand itself utilizes the same leaf-spring arrangement as used in the monopropellant system, with the same combination of strain gage and hydraulic thrust-measuring devices. The liquid-oxygen line is insulated with felt, waterproofed by plastic tape and Glyptal.

Figure 4 is a photograph of the rocket motor, which has an L^* of 57" in its present configuration. Operations at higher chamber pressures and different values of L^* are provided by the use of interchangeable injector plates and chamber bodies. Only the nozzle is cooled. The photograph shows only a single chamber pressure pickup, but additional pickups will be installed in the chamber and in each injector manifold after completion of shakedown testing. A schematic layout of the motor appears in the Fifth Quarterly Progress Report.

The flow modulating unit is shown in Figure 5 with its 5 HP U.S. Motors Varidrive. This unit was installed with a pump-pressurized lubricating system for the connecting-rod bearings, and features a continuously adjust-

able phase difference from zero to 360° between fuel and oxidant pistons. Details of the design were included in the previous Quarterly Progress Report.

Other system components, mounted on the same panel which services the monopropellant test stand, appear in Figure 6. The control, gage and instrument panels are shown in Figure 7. As in the case of the monopropellant stand, only those instruments necessary for operation of the test stand are located in the control room, all other instrumentation being mounted remotely in the central recording room over 50 feet removed.

Flow and pressure checks of the system have begun and shakedown operation of the system will be carried out when these checks are completed. The first tests will be made at 300 psi chamber pressure with rich mixture ratios in order to insure avoidance of high-frequency instability, increasing gradually to maximum performance ratios before beginning tests with flow modulation. The flow modulating unit will be checked before beginning shakedown tests, so that any necessary repairs will not cause delays in the test program.

C. Instrumentation:

The results of the series of monopropellant test runs completed during this report period indicated that the required instrument accuracy has not yet been achieved. (See Appendix B) An instrument refinement program has therefore begun to reduce the overall system error from its present value of approximately 5%, aiming at the goal of better than 1% on all measurements.

This program will not require the use of any additional instruments (other than a set of extremely simple filters to be constructed at Princeton) but is expected to involve a number of detailed changes in circuitry, installations and calibration techniques. For example, an electronic

method for determining the phase difference between two signals has been conceived, using available equipment, in order to eliminate the large error involved in manual reading of this important quantity. A complete revamping of the Central Recording Room has been initiated to reduce electrical and magnetic "noise" pickup, poor connections, and operations errors, and also to streamline operation of the room for better test efficiency.

Additional major items necessary for the bipropellant tests which are now on hand include a four-channel oscilloscope and a four-channel conversion of the original two-channel magnetic tape recorder. (See Figure 8). During conversion of the latter, a number of circuit changes were made which are expected to vastly improve the performance of this instrument. The original two-channel recorder was the first of its type to be sold, and thus possessed a number of "bugs" which hampered its use at the accuracy levels required. These have been eliminated in the four-channel version, and preliminary acceptance tests revealed significant improvements in performance of the recorder.

Additional items which have not yet been received include four additional Li-Liu pickups of the differential type, and repairs to three absolute pressure pickups which had been damaged on tests at N.A.C.A. and Princeton. A set of high-sensitivity steady-state differential pickups (0 to 1 psi full-scale) were ordered some time ago for use in determining location of the combustion zone in the bipropellant rocket, but these items are not expected until January 1954.

A failure of the main drive shaft of the Li mass flowmeter necessitated return of the instrument to the vendor. In view of the large number of mechanical difficulties encountered in operating this instrument, it has been decided to eliminate it from the dynamic flow calibration program despite its theoretically sound principle of operation. The unsatisfactory performance of this meter and of the Mittelman electromagnetic flowmeter leaves only the liquid hot-wire as a check on the theoretical phase correction between flow and pressure drop across the injector orifices. The existing hot-wire probe has been modified to provide more reliable operation, and meanwhile a new tungsten probe, which will provide much greater sensitivity, has been designed. A preamplifier has also been installed between the balancing bridge and the constant temperature amplifier in order to increase the signal-to-noise ratio. This meter is available for dynamic calibrations, which will be run on the monopropellant flow stand as soon as repair of the flow modulating unit is complete.

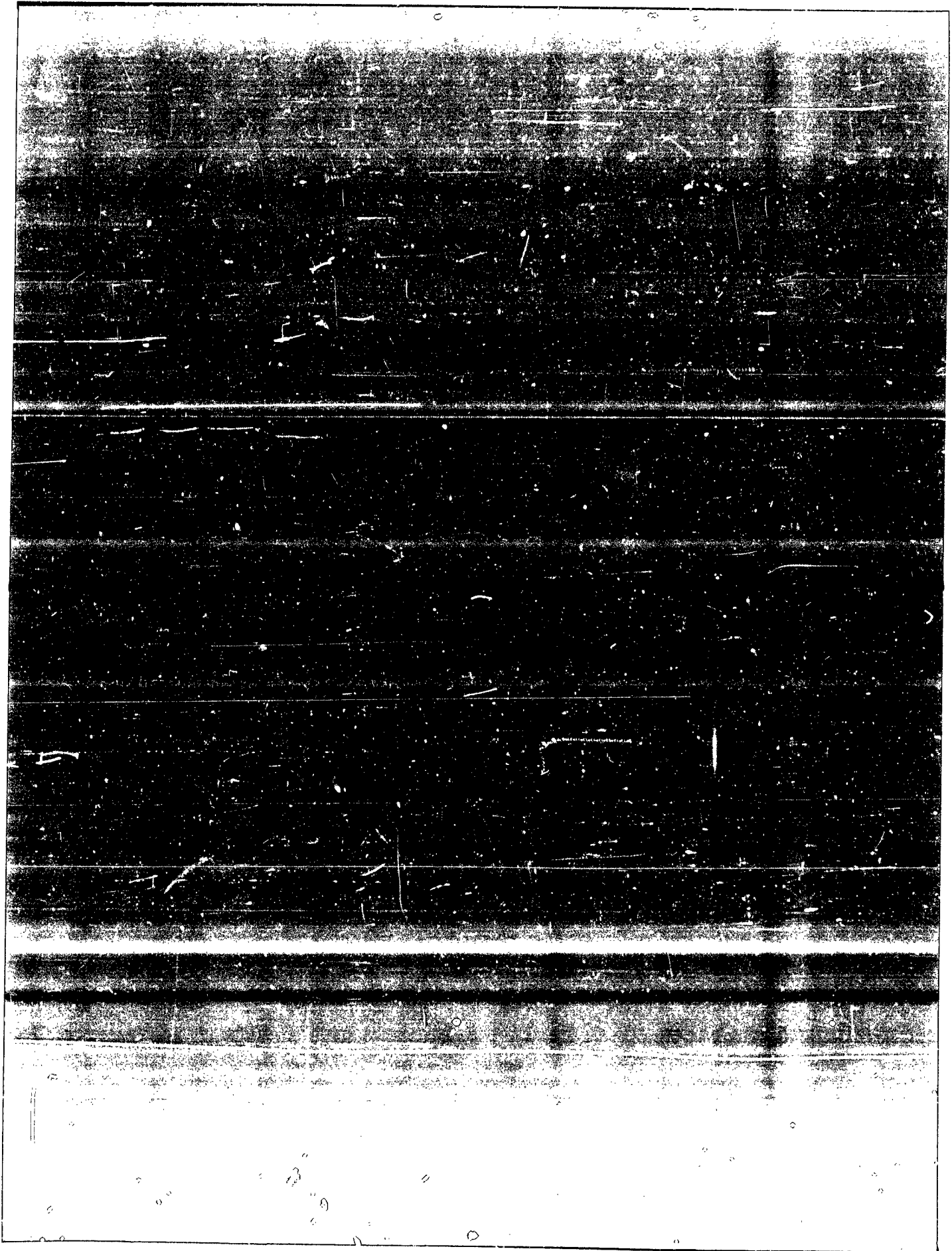
IV. INFORMATION AND DATA:

All subject matter normally appearing in this section has been included in the appendices as follows:

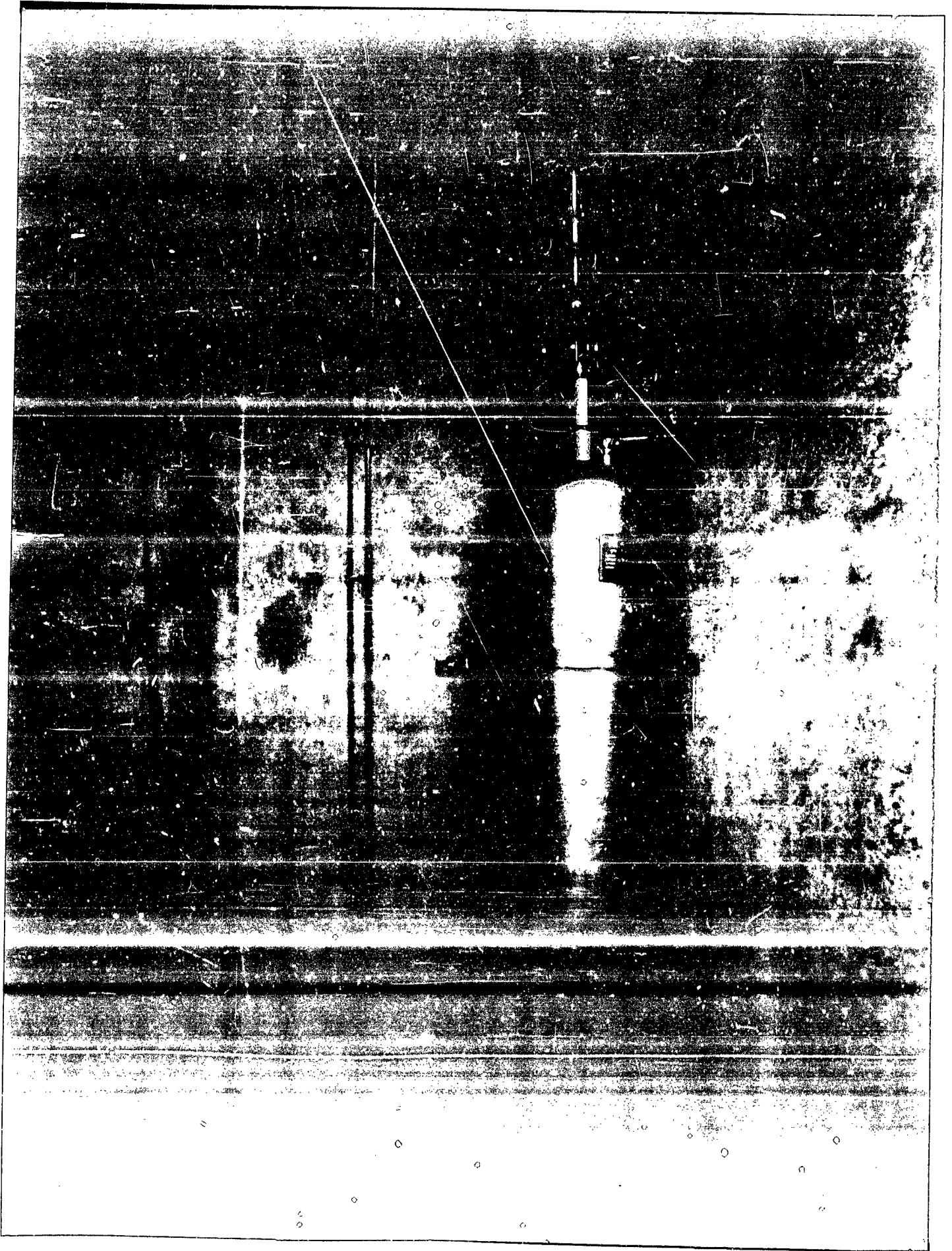
- (a) Theory: Appendix A.
- (b) Monopropellant Rocket Motor Tests: Appendix B
- (c) Pressure Pickups:

V. DISCUSSION:

All pertinent discussion may be found in the appendices as indicated previously.



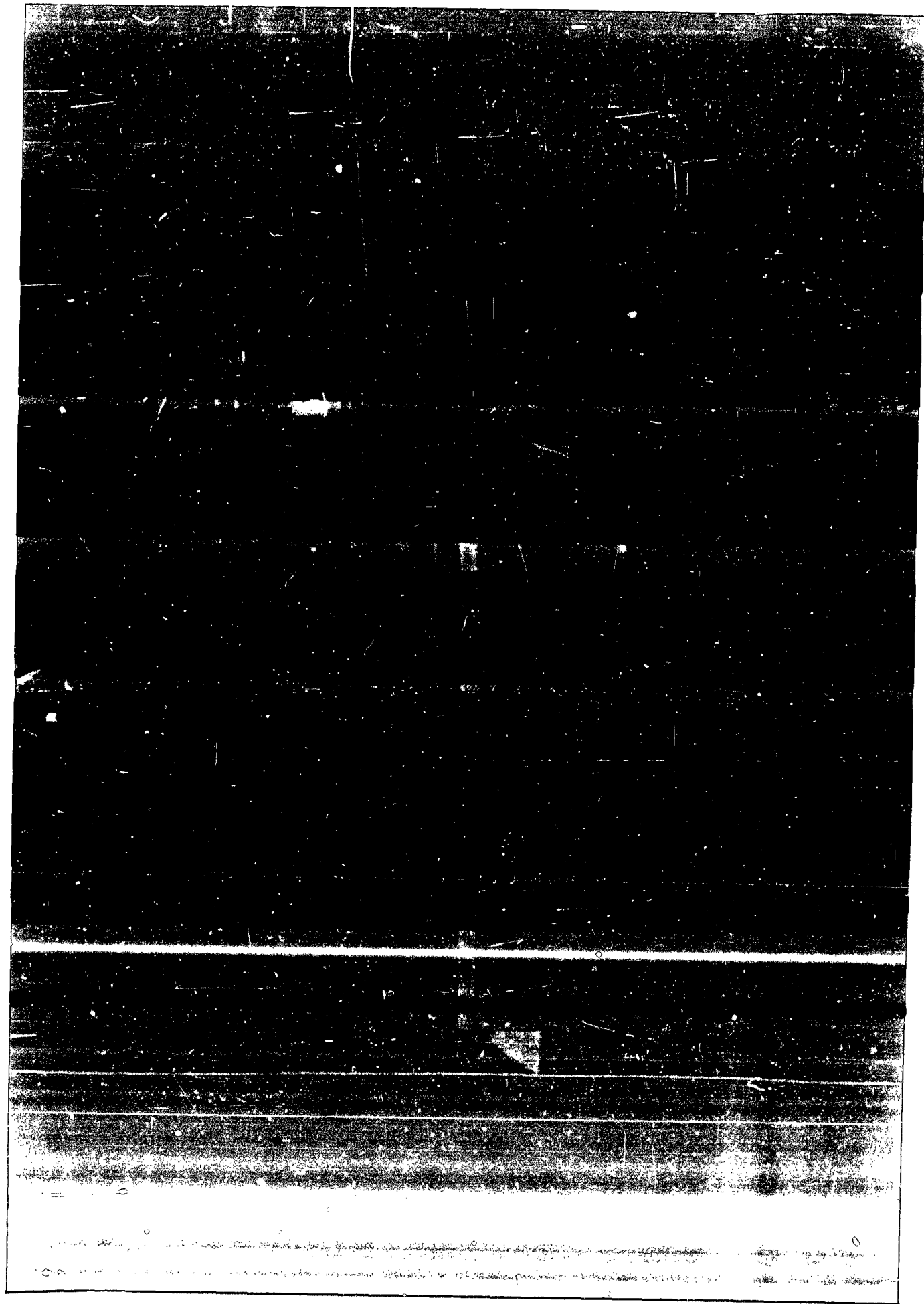
INSTALLATION OF LIQUID OXYGEN TANK
Figure 1



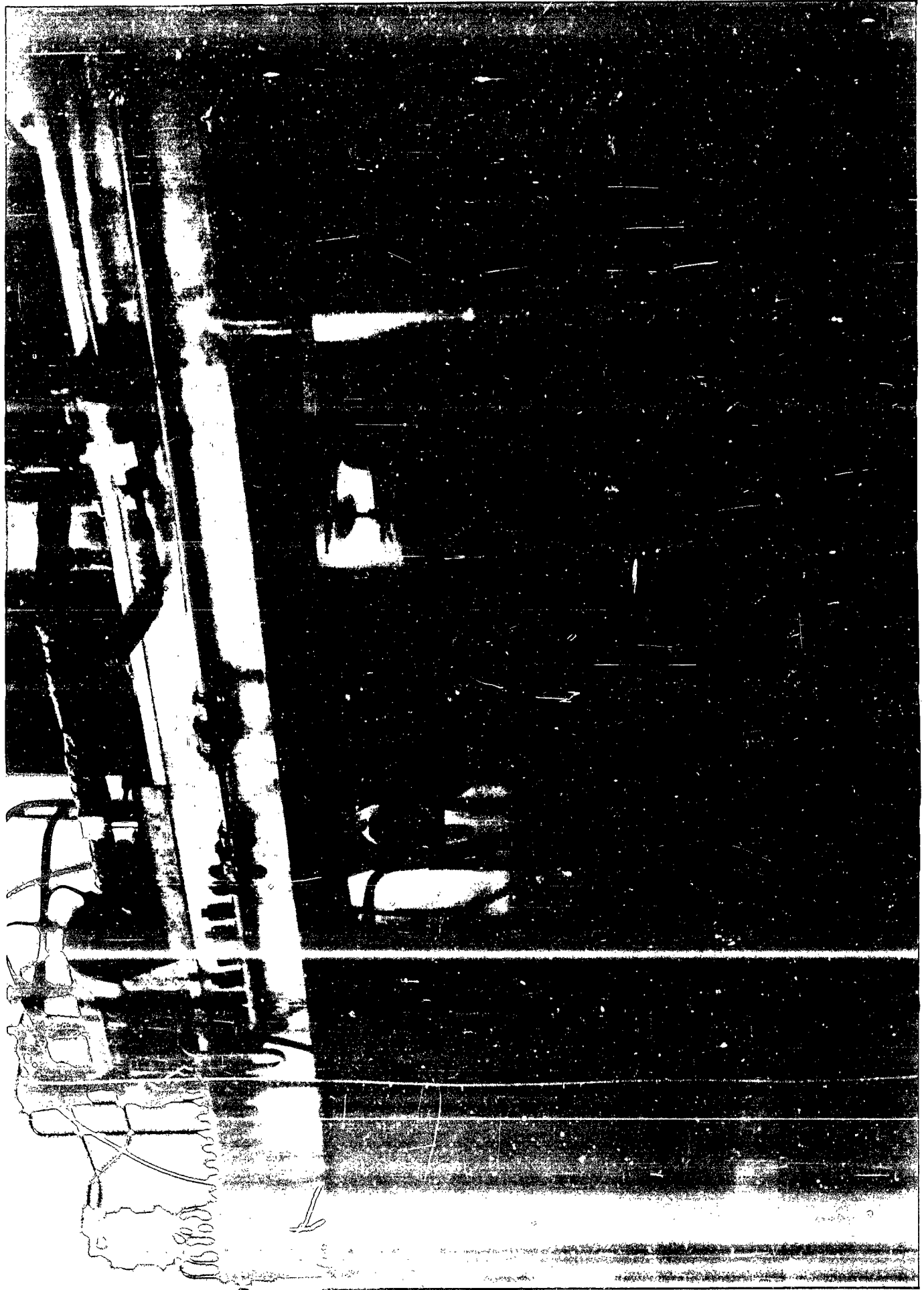
INSTALLATION OF ALCOHOL TANK
Figure 2



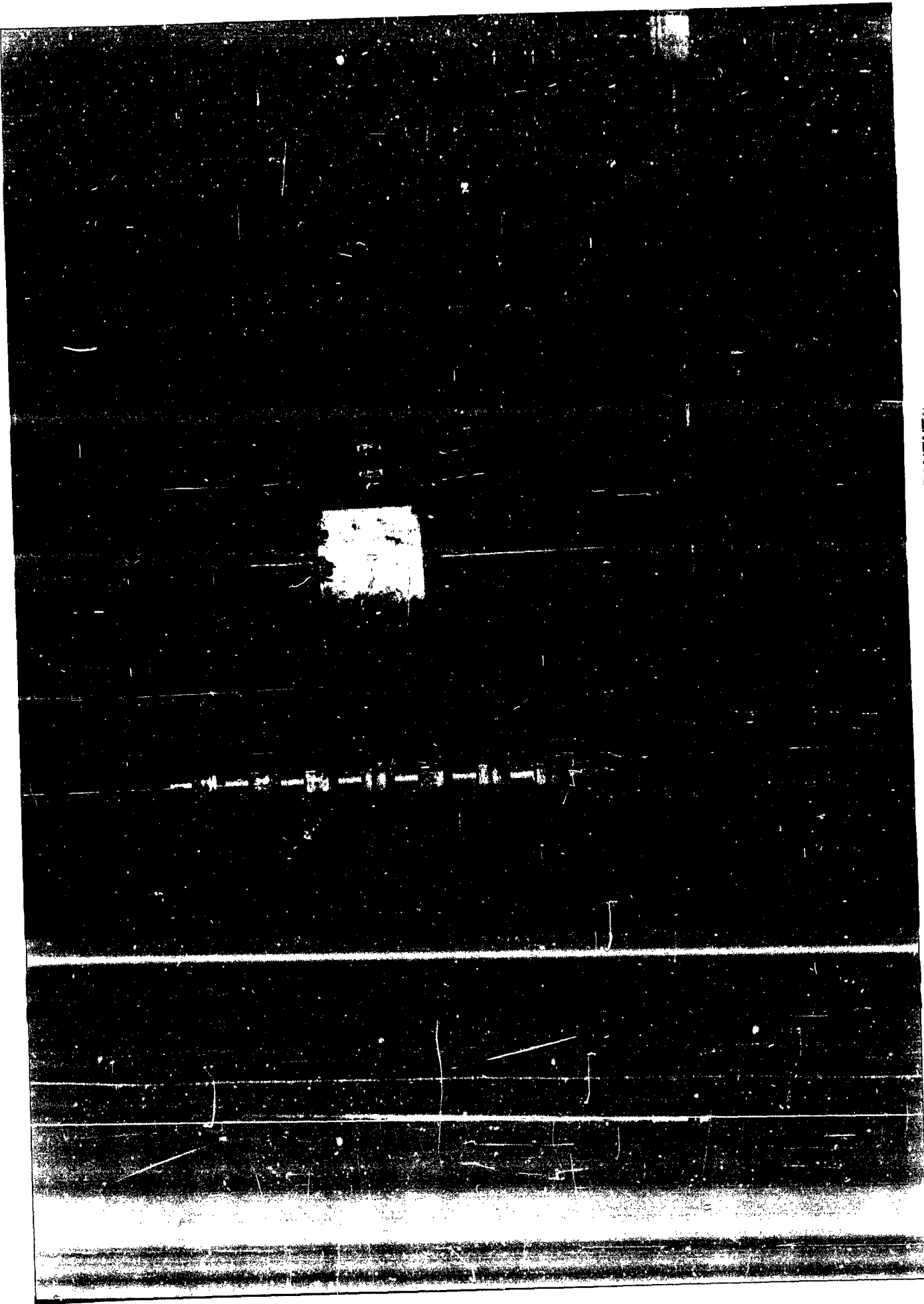
BIPROPELLANT THRUST STAND
Figure 3



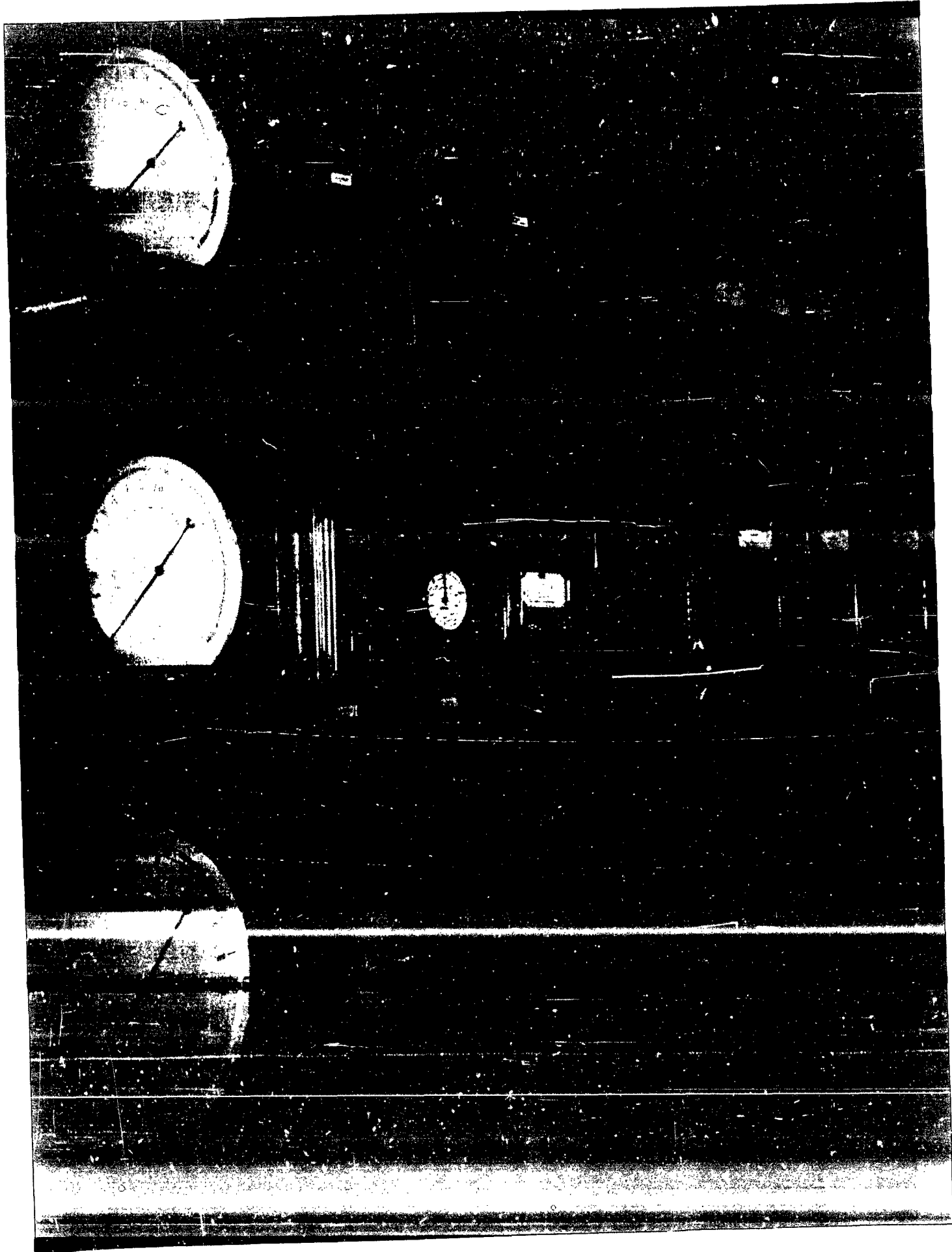
BIPROPELLANT ROCKET MOTOR
Figure 4



BIPROPELLANT FLOW MODULATING UNIT
Figure 5

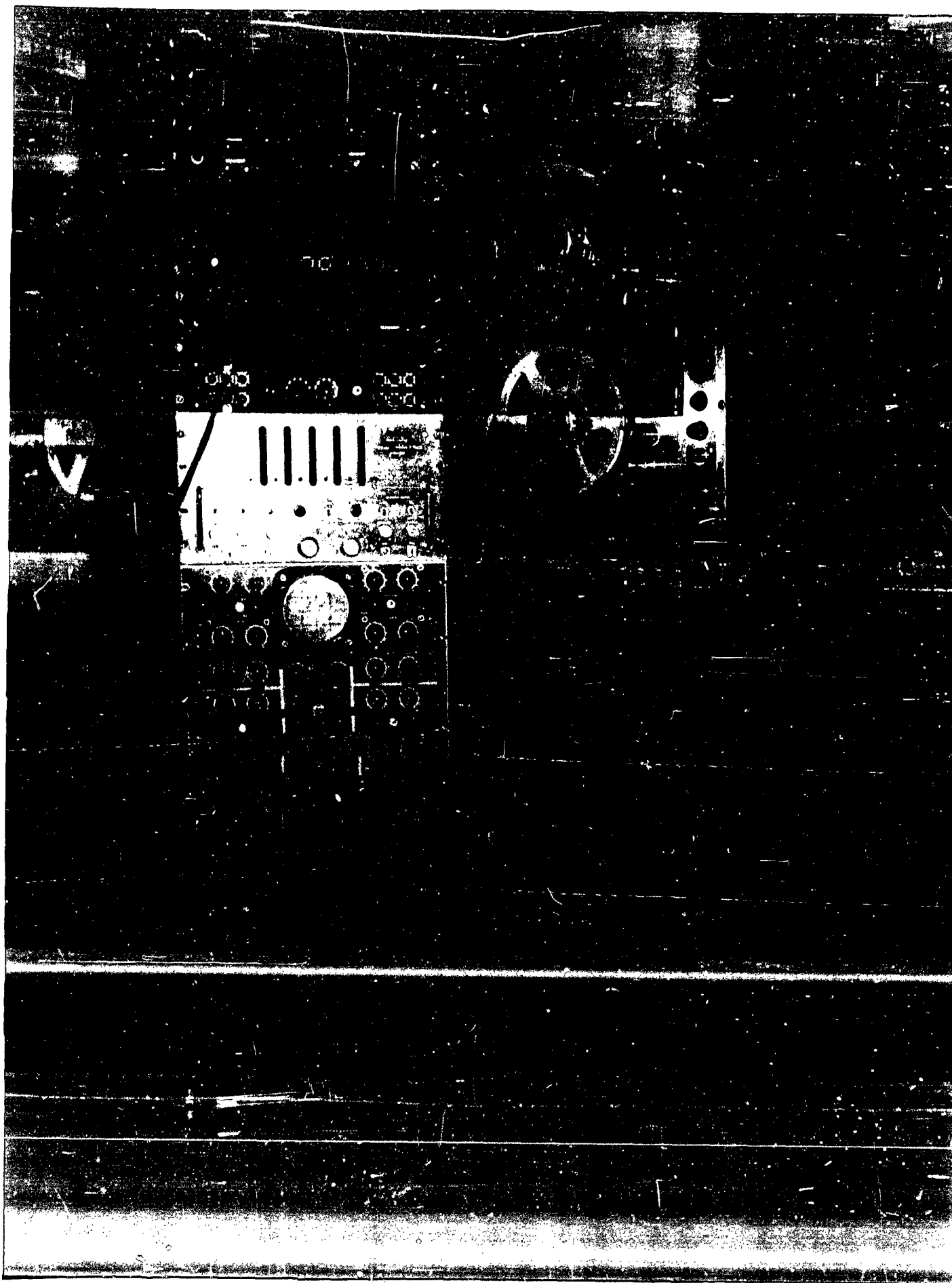


BIPROPELLANT FEED SYSTEM COMPONENTS
Figure 6



BIPROPELLANT CONTROL PANELS

Figure 7



FOUR-CHANNEL AMPEX FM MAGNETIC TAPE
RECORDER

Figure 8

AD No. 36 005-A

ASTIA FILE COPY

APPENDIX A

CONCEPTS AND THEORY OF COMBUSTION INSTABILITY

Concepts and Theory of Combustion Instability

Combustion in a rocket motor is never perfectly smooth. The pressure fluctuation at a given position in the combustion chamber of most of the liquid rockets is very irregular and analysis of such fluctuations shows that no particular frequency is persistently of predominating magnitude. As a result of such randomness, the mechanical and the thermal stresses when averaged over a sufficiently long period of time, remain substantially constant. Therefore, no serious consequences are encountered under such circumstances and the rocket motor is said to be operating under steady state conditions. These random fluctuations may be originated from either fluid dynamical processes or chemical kinetic processes or both and are evidenced by the extremely turbulent conditions in the combustion chamber. The origin and the nature of this random or turbulent fluctuation are not the present subjects of consideration. Under certain operating conditions, the pressure fluctuation at a given position is more or less periodic. Analysis of such fluctuations shows that one or several particular frequency components are persistently of predominating magnitudes as compared to the magnitude of the random noise that invariably occurs in the combustion chamber. When a rocket is operating under such circumstances, the thermal and the mechanical stresses, when averaged over a sufficiently long period of time, attain magnitudes considerably higher than those corresponding to steady state conditions. Therefore oscillations of this kind will have detrimental effects on the life and the

reliability of the motor. If such undesirable oscillations are present, we call the combustion unstable.* It is the purpose of this paper to review the investigations concerning the origin and the mechanism of producing such undesirable oscillations with a view to its elimination.

These regular oscillations of large amplitude can be generated in either of the following two ways:

1. Any small disturbance, existing in the combustion chamber is unstable and amplifies with time until it attains a finite magnitude which is determined by the presence of nonlinear damping agents. (If the motor is not strong enough to bear the mechanical and the thermal stresses produced by the fully developed unstable oscillation, the motor will fail during the period of amplification, and the unstable oscillation appears to be diverging all the way up to the failure of the motor). This type of unstable combustion can be distinguished from other types by the fact that there is a transition stage preceeding the fully developed unstable combustion. During this transition stage, the unstable oscillation gains in amplitude continuously without significant change in its frequency. Such transition stage has been recorded in rocket motor with transparent slit window by Berman and Cheney as is reproduced in figures 1a and 1b, from reference 1. The magnitude of the fully developed unstable oscillation is large but such large amplitude oscillations are originated from the instability of oscillations of much smaller amplitudes. While the nonlinear effects should be taken into account for the analysis of the fully developed unstable oscillation, the stability of the small disturbances which are responsible for the presence of the large amplitude oscillations can be analyzed by linearized treatment. Consequently we call this type of combustion instability the "linear instability."

*This distinction of the rough but stable combustion and the unstable combustion was advanced by Prof. L. Crocco in the Annual Meeting of the ARS, 1952. A detailed account is presented in the Monograph "Combustion Instability in Liquid Propellants Rockets" by L. Crocco and S. I. Cheng to be published by AGARD, NATO.

2. Disturbances smaller than a certain magnitude are stable and die with time. But disturbances larger than this magnitude either remain finite or amplify with time. Nonlinear effects are essential for this type of instability. The occurrence of this type of instability is not necessarily preceded by a transition stage and can be initiated by accidental or functional disturbance of sufficient magnitude; for example the starting transient that initiates unstable combustion before the rocket has ever come to a steady state. Because of the fact that nonlinearity is an essential feature of this type of unstable combustion, we call this type "the nonlinear instability". Nonlinear instability can be avoided if both the functional and the accidental disturbance and the random noise are kept below a certain magnitude. In this respect, the nonlinear instability differs from the linear instability.

Only linear instability has so far been subjected to analysis. Since combustion plays an important role in the unstable phenomenon and since our knowledge of mixing processes and of chemical kinetics is too meager to permit a detailed formulation of the combustion processes, the stability analysis can be made only when the combustion processes are successfully described by a simplified model. The following model is found very useful. It is based on two essential assumptions:

(1) The unburned propellant elements occupy negligible volume in the combustion chamber. Thus, it is only the flow of the burned gas that enters into the dynamics of the gas system in the combustion chamber.

(2) The propellant element after leaving the injector takes a definite amount of time called the time lag to prepare itself for combustion which takes place instantaneously at the end of the time lag.

This concept of delayed instantaneous combustion has long been introduced for the analysis of combustion processes; for example, the concept of ignition temperature. The time lag consists essentially of two parts, a constant part during which processes insensitive to the thermodynamic states of the surrounding gas, like mixing, take place; and a variable part during which processes sensitive to the states of neighboring gas like activation processes occur. We call them insensitive and sensitive time lag respectively. This schematic representation is very rough because both processes take place simultaneously. However, this permits a "simple" description of the combustion processes and of their variations under unsteady conditions. Combustion in this schematic representation is just a process of mass generation, and so far as the dynamics of the gas is concerned, the local rate of gas generation is the source strength from the point of view of aerodynamicists. All that we need to know in analyzing the dynamic behavior of the system is the instantaneous source strength at any instant at every location in the chamber volume.

This description of combustion in steady state can be effected by specifying both the total space lag ξ , that is the position where a given propellant element is transformed into burned gas and the sensitive time lag τ of the element. The motion of the unburned element during the sensitive time lag is assumed to be the same as the motion of burned gas in steady state. The description of combustion in unsteady state will require a knowledge as to how the local source strength or local rate of burned gas generation responds to oscillations in the combustion chamber.

The rate of burned gas generation can be affected by chamber oscillations in a number of ways. But all these fall in two categories, one modifies the

rate of supply of unburned elements through the sensitivity of feeding system to chamber oscillations, and the other modifies the specific rate of conversion of unburned elements into combustion products through the sensitivity of activation processes to chamber oscillations. Instability excited by agents of the first category, has been studied by Prof. von Karman and his group since 1942 and also by many other authors. Their analyses are limited to chugging (or low frequency instability). Since the specific rate of conversion of unburned elements into burned gas is unaffected by and remains constant throughout the oscillations, this type of instability depends very much on the behavior of the feeding system. Instability excited by agents of the second category was conceived and studied in 1951 by Prof. L. Crocco, who demonstrated the possibility of instability of both chugging and screaming (or high frequency instability) even when injection rate is constant. This type of instability has been called intrinsic instability. To overcome the difficulty of our incomplete knowledge of combustion processes and of their relations with chamber oscillations, Crocco introduced an interaction index n which determines the course of variations of the sensitive time lag. This interaction index n is a characteristic quantity of a given propellant combination and the mixture ratio and also depends upon a number of factors like the design chamber pressure and temperature of the rocket. Let τ_t be the total time lag of an element, τ_i the insensitive part, and τ the sensitive part with $\tau_t = \tau_i + \tau$. The sensitive time lag τ of an element burning at instant t is assumed to be determined by the following integral relation:

$$\int_{t-\tau}^t p^n [x'(t'), t'] dt' = \text{constant} \quad (1)$$

where $x'(t')$ is the path of each individual unburned element. The integrand indicates the local rate of activation processes, and the constant of the integral indicates the total amount of activation energy required to initiate instantaneous combustion except for a proportionality constant. The local rate of activation processes depends on a number of thermodynamic variables like the neighboring burned gas pressure and temperature and also on the relative velocity, mixture ratio and so forth. For small oscillations the variation of these physical quantities may be assumed to be correlated. Therefore, the local activation rate can be related to a single variable which is taken to be local gas pressure acting on the unburned element as shown in equation (1). As a result the interaction index n is an average or overall parameter including the effects of all the relevant physical factors. The value of the interaction index n for given propellant can therefore be best determined experimentally because, as previously explained, our knowledge as to the detailed processes of mixing and chemical reactions is too meager. The constant value of the integral indicating the total amount of activation energy also varies between different propellant elements. This constant is equal to $\bar{p}^n \bar{\tau}$ if the chamber pressure \bar{p} is uniform everywhere in the chamber at any instant which is approximately true in conventional liquid rocket operating in steady state (except for the case of throatless motor). The variation of this constant means that the steady state value of the sensitive time lag $\bar{\tau}$ varies between propellant elements. For simplicity, analyses are performed for systems in which all elements have the same value of $\bar{\tau}$. The effect of the unequal $\bar{\tau}$ of different elements has also been treated.

That the variation of this time lag leads to the variation of rate of gas generation can be seen graphically as shown in figure 2. Consider a

given amount of elements injected during the interval Δt . If τ remains constant for elements injected at different instants, these elements are transformed into gas in an equal but later time interval Δt . If τ is larger for elements injected later, the same amount of gas would be generated in a time interval longer than Δt , and the gas generated per unit time is decreased as indicated in figure 2 as a rarefaction or dilution of the combustion processes. Thus, increasing τ leads to decreasing gas generation rate \dot{m}_p and vice versa. Since the integral in equation (1) indicates a variation of τ with p , an oscillation \dot{m}_p' of burned gas generation rate is generated when there is a pressure oscillation p' in the chamber. Now if the oscillation of \dot{m}_p is so coordinated as indicated in the figure, the response of \dot{m}_p will tend to magnify the pressure oscillation. Furthermore if the response of \dot{m}_p is big enough as indicated by a sufficiently large value of the interaction index n , unstable oscillations can be excited.

Here lies the fundamental difference between oscillations in an organ pipe with closed ends and those in the chamber - nozzle combination. If the walls are rigid and all the usual dissipative agents like viscosity and conductivity are neglected, a small disturbance in the organ pipe will remain neutral without losing its strength or energy. However, a disturbance in the chamber is only partially reflected from the nozzle and is partially transmitted downstream with a consequent loss of energy of the disturbance in the chamber. If there is a sustained oscillation in the combustion chamber, the energy of the disturbance is continuously being dissipated through the successive wave reflections at the nozzle. Therefore, sufficient amount of energy must be supplied to the oscillation to make up for the dissipation. This energy dissipation can also be visualized as the flow work in excess of

the steady state value, that is performed by the gas in the chamber on the gas in the nozzle. This amount of energy must be supplied by the exciting agent in forcing into the combustion chamber the excess amount of the burned gas that is generated. This energy supply is proportional to the magnitude of the variation of burned gas generation. The dissipative action of the nozzle therefore sets up a minimum magnitude of excitation that is required to maintain neutral oscillation. In the case of intrinsic instability where the injection rate is constant, this minimum amount of excitation is indicated by a minimum value of n which is approximately $\frac{1}{2}$ for chugging and increases with increasing frequency as will be shown later. If additional dissipative agents like viscosity and conductivity are taken into account, the value of n_{\min} would be correspondingly increased. The existence of the nozzle dissipative action even in absence of viscosity and conductivity is a very important feature of the oscillations in rockets. Therefore, a system can exhibit instability only when both the excitation agent is sufficiently strong to overcome the energy loss due to dissipation through the nozzle and the time lag is in ^{the} proper range or ranges of values to bring about an increase of ^{the} burning rate during ^{the} pressure excess period.

For the analysis of chugging or low frequency oscillation the period of the oscillation is very large as compared to the time required for a pressure wave to travel the length of the combustion chamber. The effect of the variation of burning rate at any point is felt everywhere in the chamber practically instantaneously. The gas pressure can be assumed to be uniform at any instant everywhere in the combustion chamber, and oscillate as a whole about the mean or steady state value. Thus the position where an unburned element sensed the pressure oscillation and the position where the element

burns are not of importance in the low frequency analysis, and only the timewise description of combustion in terms of the time lags need be considered. It is further assumed for simplicity in the low frequency analysis that the temperature of the burned gas generated from a given element remains unchanged throughout the pressure variations during its travel toward the nozzle end. This assumption is equivalent to the assumption of $\gamma - 1 \ll 1$ for the case of isentropic oscillation. The stagnation temperature or adiabatic flame temperature of the burned gas element is assumed to be the same for all elements in the case of monopropellant, and to be dependent only on the mixture ratio of the element in the case of bi-propellant regardless of the pressure variation under which combustion takes place. The final equation for the fractional pressure variation ϕ in a monopropellant motor is given as

Rate of Mass Accumulation or Pressure Change	Variation of Mass Ejection Rate	Variation of Rate Gas Generation Due to the Sensitivity of
		Feeding System Combustion Processes
$\frac{d\phi}{dz} + \phi = N \cdot \phi(z - \delta_t) + \eta [\phi(0) - \phi(z - \delta)] \quad (2)$		

The course of variation of chamber pressure is determined by the mass balance of the system. λ is the reduced time defined in terms of the average gas residence time in the chamber. δ_t and δ are the reduced or dimensionless total and sensitive time lag. N is the transfer function of the feeding system defined as the ratio of the fractional variation of the injection rate μ_i and the fractional variation of chamber pressure at a given instant. For systems with constant injection rate, $N = 0$, and the instability of such systems is due to the sensitivity of the combustion processes only and is called the intrinsic instability. For practical systems, N is a complicated function of the frequency of the chamber pressure

variation and the different feeding system constants representing the pump characteristics, the pressure drop across the system, the elasticity and the inertia of the system. A number of investigations have been made for low frequency combustion stability in systems with different ideal feeding systems characterized by different forms of the transfer function $N(1 - 7)$. These analyses are quite involved algebraically primarily because of the sensitivity of the feeding system. The effect of varying individual constants on the stability of the system cannot be easily drawn except that as a general trend, decreasing interaction index n and increasing the pressure drop in the feeding system are stabilizing.

When the frequency of chamber pressure oscillation is sufficiently large so that the period of oscillation is comparable to the time that a pressure wave will take in travelling the length of the feeding system, the elasticity and the inertia characteristics of the feeding system can not be successfully represented by concentrated capacitance and inertia. The idealized simple systems as described in the analysis of low frequency oscillations cannot possibly be admitted for the analysis of high frequency oscillations. The situation is further complicated by the presence of valves and other sudden changes in sections and bends in the feed lines. Except for the much too idealized "feeding system" consisting only of a uniform straight tubing it is practically impossible to formulate analytically the response of injection rate to high frequency chamber oscillations even approximately. Therefore the analysis of high frequency oscillations has been primarily limited to intrinsic stability. Even in this case the mathematical complications are quite formidable and only the longitudinal modes have so far been treated.

The mathematical complication arises because the time of propagation of pressure waves in the chamber and that in the nozzle is comparable with the period of oscillation. The response of the flow in the nozzle to high frequency oscillations is of fundamental importance to the stability problem because it is the energy dissipation associated with this outflow which constitutes the essential damping action. The mathematical treatment for longitudinal oscillations in the nozzle was initiated by Prof. Tsien (8) and solutions for the whole frequency range were obtained by Prof. Crocco (9). The result is presented and reproduced as figure 3 with the specific admittance ratio defined as the ratio of the fractional variation of velocity to fractional variation of density at the entrance to the nozzle plotted against the reduced frequency β which is the angular frequency divided by velocity gradient in the subsonic portion of the nozzle.

The situation in the combustion chamber can be visualized as a number of sources distributed over the chamber volume and generating pressure waves through the variation of source strength or local burning rate. Pressure waves are reflected from the solid boundaries, and are partially transmitted and partially reflected at the nozzle entrance. All these waves that are present in the combustion chamber interact in a complicated manner to set up a definite wave form somewhat different from the standing acoustical or organ pipe mode even without considering any nonlinear effects. It is therefore necessary in the formulation of the problem to consider the balance of mass, momentum, and energy of each individual differential element instead of the overall mass balance of the entire combustion chamber as indicated in equation (2) for low frequency oscillations. As a result, we obtain (11) an integro-differential equation with

retarded variable for the pressure perturbation in the chamber. An analytic solution of this equation satisfying the necessary boundary conditions cannot be obtained explicitly. However, approximate solutions can be determined if we introduce several additional assumptions. Besides such mathematical complexity, the spatial description of combustion distribution becomes an important factor in addition to the timewise description in the stability analysis. The capability of an element in exciting instability under non-uniform pressure at any instant in the chamber depends not only on the time interval but also on the spatial range in which this element sensed pressure variations. The evaluation of the exciting action will require a complete description of the spatial distribution of combustion and its variations in response to chamber oscillations in addition to the timewise description. In other words, we have to specify both the space lag and the time lag of each propellant element. In general, the space lags are different for different elements. Both the magnitudes and the distribution of the space lags of the propellant elements are different in different rockets. The spatial distribution of combustion in the chamber is therefore arbitrary. The sensitive time lags of different elements are also distributed in a certain range of values. Both of these have important consequences on the stability of the system. These qualitative pictures pertain to any high frequency modes of oscillations, pure longitudinal mode or combined with transversal modes. The presence of the transversal modes introduces only additional mathematical complications, for example the space lag of an element will have to be described by a vector instead of a scalar distance from injector end. The mechanisms of excitation and of wave interaction are the same.

The importance of the spatial distribution of combustion is best illustrated by considering the simplest case of longitudinal oscillations in systems with concentrated combustion front, that is, when all elements have the same space

lag ξ and the same sensitive time lag τ . In this configuration, if τ is sufficiently small, propellant elements sense only the pressure variation at the combustion front and the effect of spatial distribution of combustion is brought out most significantly. Another important extreme case is the configuration with combustion uniformly distributed over the entire length of the chamber. Both of these two extreme cases have been treated analytically (10, 11). Typical results are given below.

In figure 4 the unstable ranges of the steady state values of time lag $\bar{\tau}$ for systems with combustion concentrated at different axial position ξ and when the interaction index $n = 1$ are shown. The solid curves are the stability boundary which separates the stable and the unstable regions for systems with "long nozzle" with the length of the subsonic portion of the nozzle approximately equal to $1/3$ of chamber length. The dotted curves are those for systems with "short nozzle" with negligible length of its subsonic portion as compared to chamber length. The strong stabilizing effect of a long nozzle in reducing unstable ranges of $\bar{\tau}$ and of ξ for given n is obvious. The most important aspect of this stabilizing effect of the nozzle is that it is much stronger toward higher modes of oscillation. While the "short nozzle" leads to definite unstable regions for all modes of oscillations when n is bigger than $\frac{1}{2}$, the "long nozzle" stabilizes all modes higher than the second mode when $n = 1$. If n decreases from unity, the long nozzle makes all modes except the fundamental one and eventually all modes always stable before reaching $\frac{1}{2}$. The physical reasons for the increasing stabilizing effect of a given nozzle toward higher modes of oscillations are:

(1) The energy outflow through the nozzle as evaluated from the specific admittance ratio is larger for oscillations of higher frequency. This leads to

larger dissipation or damping. (2) The increasing spread of the reflected waves as compared to period of oscillations of higher modes leads to poorer timing or coordination and therefore less effective excitation.

For given position ξ of the combustion front, proper coordination of the exciting agent is obtained only when the time lag $\bar{\tau}$ lies in certain discrete range of values. It is clear also that if combustion is concentrated in the neighborhood of the node of a given mode ($\xi = \frac{1}{2}$ for fundamental mode) there is no such unstable ranges of $\bar{\tau}$ and that mode is always stable. If combustion is concentrated at an anti-node of a given mode, the unstable range of $\bar{\tau}$ is the widest and that mode is most likely to become unstable. This is obvious physically as there is little pressure variation at a pressure node to excite the oscillation while the pressure variation at an antinode is the largest. It should be remarked that a nodal position of a given mode need not be the desirable position for a stable concentrated combustion front because a node of a given mode can be the antinode of some other mode or modes. For example, the middle of the chamber is roughly a node of the fundamental mode and an antinode of the second mode. Thus if combustion is concentrated at the middle section of the chamber length, the fundamental mode is always stable while the second mode is most likely to become unstable. Since a motor can be considered as stable only when all modes are stable, it cannot be concluded from this simple analysis which is the best axial position for a concentrated combustion front to be stable. However, this simple consideration does indicate, on the other hand, that the injector end being an antinode of all modes of pressure oscillations, is the position where a concentrated combustion front is most likely to exhibit instability.

In figures 5 and 6 the magnitudes of n required to maintain neutral oscillations of different frequency $\omega = \beta \pi$ in the neighborhood of the fundamental and the second acoustical mode respectively are plotted for several combustion configurations (systems with combustion concentrated at different axial positions ξ and for system with uniformly distributed combustion). For each configuration, there is a particular frequency, corresponding to a particular value of the sensitive time lag where the value of n that is required to maintain neutral oscillation or to excite unstable oscillation is a minimum. We call it n_{\min} . This n_{\min} is a characteristic of the given configuration, designating the minimum amount of excitation required to initiate unstable oscillations under the condition of optimum timing. Therefore this n_{\min} serves as a very good criterion in comparing the relative tendency of different combustion configurations to exhibit instability independent of the values of the time lag. The values of n_{\min} for systems with combustion concentrated at different ξ 's are shown in figure 7. It is clearly seen here that when the combustion front is shifted away from injector end, n_{\min} for all modes increase gradually and the system becomes more stable. The value of n_{\min} for a given mode becomes very large when a pressure node is approached. The curve of n_{\min} vs. ξ for a given mode is roughly symmetric with respect to the node. When all modes of high frequency oscillations are taken into consideration, we see that the smallest value of n_{\min} , when the concentrated combustion front is at a given position ξ , is in most cases given by the n_{\min} of either the fundamental or the second mode whichever is the smaller. The values of n_{\min} for the fundamental and the second mode in a system with uniformly distributed combustion can be read from figures 5 and 6 and these values are considerably larger than the

value of n_{\min} when combustion is concentrated at any axial location when all high frequency modes are considered. Therefore a system with uniformly distributed combustion is considerably more stable than systems with combustion concentrated at any axial position. Accordingly, a system with uniformly distributed combustion can be considered as one of the most desirable stable configurations.

Analysis for systems with arbitrarily distributed combustion has been carried out (12). Instead of specifying the local source strength, the combustion distribution is more conveniently described by the steady state velocity $\bar{u}(x)$ which is equal to the Mach number M of the gas flow at the entrance of the nozzle. The stability boundary can be determined by the method of successive approximation and the value of n_{\min} corresponding to each configuration of combustion distribution $\bar{u}(x)$ is given for the first approximation as:

$$n_{\min} = \frac{1 + R(\omega_0) \cos^2 \omega_0}{2\gamma \int_0^1 (\bar{u}_x/M) \cos^2 \omega_0 x dx} \quad (3)$$

where ω_0 is the frequency of a given mode of oscillation with optimum timing determined by the following algebraic relation:

$$\omega_0 = k\pi - \tan^{-1} [MS(\omega_0)] \quad k=1, 2, 3 \dots \quad (4)$$

with $R + 18$ representing the nozzle admittance ratio which is the ratio of the fractional variations of gas velocity to that of gas density at the entrance of the nozzle. Since M is a small quantity and $S(\omega_0)$ is of the order of unity, equation (4) shows that ω_0 is in the neighborhood of integral multiples of π with deviation of the order of M . Hence, if n is not much bigger than n_{\min} the frequency of the unstable oscillation is slightly less than the acoustical frequency of the gas column in the combustion chamber.

This decrease in frequency of the oscillations can be interpreted as due to the inertia of the gas in the subsonic portion of the nozzle which constitutes an increase of the effective length of the gas column in the chamber. Following the conventions in acoustics, this may be interpreted as an end correction of the chamber length. But it should be noted that this end correction depends on the function S which is the imaginary part of the acoustical admittance ratio of the nozzle and is a complicated function of the nozzle shape, the entering Mach number of the gas and in particular the frequency of the oscillation in question.

Equation (3) represents the balance of excitation and damping for neutral oscillations with optimum timing. The numerator of the right hand side represents damping. The denominator multiplied by n represents excitation. The denominator itself is a factor that takes into account the unequal exciting contributions of different propellant elements. In first approximation, it is only the averaging factor of excitation that is affected by the combustion distribution. With $n > n_{\min}$, excitation may be larger than damping. Unstable oscillation will occur if timing is optimum and neutral oscillation can be maintained if the timing is not quite optimum.

In figure 8 the computed values of n_{\min} are shown for systems with combustion uniformly distributed along the first part ξ of the chamber length. It is interesting to note that the combined effect of the nozzle and the spatial combustion distribution makes the second mode always more stable than the fundamental mode. Furthermore, the most stable configuration (biggest n_{\min} when all modes are considered) corresponds to a system with combustion uniformly distributed through most but not all of the chamber length.

In figure 9 the values of n_{\min} of the fundamental modes for systems with combustion uniformly distributed in an intermediate portion of chamber length

are presented. It is found that the spatial spread about a mean position has in general a stabilizing tendency when all modes are being considered; but the effect is relatively insignificant if the total spatial spread is roughly less than $1/8$ of the wave length.

So far we have discussed the effect of spatial distribution of combustion or spread of the total space lag while the sensitive time lag is assumed to be the same for all elements. In actual situation they may vary in a certain range and distributed in some definite manner. Analysis shows that the spreading of the time lag, in general, tends to decrease the unstable ranges for given n and to increase the value of n_{\min} , for a given spatial distribution of combustion. The magnitude of the stabilizing effect for a given type of distribution of the sensitive time lag increases when the ratio of the actual spread of the time lag and the period of oscillation increases. Computed results for a particular type of time lag distribution about the mean value and for $n = 1$ are given in figure 10. The unstable ranges for the fundamental mode of oscillations are seen to be decreasing with increasing magnitude of ϵ_s , which is the fractional extent of time lag spread. Thus, the stabilizing effect toward a given mode of oscillation increases with increasing extent of spread of the sensitive time lag. Figure 10 also indicates that a fractional extent of spread of less than $\frac{1}{4}$ has negligible effect on the stability of the fundamental mode. The stabilizing effect of a given extent of the time lag spread increases toward higher modes of oscillation because of their smaller oscillation periods. The larger stabilizing effect of the nozzle and that of the spread of the sensitive time lag make the higher modes of the high frequency oscillations not likely to become unstable, as compared to the fundamental and the second modes. The

investigation of the stability of the fundamental and the second mode will therefore usually be sufficient. The effect of the spread of sensitive time lag in systems with arbitrary combustion distribution has been studied (14) and is shown to be likewise stabilizing.

The effect of a pressure sensitive feeding system can be analyzed if we know the transfer function $N(\omega) = \mu/\rho$ which is defined as the ratio of the fractional variation of the injection rate and the fractional variation of pressure at injector end. The following expression for n_{min} for arbitrary combustion distribution is obtained (15)

$$n_{min} = \frac{1 + R(\omega_0') + S_f(\omega_0')}{2\gamma \int_0^1 (\bar{u}_x/M) \cos^2 \omega_0' x \, dx} \quad (5)$$

where ω_0' is the frequency of optimum timing, determined by

$$\omega_0' = k\pi - \tan^{-1} M[S(\omega_0') + S_f(\omega_0')] \quad (6)$$

with R_f and S_f defined by the following complex integral

$$R_f + i S_f = \int_0^1 (\bar{u}_x/M) \frac{\cos \omega x}{i \omega} N(\omega) e^{-i \omega \bar{\tau}_i(x)} \, dx \quad (7)$$

The order of magnitude of R_f and S_f is roughly given by $|N|/\omega^2 \bar{\tau}_i$. The nondimensional $\bar{\tau}_i$ used in this formula is a mean value of the insensitive time lags τ_i of different elements nondimensionalized by the wave propagation time. Simple physical considerations show that this quantity $\bar{\tau}_i$, at least for the case of distributed combustion must be considerably bigger than unity. On the other hand, the dimensionless frequency ω is at least of the order of π . Thus both R_f and S_f are very small compared to unity unless N is very large, that is, unless the feeding system is in resonance with the acoustical frequency of the chamber - nozzle combination. Neglecting this possibility,

we see that the magnitudes of R_f and S_f decrease very fast with ω and that the effect of the feeding system on high frequency modes is very small. Consequently, the present author is inclined to conclude that screaming or unstable high frequency oscillation is essentially a phenomenon of intrinsic instability as compared to the case of chugging or low frequency oscillation which is strongly interfered by the pressure sensitivity of the feeding system. The exceptional case of resonance would need further study.

As has been remarked, all the previous results concern the stability of small high frequency longitudinal oscillations only. The stabilizing effect of the spatial spread of combustion and that of the timewise spread of the sensitive time lag are well established theoretically and the important role of stabilization played in this case by the energy dissipation due to the response of flow in the nozzle to oscillations at the entrance has been verified. The trend of design to eliminate or avoid the linear instability of longitudinal oscillations with frequencies in the neighborhood of acoustical values is clearly indicated in the previous theoretical results.

Fully developed unstable oscillations of combined longitudinal and transversal modes of the acoustical type are more often found in large thrust units especially when the length to diameter ratio of the combustion chamber is not large. The stability of the small cylindrical acoustical oscillations in the combustion chamber can be analyzed based upon the same physical concept of the mechanism of self-excitation as ^{that} for pure longitudinal oscillations. However, if we bear in mind the important dissipative action of the nozzle in the stability analysis of the longitudinal modes, we would have to determine the acoustical admittance ratio of the nozzle in response to combined transversal and longitudinal oscillations before we can evaluate the stability

boundary or even the minimum criterion of n_{min} . The determination of this admittance ratio is under way but has not yet been completed. Much theoretical work remains to be done concerning the stability of such combined modes.

The phenomenon of combustion instability is an extremely complicated one. The proposed mechanism of self-excitation is by no means the only one but is believed to be the most important mechanism which is responsible for unstable oscillations with frequencies closely related to the frequencies of acoustical modes; both pure longitudinal and combined modes. Some of the theoretical deductions as presented in the present paper have received experimental verifications. This is rather encouraging. However it is all the more important to investigate the basic postulate of the present theory, that is the empirical law concerning the variation of the sensitive time lag with chamber oscillations as expressed in terms of gas pressure. The qualitative stability behavior as influenced by the variation of different parameters, predicted by the present theory should be verified by a systematic experimental research. It is only through the careful investigation from both the theoretical and the experimental side, can we hope to understand the complicated phenomenon of combustion instability. It should be repeated here that the present theoretical results are concerned only with linear instability of acoustical type. Both the nonlinear instability and the linear instability with frequencies not apparently correlated with any acoustical frequencies would obviously require separate considerations.

REFERENCES

1. "Stability of Flow in a Rocket Motor" by D. F. Gunder and D. F. Friant, *Journal of Applied Mechanics (Trans. A.S.M.E.)* vol. 17, 1950, p.p. 327-333.
2. Discussion of Reference 1 by M. Yachter, *Journal of Applied Mechanics (Trans. A.S.M.E.)* vol. 18, 1951, p.p. 114-116.
3. "A Theory of Unstable Combustion in Liquid Propellant Rocket Motors" by M. Summerfield, *Journal of the American Rocket Society*, vol. 21, Sept., 1951, p.p. 108-114.
4. "Aspects of Combustion Stability in Liquid Propellant Rocket Motors" by L. Crocco, *Journal of the American Rocket Society*, Part 1, vol. 21, No. 6, Nov. 1951, p.p. 163-178, Part II, vol. 22, No. 1, Jan., 1952, p.p. 7-16.
5. "Servo-Stabilization of Combustion in Rocket Motors" by H. S. Tsien, *Journal of the American Rocket Society*, vol. 22, No. 5, Sept., 1952, p.p. 256-262.
6. "Servo-Stabilization of Low Frequency Oscillations in a Liquid Bipropellant Rocket Motor" by F. E. Marble and D. W. Cox, Jr. *Journal of the American Rocket Society*, vol. 23, No. 2, March, 1953, p.p. 63-74.
7. "Stability and Control of Liquid Propellant Rocket Systems" by Y. C. Lee, M. R. Gore, and C. C. Ross, *Journal of the American Rocket Society*, vol. 23, No. 2, March, 1953, p.p. 75-81.
8. "Transfer Functions of Rocket Nozzles" by H. S. Tsien, *Journal of the American Rocket Society*, vol. 22, No. 3, May, 1952, p.p. 139-143.
9. "Supercritical Gaseous Discharge with High Frequency Oscillations" by L. Crocco, *L'Aerotecnica*, vol. 33, No. 1, Feb., 1953, (Text in English).
10. "High Frequency Combustion Instability in Rocket Motor with Concentrated Combustion" by L. Crocco and Sin-I Cheng, presented at the 8th International Congress of Applied Mathematics and Mechanics, Aug., 1952, Istanbul, Turkey. Also published in *Journal of American Rocket Society*, vol. 23, No. 5, Sept.-Oct., 1953.
11. "High Frequency Combustion Instability in Rockets with Distributed Combustion" by L. Crocco and Sin-I Cheng, *Proceedings of the 4th Symposium of Combustion*, Sept. 1952, U.S.A. p.p. 865-880, Williams and Wilkins Co.
12. "Longitudinal Combustion Instability in Liquid Rockets with Arbitrary Combustion Distribution," by Sin-I Cheng will be submitted to the Bureau of Aeronautics U.S. Navy with Progress Report under Contract No. NOas 53-817-c.

13. "High Frequency Combustion Instability in Liquid Rockets with Concentrated Combustion and Distributed Time Lags" by Sin-I Cheng, Report No. 246, Aero. Eng. Report, Princeton University. Submitted to the Bureau of Aeronautics, U. S. Navy with Progress Report under Contract No. NOas 53-817-c.

14. "On the Approximations of the Analyses of Longitudinal High Frequency Combustion Instability in Liquid Rockets" by Sin-I Cheng will be submitted to the Bureau of Aeronautics, U.S. Navy with Progress Report under Contract No. NOas 53-817-c.

15. "Effect of Feeding System on High Frequency Longitudinal Combustion Instability in Liquid Rockets" by Sin-I Cheng. Will be submitted to the Bureau of Aeronautics, U. S. Navy with Progress Report under Contract No. NOas 53-817-c.

Legend of Figures

- Fig. 1a Radiation pattern of transition of unstable oscillations from weak to strong shock type. Modified impinging head, 41° convergent nozzle, $16 \frac{5}{8}$ in long chamber, frequency ~ 1200 cps.
- Fig. 1b Dynagage chamber pressure record of transition.
- Fig. 2 Schematic diagram for burning rate variation.
- Fig. 3 Specific acoustical admittance ratio of deLaval nozzle with linear steady state velocity in converging section.
- Fig. 4 Unstable ranges of sensitive time lag $\bar{\tau}$ and of total space lag ξ , $n = 1$.
- Fig. 5 Critical value of interaction index n to maintain neutral oscillations of reduced frequency $\beta = \omega/\pi$, concentrated combustion and uniformly distributed combustion, fundamental mode.
- Fig. 6 Critical value of interaction index n to maintain neutral oscillations of reduced frequency $\beta = \omega/\pi$, concentrated combustion and uniformly distributed combustion, second mode.
- Fig. 7 Minimum interaction index, n_{\min} , compatible with unstable oscillations in systems with combustion concentrated at ξ , fundamental mode $k = 1$, second mode $k = 2$, third mode $k = 3$.
- Fig. 8 Minimum interaction index, n_{\min} , compatible with unstable oscillations in systems with combustion uniformly distributed in $x = 0$ to $x = \zeta < 1$, fundamental mode $k = 1$, second mode $k = 2$.
- Fig. 9 Minimum interaction index, n_{\min} , compatible with unstable oscillations in systems with combustion uniformly distributed in region ζ about mean position σ , fundamental mode $k = 1$.
- Fig. 10 Unstable ranges of effective sensitive time lag $\bar{\tau}_e$ and position ξ of concentrated combustion front with $n = 1$. The fractional amount of propellant elements having their sensitive time lags lying between $\bar{\tau}_m(1 + \epsilon)$ and $\bar{\tau}_m(1 + \epsilon + d\epsilon)$ is given as $(\pi/4\epsilon_0) \cos(\pi\epsilon/2\epsilon_0)$ where $\pm \epsilon_0$ define the total fractional extent of time lag spread.

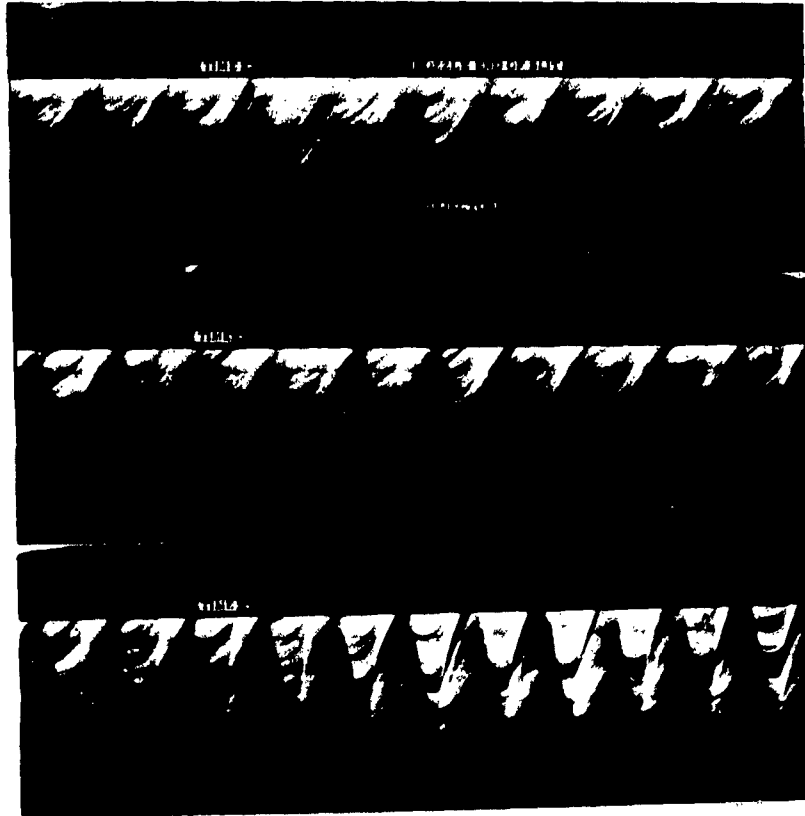


Figure 1a

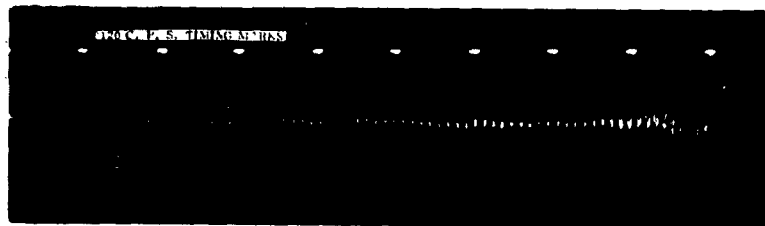
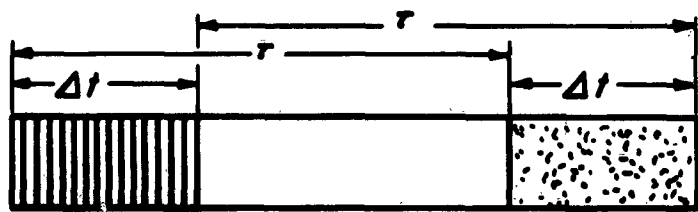


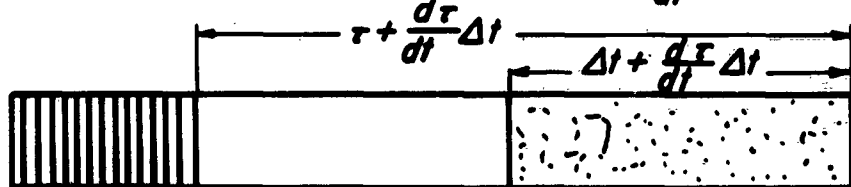
Figure 1b

$$\int_{t-\tau}^t p^n [x'(t'), y'] dt' = \text{constant}$$

STEADY STATE



SMALLER BURNING RATE $\frac{d\tau}{dt} > 0$



LARGER BURNING RATE $\frac{d\tau}{dt} < 0$

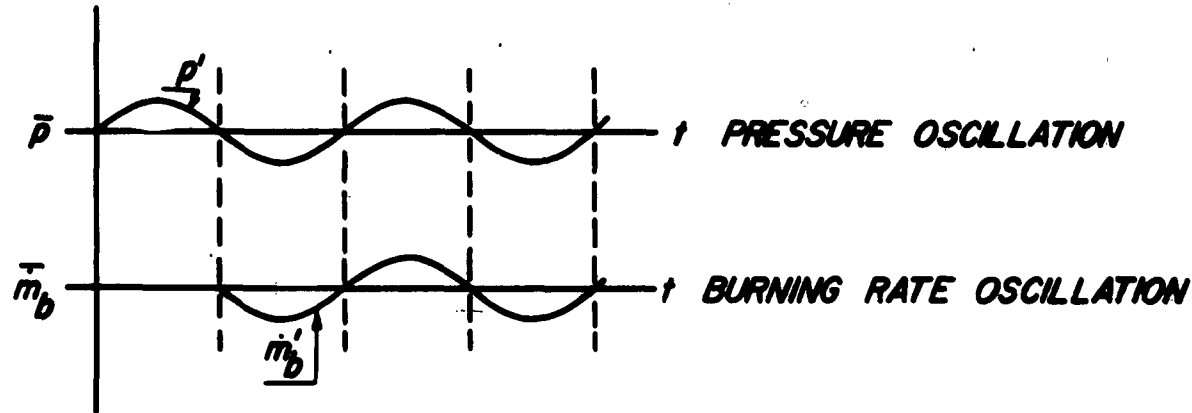
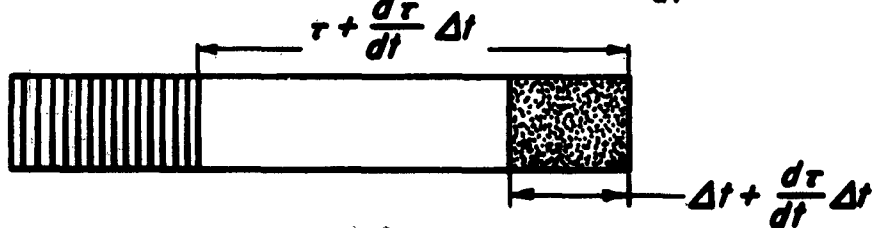


Figure 2

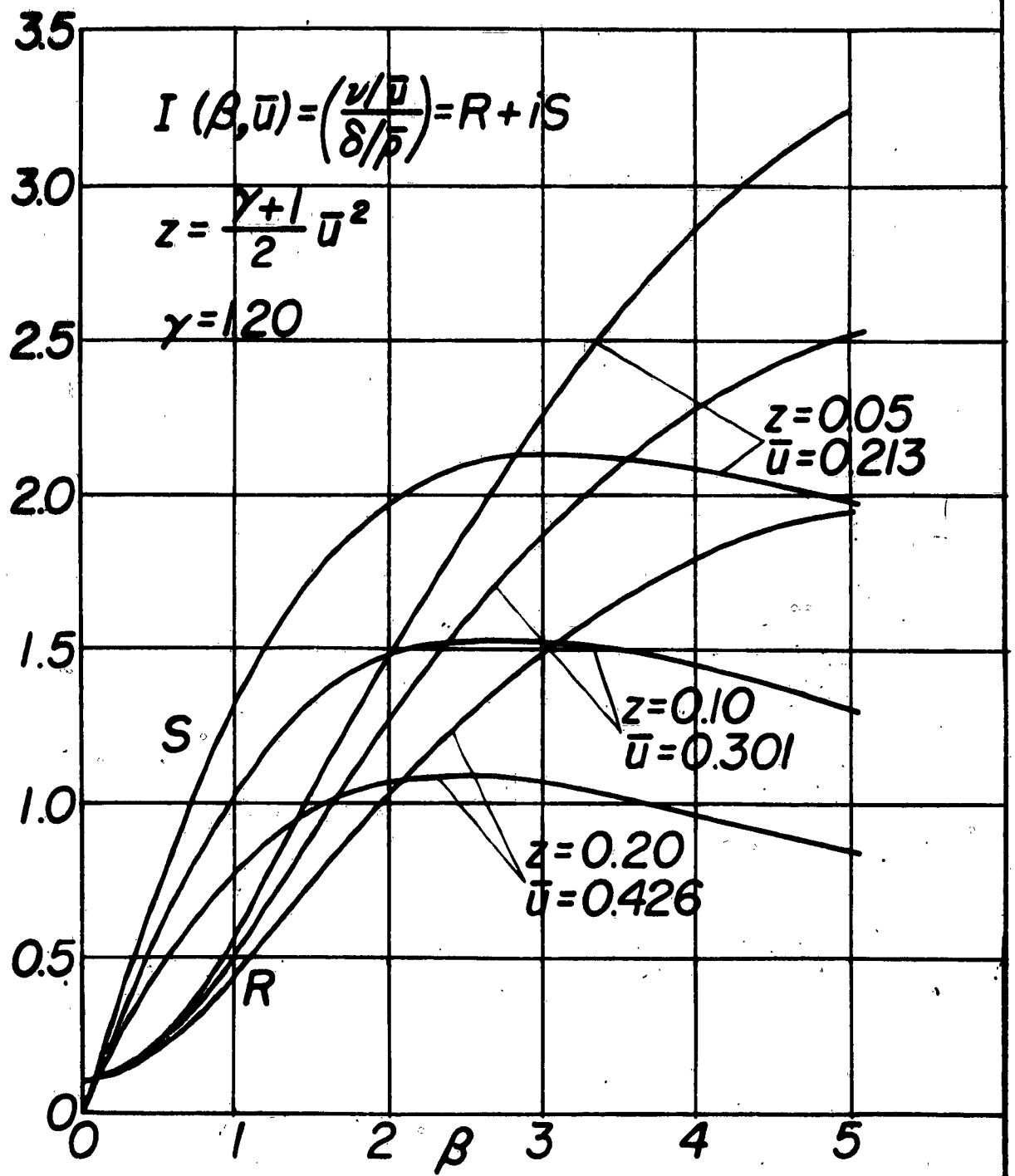


Figure 3

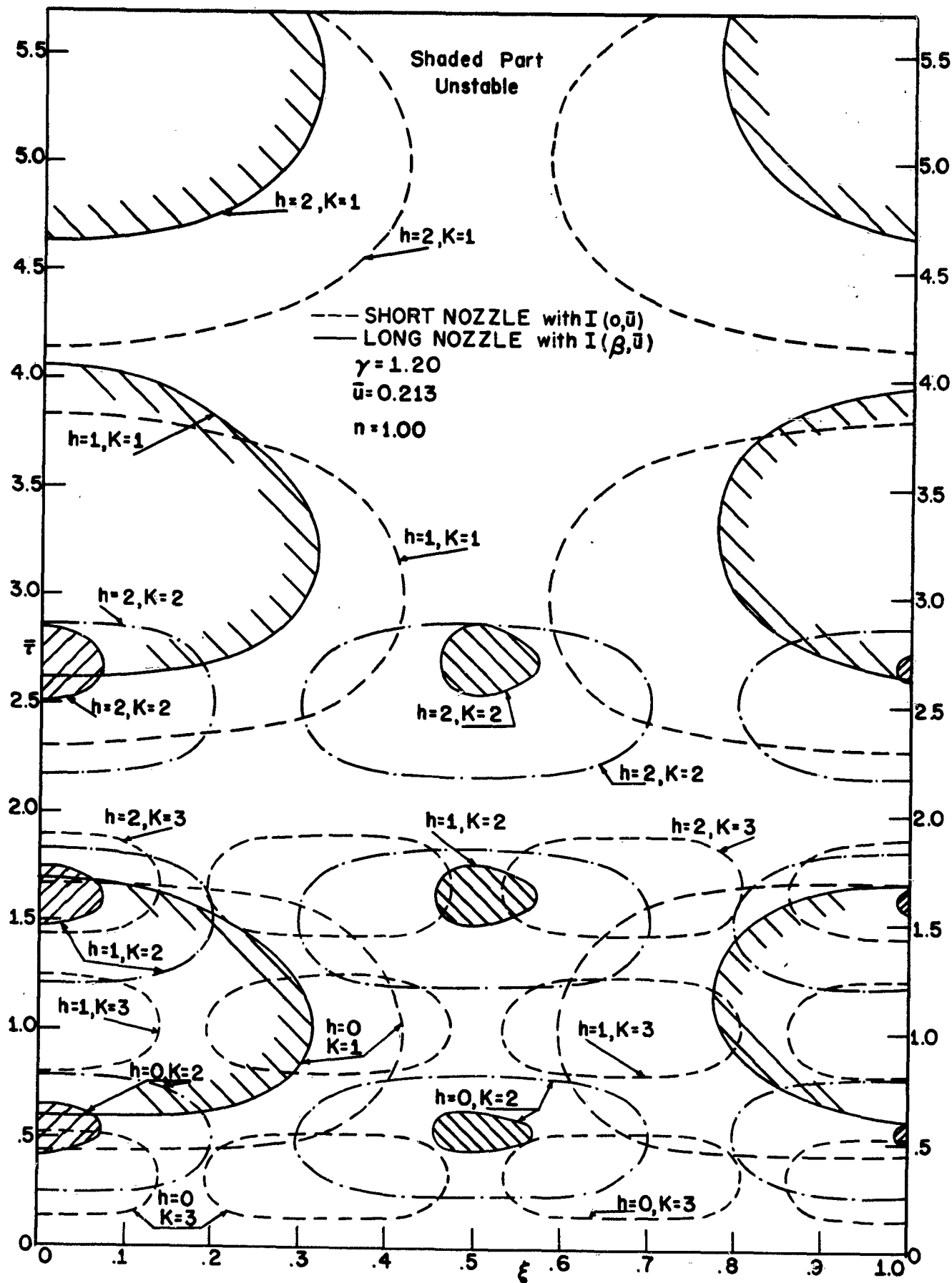


Figure 4

$\beta = \omega/\pi$
 $\gamma = 1.20$
 $\bar{u} = 0.213$

— long nozzle
--- short nozzle

fundamental mode

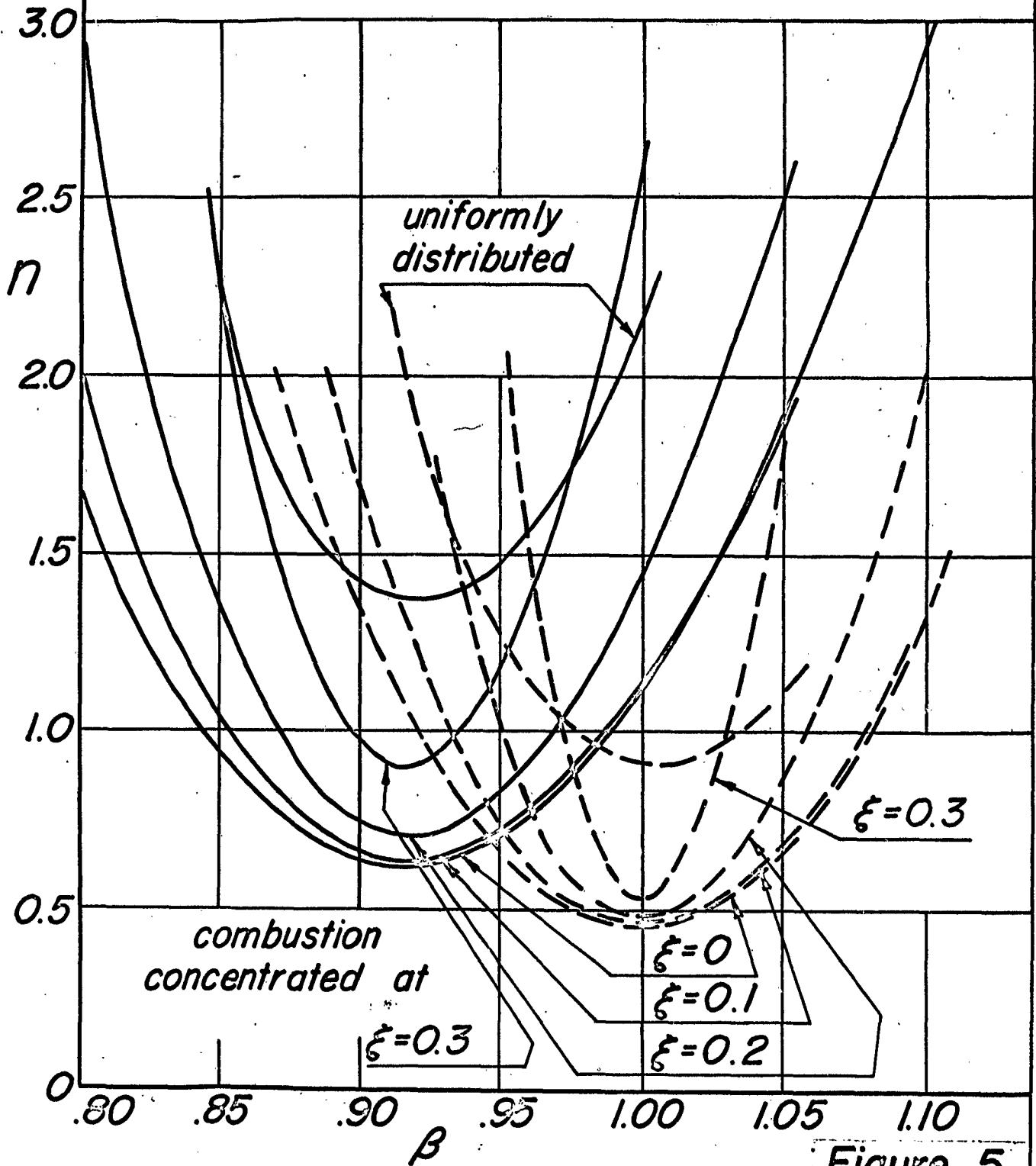


Figure 5

$$\beta = \omega/\pi$$
$$\gamma = 1.20$$
$$\bar{u} = 0.213$$

— long nozzle
--- short nozzle

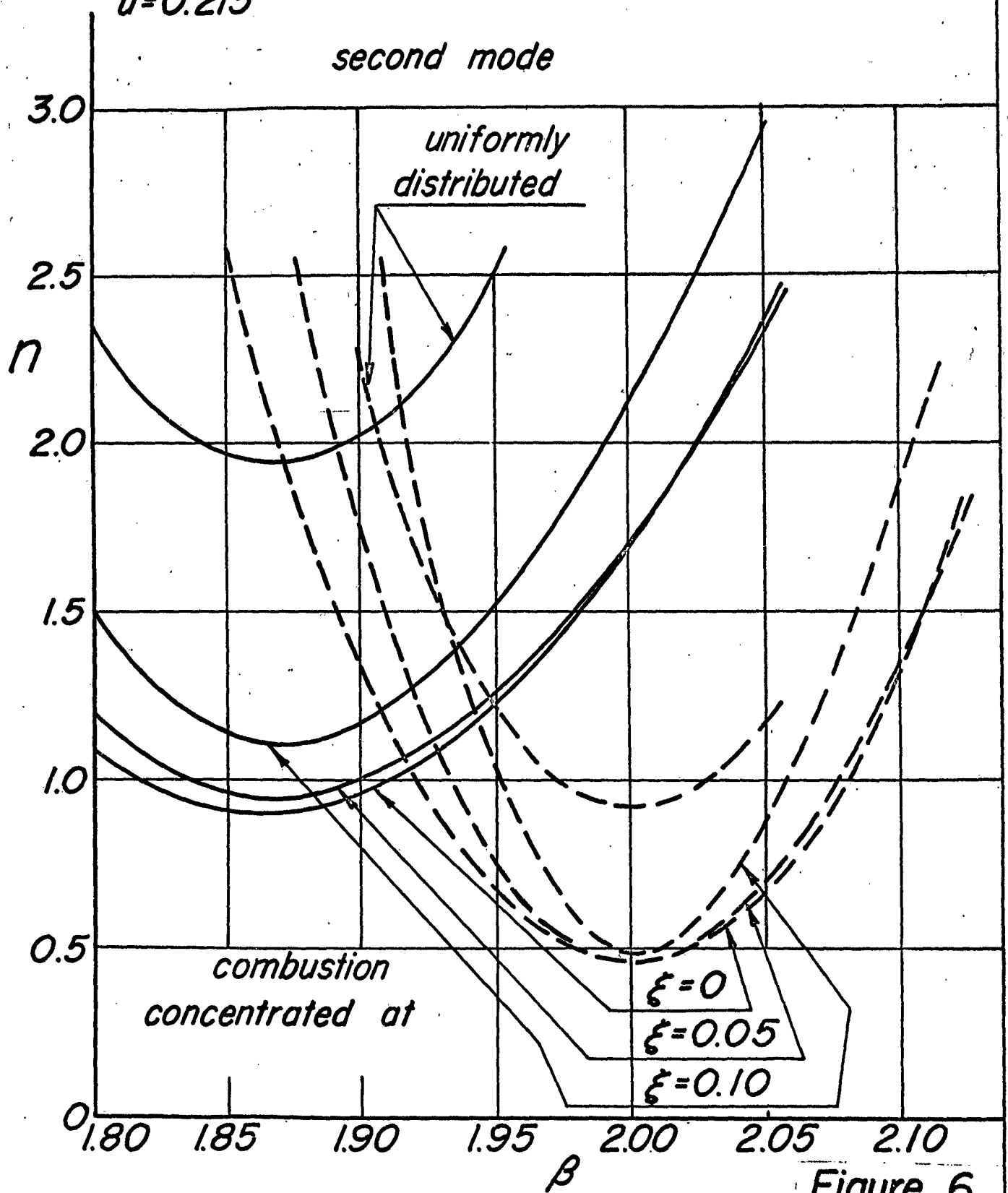


Figure 6

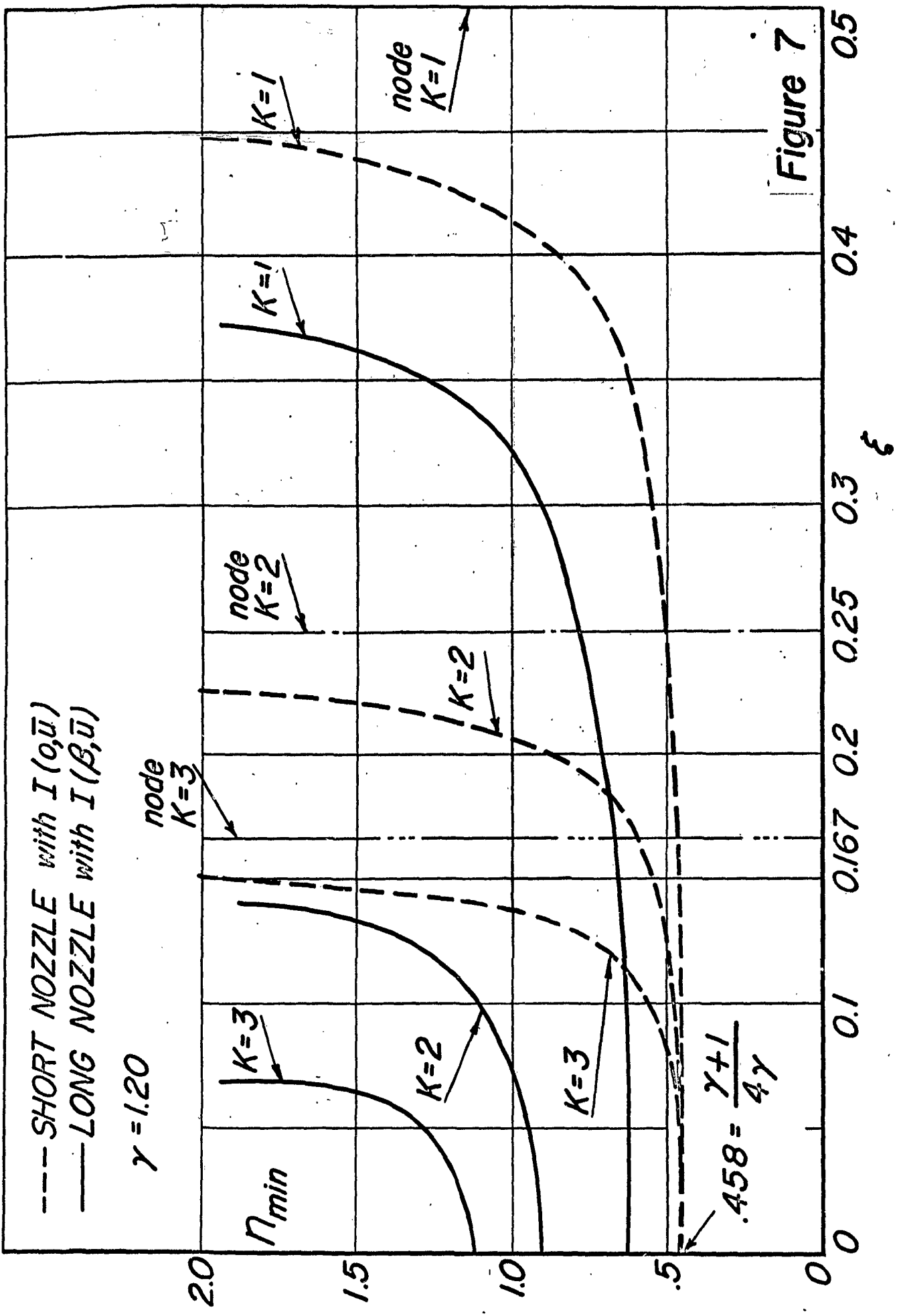


Figure 7

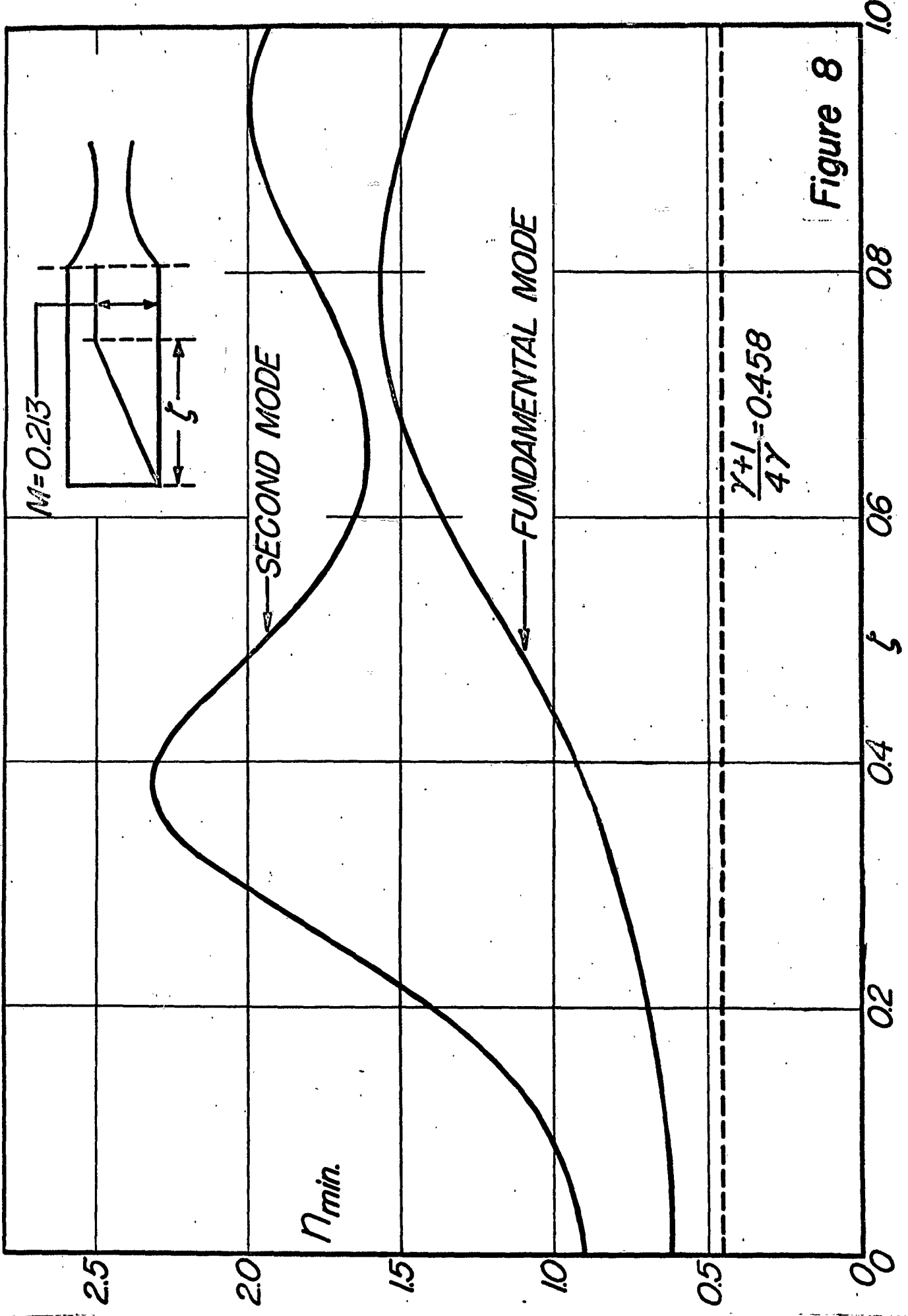


Figure 8

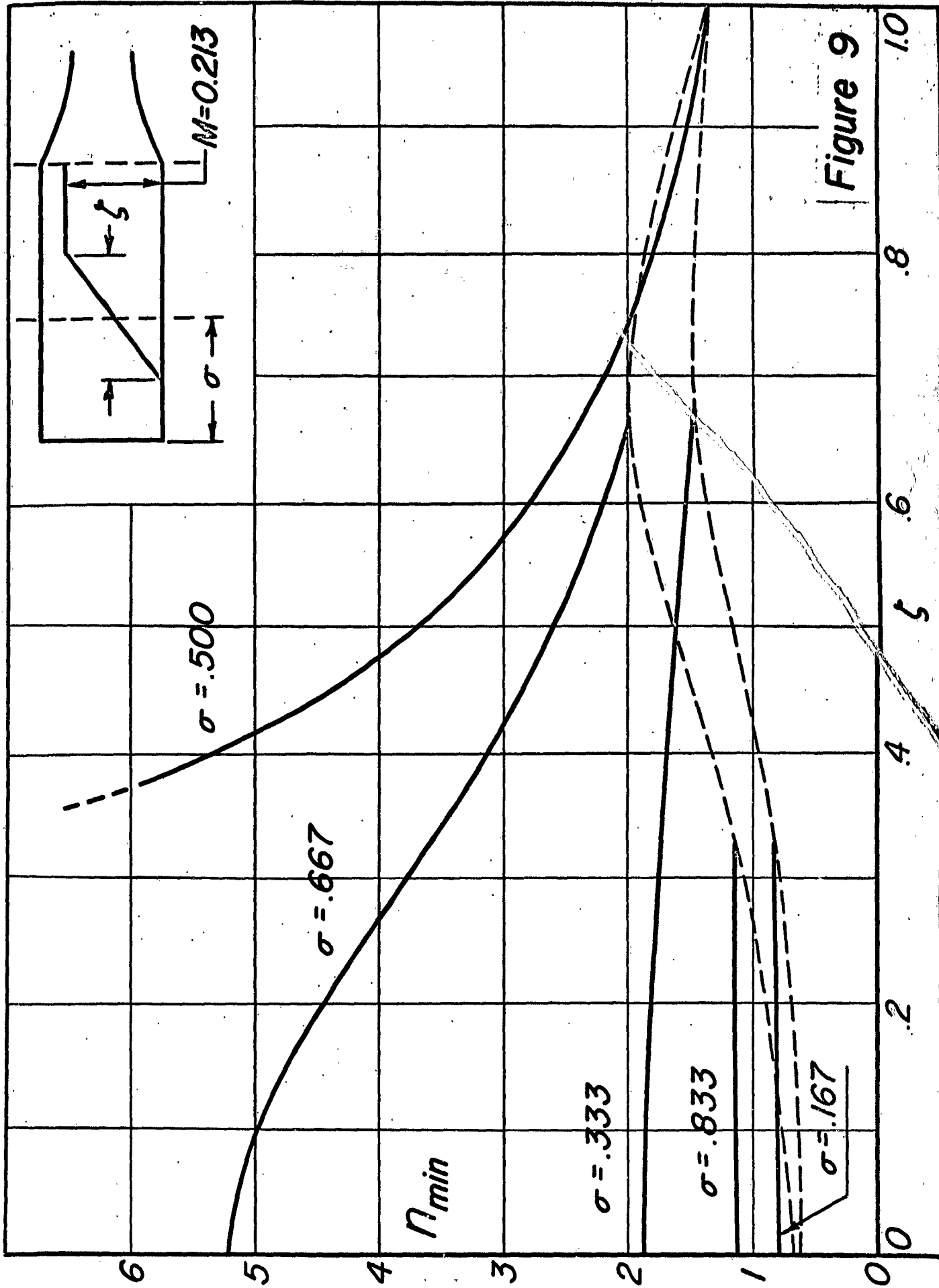


Figure 9

Fundamental

mode

$$\gamma = 1.20$$

$$n = 1$$

$$h = 0$$

$$G_2 = \frac{\cos \alpha \sqrt{\epsilon_0}}{1 - \left(\frac{2\alpha \sqrt{\epsilon_0}}{\pi}\right)^2}$$

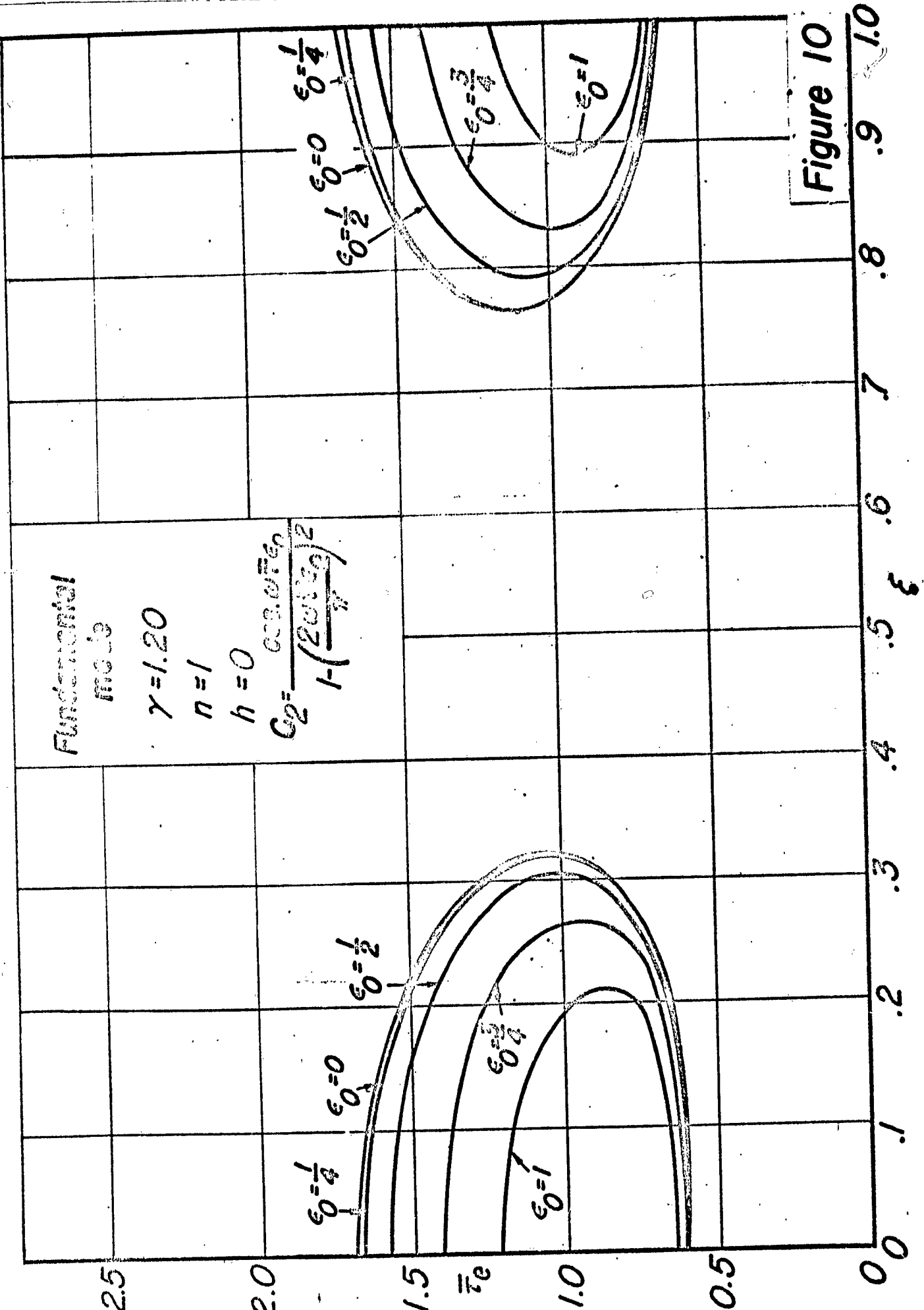


Figure 10

AD No. 36005-B

ASTIA FILE COPY

APPENDIX B

COMBUSTION TIME & IAO MEASUREMENTS

PHASE I: 31 OCTOBER, 1953

INTRODUCTION

The problem of combustion instability in liquid propellant rocket motors has long been recognized as one of the major difficulties in their development. In particular, the effect of extreme rates of heat transfer which have been shown to result from the high-frequency oscillations commonly called "screaming" will become even more significant as the industry progresses to the use of higher thrust, higher performance rocket engines.

In view of the present lack of correlation among so many of the recorded instances of instability, a program directed by L. Crocco was introduced at Princeton under the sponsorship of the Bureau of Aeronautics to examine the fundamental nature of this phenomenon from both theoretical and experimental viewpoints. The long-range objective of this program is to define a parameter or system of parameters which can be used to describe quantitatively the tendency of a given rocket motor configuration to exhibit one or more of the various forms of instability, and hence to supply the rocket motor designer with criteria which will permit elimination of combustion instability either in the design phase or by rational changes and adjustments in the course of development.

The first task encountered in setting up a systematic investigation is the formulation of a suitable framework to be used as a basis of operations. The concept of a combustion timelag, although presented some time ago by von Karman's group at the California Institute of Technology, was first subjected to analysis by Gunder and Friant (Ref. 1). Modifications were later introduced by

Yachter (Ref. 2) and Summerfield (Ref. 3), both of whom demonstrated that low-frequency instability could be coupled to the feed system through a constant combustion time lag. However, it was not until the concept of a pressure sensitive time lag was created by Crocco (Ref. 4) that the mechanism of high-frequency instability could be analyzed, and thus it was Crocco's theory which was selected to comprise the required framework for the experimental program.

Crocco's analysis is based on the assumption of a combustion model which considers all atomization, mixing, heating, and reaction of the liquid propellants in rocket combustion to be characterized by the time delay between the instant a particle of propellant enters through the injector orifice and the time its evolution into hot combustion gases is complete. This time delay consists of two parts; (which are, however, physically inseparable) a constant portion, which is a function primarily of motor configuration, and a variable portion which is sensitive to the variable combustion chamber parameters (e.g., pressure, temperature, velocity, etc.). For mathematical and experimental simplicity, and also because it appears to best characterize the grouping of physical and chemical processes we call combustion, this variable portion of the time lag was taken to be a reasonable function of chamber pressure, and development of the analysis was completed on this basis. A summary of the theoretical treatment in its present state of completion may be found in Ref. 5.

The experimental attack logically breaks down into two basic problems:

- (1) Test, verification, and/or modification of the fundamental assumptions

which comprise Crocco's model of the rocket combustion process, and (2) Determination of the effects on stability of varying the time lag and other significant parameters by means of variations in the standard rocket motor components; e.g., propellants, injectors, chamber geometries, nozzle geometries, etc. In view of the extreme interest in the detrimental effects of high frequency instability on liquid bipropellant motors, this particular case has received primary emphasis in planning both the theoretical and experimental attack. The theory presents an analysis of only the longitudinal type of instability, although extension of the basic fundamentals to mathematical and experimental analysis of the transverse modes is now being undertaken.

In order to facilitate development of the necessary experimental techniques and instrumentation, a "workhorse" monopropellant test stand was constructed. The monopropellant system was selected primarily for its simplicity, low temperature, flexibility and reliability of operation, since the rocket motor was to serve in this phase only as a test vehicle for the instrumentation. The monopropellant data, however, can easily be applied as a check on the basic assumptions of the theory for monopropellants as set forth in Ref. 4, once development of techniques and instrumentation have progressed to a satisfactory degree, but, as mentioned above, the heart of the experimental program actually lies in the bipropellant system.

The present paper describes the techniques which have been developed to conduct the experimental investigation, together with preliminary results of monopropellant test program. These results must be considered to be merely

an indication of the capabilities of techniques which are still undergoing a process of refinement, with the final aim of reducing the scatter of the observations to the minimum possible amount.

APPARATUS

Although construction of a bipropellant system is nearing completion at the present time, only the equipment used to obtain monopropellant rocket motor data will be described here. Basically, this equipment consists of a gas-pressurized feed system, a monopropellant rocket motor, flow and pressure sensing elements, and electronic recording equipment.

The feed system and rocket motor layout is illustrated in Fig. 1. The inert gas pressurizes ethylene oxide in the high-pressure tank, forcing it through a Potter turbine-type flowmeter, a cavitating venturi, a flow modulating unit, and into the rocket motor injectors. All components downstream of the propellant valve are mounted on a flexure type thrust stand (see Fig. 2) which uses leaf springs to provide one degree of frictionless freedom. The rocket motor, shown in Figure 3, is of stainless steel and has an inner diameter of 5 inches. It is of sectional construction, providing a simple method of changing L^* , and uses eight radial injectors of the full-cone spray type. A small amount of gaseous oxygen is injected through an orifice located on the motor axis at the head end, and ignition is accomplished by means of standard sparkplugs (two are used to provide reliability).

The flow modulating unit, a simple piston arrangement diagrammed in

Figure 4, is mounted in the propellant feed line between the rocket motor and a cavitating venturi. The venturi serves to maintain the steady-state component of the flow rate, and also to damp out disturbances traveling upstream from the modulating unit. The flow modulating unit itself is a straightforward crank-piston arrangement with a 0.20-inch stroke and interchangeable pistons to provide different displacements. The data included in this report have been taken using a piston with 0.802-inch diameter and a resulting displacement of 0.1 cubic inches. The unit can be driven at speeds ranging from 3,000 to 12,000 RPM (50 to 200 cycles per second) by a U. S. Motors 3/4 HP Varidrive. It was found during the course of testing that the flywheels shown in Figure 4 were not necessary to maintain constant speed under load, and hence most of the data were taken with the flywheels removed. Piston sealing is provided by a double-ridged teflon gasket (as shown in Figure 4), but it was found necessary to replace this seal after every ten or twelve runs.

Operation of the monopropellant motor is performed from the control panel shown in Figure 5. Photographs of the Heise bourdon-tube gages are used to obtain checks on the steady-state values of thrust, chamber pressure, injector pressure, and pickup reference pressure. The power supplies and balancing bridges for strain-gage sensing elements also appear in Figure 5, but all other electronic operations and recording are done in a separate building, to which the signals are piped via coaxial cables.

Steady-state flow rates are measured with a Potter turbine-type flowmeter, and values checked by a high-pressure sight glass located on the propellant

tank. Thrust is measured simultaneously with an Emery hydraulic load cell and indicator and a Li strain gage load cell recording on a Leeds and Northrup potentiometer. Two Li-Li pressure pickups are used to record instantaneous pressures at the injector and in the chamber. This type of pickup (see Fig. 6) is a double catenary diaphragm, water-cooled strain-gage transducer which is designed to be flush-mounted in a rocket combustion chamber. A detailed description of this device is presented in Ref. 6.

The pickups are mounted as shown in Figure 7, the diaphragm of one pickup being flush with the inner combustion chamber wall, and the other installed as closely as possible to one of the injector orifices. The signals from the pickups are recorded as shown in Figure 8. Each signal is branched four ways; first, directly to an Electronic Tube Corporation four-channel oscilloscope recording on a General Radio strip-film camera (see Fig. 9). A 200 cps timing trace, checked for exact frequency with a Berkeley electronic counter, also appears on the oscilloscope screen. The second signal branch is passed through a constant-phase AC amplifier into a two-channel FM Ampex magnetic tape recorder which features a 20 to 1 tape-speed reduction for playback. (See Fig. 9). The recorder's low-speed playback permits ultimate viewing of the taped signals on a Hathaway six-channel recording oscillograph whose galvanometer frequency response is flat to only 1,000 cps. The third signal branch is amplified by a chopper feedback DC amplifier and recorded on the Hathaway oscillograph, serving primarily as a complete history of the run. The fourth branch is passed through a cathode follower (necessary because of poor circuit impedance matching characteristics) to a low-response Leeds and Northrup continuously

recording potentiometer, which provides an accurate determination of average chamber and injector pressures.

Measurement of the instantaneous flow rate through the injectors was attempted in a number of different ways. A Mittelmann electromagnetic flowmeter was obtained on a loan basis, but circuit inadequacies prevented its use in the program, despite extensive development work on the part of project personnel. A true mass flowmeter designed by Y. T. Li was also procured for this purpose, but mechanical difficulties (e.g., leakage, etc.) have prevented its use for instantaneous flow measurement purposes up to the present time. Constructional details and principle of operation of this instrument, which is pictured in Figure 10, are described at length in Ref. 7.

A third approach to the flow-measuring problem, which appears to show some promise for calibration purposes in conjunction with the fourth technique (to be discussed later) was the adaption of constant-temperature hot-wire anemometer techniques to the flow of liquids. This system required extensive development but has been successful in producing an instrument which will respond in approximately 0.15 milliseconds to variations in flow velocity. The method is fundamentally the same as that used in wind-tunnel hot-wire anemometry, but involves a number of rather extreme changes in the basic components. For example, the strength requirement dictates use of a wire diameter ten times that of conventional systems. The resulting enormous decrease in resistance, coupled with the high heat capacity of the liquid medium, necessitates wire heating currents of the order of one or two

amperes, as compared with the few milliamperes generally used, in order to approach sensitivity requirements of the system. The solutions to this and other problems are described at length in Ref. 8.

The experimental method used for determining the time constant of the hot-wire apparatus is shown in Figure 11. A steel weight is dropped on a piston, moving a water column of known dimensions past the hot-wire probe. Knowing the instant at which the weight strikes the piston and the wave travel time through the water column, the response time of the hot-wire probe can be measured. Typical data obtained with this system are shown in Figures 12a and 12b. The uppermost trace in each case is the electrical contact which marks the instant at which piston motion begins. The hot-wire signal appears in the center, and the lowest trace is ^a1,000 cps timing marker. Figure 12a indicates the response time of the hot-wire to the water velocity induced by the piston motion, showing also the expected linear velocity increase. The response time of the probe was approximately one-seventh of a millisecond, as shown in the figure. Figure 12b indicates the excellent resolving power of the hot-wire, demonstrating its ability to detect wave reflections which traveled at 5500 ft/sec in the cylinder of water.

Amplitude response characteristics of the hot-wire have not yet been determined, but its use as a liquid flow phasemeter is now feasible up to frequencies of at least 1,000 to 2,000 cps.

The fourth technique to be applied to the measurement of flow is the use of two high-response pressure pickups and an orifice. For an oscillating flow

rate, it can be shown theoretically (see Ref. 9) that there are both an amplitude change and a phase difference between instantaneous flow and pressure drop, and further, that these quantities vary as a known function of frequency. This method appears to show far better promise than any of the others, but some check on the theoretical correction is necessary before it can become fully reliable. Such a check on the phase correction will be provided by forthcoming tests utilizing the hot-wire meter in conjunction with two pressure pickups and one of the injector orifices in a pulsating water flow, using the test rig illustrated in Figure 13.

DISCUSSION OF RESULTS

As mentioned earlier, the primary purpose of the monopropellant rocket test stand was to act as a "workhorse" for instrumentation development and evolution of test techniques, particularly the application of propellant flow rate modulation. It might, at first glance, appear that application of oscillating flow and pressure data to Crocco's linearized theory would not be permissible. This could be true if the rocket motor were experiencing actual combustion instability, but it must be carefully pointed out that the motor is run under fully-controlled, stable conditions at all times. The amplitude and frequency of the flow rate modulation are set by the operator at will, and are not fixed by the characteristics of the motor and feed system, as would be the case if instability existed. This condition is in accordance with the aims of the first phase of the test program, in which it is desired to measure certain characteristic quantities which are very important for the

appearance of unstable operation during normal -- not unstable -- combustion.

The specific purpose of operating with a modulated flow rate is as follows: By causing a variation in propellant flow rate, it is possible to observe experimentally the various quantities which appear in Crocco's equation for the combustion chamber (Ref. 4). If the flow variation is sinusoidal, these experimentally measured quantities may be analyzed by the use of straightforward mathematical techniques. An illustration of this feature appears later.

The quantities which enter into the fundamental equation of the combustion chamber (Ref. 4) are the instantaneous value of chamber pressure, its derivative with respect to dimensionless time, the instantaneous value of flow rate at the injector orifice, the pressure-sensitive and pressure insensitive time delays between flow and combustion, and the "index of interaction" between combustion rate and chamber pressure described in Ref. 4.

The first two quantities can be obtained from the recorded chamber pressure and the third from the injector pressure drop, after application of the proper corrections. The remaining three quantities, however, are unknown. Crocco has devised a procedure, the details of which need not be included here, by which they may be computed and checked using the flow rate and chamber pressure data. Hence, the experiments must provide only the ratio of fractional amplitudes of oscillation of the flow rate and chamber pressure, and the corresponding phase difference at different frequencies

and chamber pressures. These quantities can be obtained, after making the proper corrections, from the ratio of fractional amplitudes of injector pressure drop and chamber pressure, and the phase difference between them.

The method is particularly reliable when the oscillations have a nearly sinusoidal shape. In this case the necessary data can be obtained very simply from the measured oscillations of feed-line pressure at the injector (instead of the pressure drop across it) and the chamber pressure.

If the injector pressure P_i is sinusoidal, it may be written

$$P_i = \bar{P}_i + \tilde{P}_i \sin \omega t$$

The chamber pressure P_c may then be written

$$P_c = \bar{P}_c + \tilde{P}_c \sin(\omega t + \alpha)$$

where α is the phase difference between injector and chamber pressure oscillations.

The pressure drop ΔP across the injector thus becomes

$$\Delta P = P_i - P_c = \bar{P}_i - \bar{P}_c + \tilde{P}_i \sin \omega t - \tilde{P}_c \sin(\omega t + \alpha)$$

But ΔP may also be expressed by

$$\Delta P = \bar{\Delta P} + \tilde{\Delta P} \sin(\omega t + \gamma)$$

These expressions can now be used to relate ΔP to P_c by straightforward

analysis, obtaining the result

$$\frac{P_c - \bar{P}_c / \bar{P}_c}{\Delta P - \bar{\Delta P} / \bar{\Delta P}} = R e^{i\beta}$$

where the amplitude ratio R is given by

$$R = \frac{(\bar{P}_i / \bar{P}_c - 1)}{\sqrt{1 + (\tilde{P}_i / \tilde{P}_c)^2 - 2(\tilde{P}_i / \tilde{P}_c) \cos \alpha}}$$

and the phase difference β is written

$$\tan \beta = \frac{\sin \alpha}{\cos \alpha - (\tilde{P}_c / \tilde{P}_i)}$$

Thus, by measuring \bar{P}_i , \bar{P}_c , \tilde{P}_i , \tilde{P}_c , and α , that is, by measuring the mean values, the amplitudes of oscillation, and the phase difference between injector and chamber pressures, the quantities R and β , which relate injector pressure drop to chamber pressure, may be obtained quite conveniently. At any given modulating frequency and chamber pressure, R and β will provide the raw data for determination of the combustion parameters.

Experimental values of R and β were obtained from recordings of chamber pressure* and injector pressure as typified by Figure 14. Figure 14a is a strip-film photograph of the oscilloscope, and Figure 14b a typical low-speed

playback of recordings made on magnetic tape. Amplitudes and phase difference (i.e., \tilde{P}_1 , \tilde{P}_c , and α) were obtained from these types of record, while average values of the required pressures (i.e., \bar{P}_1 and \bar{P}_c) were observed on recording potentiometers.

The values of R and β themselves are shown as a function of modulating frequency (at constant mean chamber pressure) in Figure 15. The data of this figure are not yet suitable for determination of the combustion parameters for the following reasons:

The present chamber has a characteristic length $L^* = 570$ inches, due to the difficulty of decomposing ethylene oxide at smaller values of L^* . Consequently, if the flow rate oscillations are kept small, the resulting variations in chamber pressure are not sufficiently large to be observed with proper accuracy. For example, in order to obtain a chamber pressure oscillation of the order of three per cent amplitude, it was necessary to increase the injector pressure drop amplitude of oscillation to the order of fifty per cent for a typical chamber pressure and modulating frequency. This means that the flow rate/pressure drop correlation is out of the approximately linear range. Moreover, the ΔP oscillation might be too large for proper range of operation of the cavitating venturi, with the result that disturbances affecting the sinusoidal nature and general regularity of the modulation can appear at each cycle. This is especially true at the higher frequencies.

*Note that at flow modulating frequencies below 200 cps, the location of the chamber pressure tap is immaterial, since the wave travel time throughout the chamber is negligible compared with the period of the oscillation, and hence changes in chamber pressure caused by the flow modulating unit may be considered to occur simultaneously at all points in the chamber.

Elimination of these causes of error is now under way, using the experience gained on the preliminary tests to attain better accuracy through the application of minor improvements and refined calibrations. In the monopropellant case, this will supply an order of accuracy sufficient to allow smaller amplitudes of oscillation in chamber pressure; in the bipropellant case the situation will be made easier by the smaller value of L^* .

Although the data shown in Figure 15 are not yet adequate for precise determination of the combustion parameters, some qualitative conclusions concerning pressure sensitivity can be drawn. If the experimentally-measured phase difference between injector and chamber pressures is converted to the dimensions of time and plotted against mean chamber pressure on log-log paper, we obtain a relation somewhat similar to Crocco's assumed relationship between chamber pressure and time lag, (Ref. 4). This data is shown in Figure 16*. It must be remembered, however, that the ordinate T in this figure is not the true combustion time lag, but merely a conveniently measured quantity which is expected to vary with chamber pressure in somewhat the same way as the time lag.

Figure 16 shows the curves of the time T vs mean chamber pressure for two different ranges of modulating frequency. The existence of two separate curves does not violate the assumption that time lag is independent of modulating frequency. It should be reemphasized that Figure 16 is included only to present qualitative trends, and although it appears to support the general nature of Crocco's assumption of the pressure-sensitivity of the time lag, it

*Note: This figure was not presented at the Symposium.

is not considered as proof that the analytical formulation of this assumption is correct. A quantitative check on Crocco's formulation will be made after the experimental data are considered sufficiently reliable and accurate, a condition which is expected to be attained in the near future.

REFERENCES

1. D. F. Gunder and D. R. Friant, "Stability of Flow in a Rocket Motor", Journal of Applied Mechanics, Vol. 17, No. 3, 1950, P. 327
2. M. Yachter, "Discussion of the Paper of Reference 1", Journal of Applied Mechanics, Vol. 18, No. 1, 1951, pp. 111-116.
3. M. Summerfield, "A Theory of Unstable Combustion in Liquid Propellant Rocket Systems", Journal of the American Rocket Society, Vol. 21, September 1951, pp. 108-114.
4. L. Crocco, "Aspects of Combustion Instability in Liquid Propellant Rocket Motors", Journal of the American Rocket Society, Vol. 21, November, 1951, pp. 163-178 (Part I); and Vol. 22, January-February, 1952, pp. 7-16 (Part II).
5. S. I. Cheng, "Concepts and Theory of Combustion Instability", (RESTRICTED). Presented at the 2nd Symposium on Liquid Propellant Rocket Engine Combustion Instability, October 28, 29, 1953.
6. G. B. Matthews, "Development of Li-Li₂ Pressure Pickup", (RESTRICTED). Presented at the 2nd Symposium on Liquid Propellant Rocket Engine Combustion Instability, October 28, 29, 1953.
7. Y. T. Li and S. Y. Lee, "A Fast-Response True Mass Rate Flowmeter", ASME Paper No. 52-A-170, presented at the Annual Meeting of ASME, New York, N. Y., December 2, 1952.
8. L. Crocco and J. Grey, "Combustion Instability in Liquid Propellant Rocket Motors", Appendix A, Fourth Quarterly Progress Report, BuAer Contract Noas 52-713-c, (RESTRICTED), June 1, 1953.
9. L. Crocco and J. Grey, "Combustion Instability in Liquid Propellant Rocket Motors", Appendix A, Third Quarterly Progress Report, BuAer Contract Noas 52-713-c, (RESTRICTED), March 1, 1953.

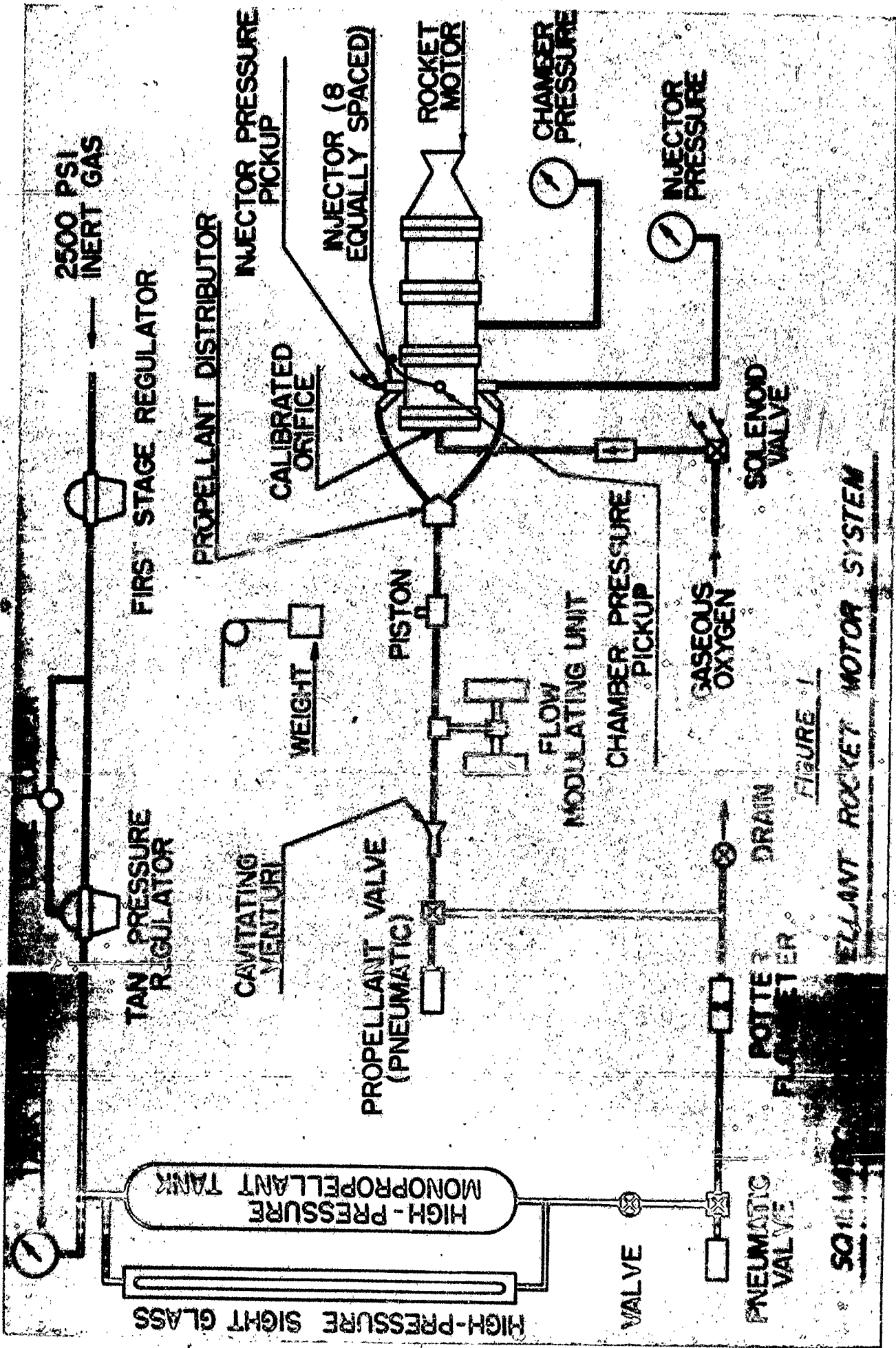


FIGURE 1

PROPELLANT ROCKET MOTOR SYSTEM

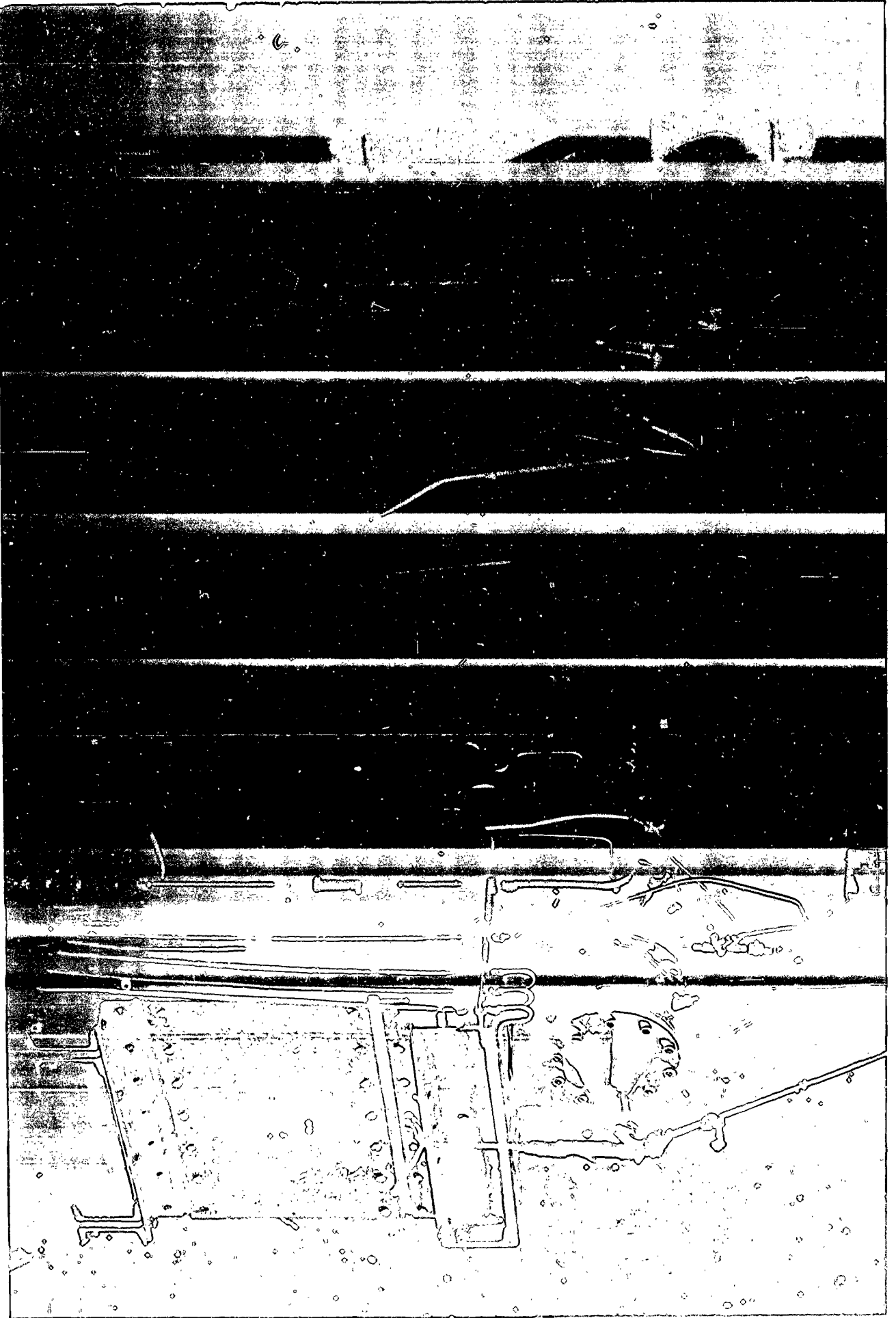


FIGURE 2
MONOPROPELLANT TEST STAND

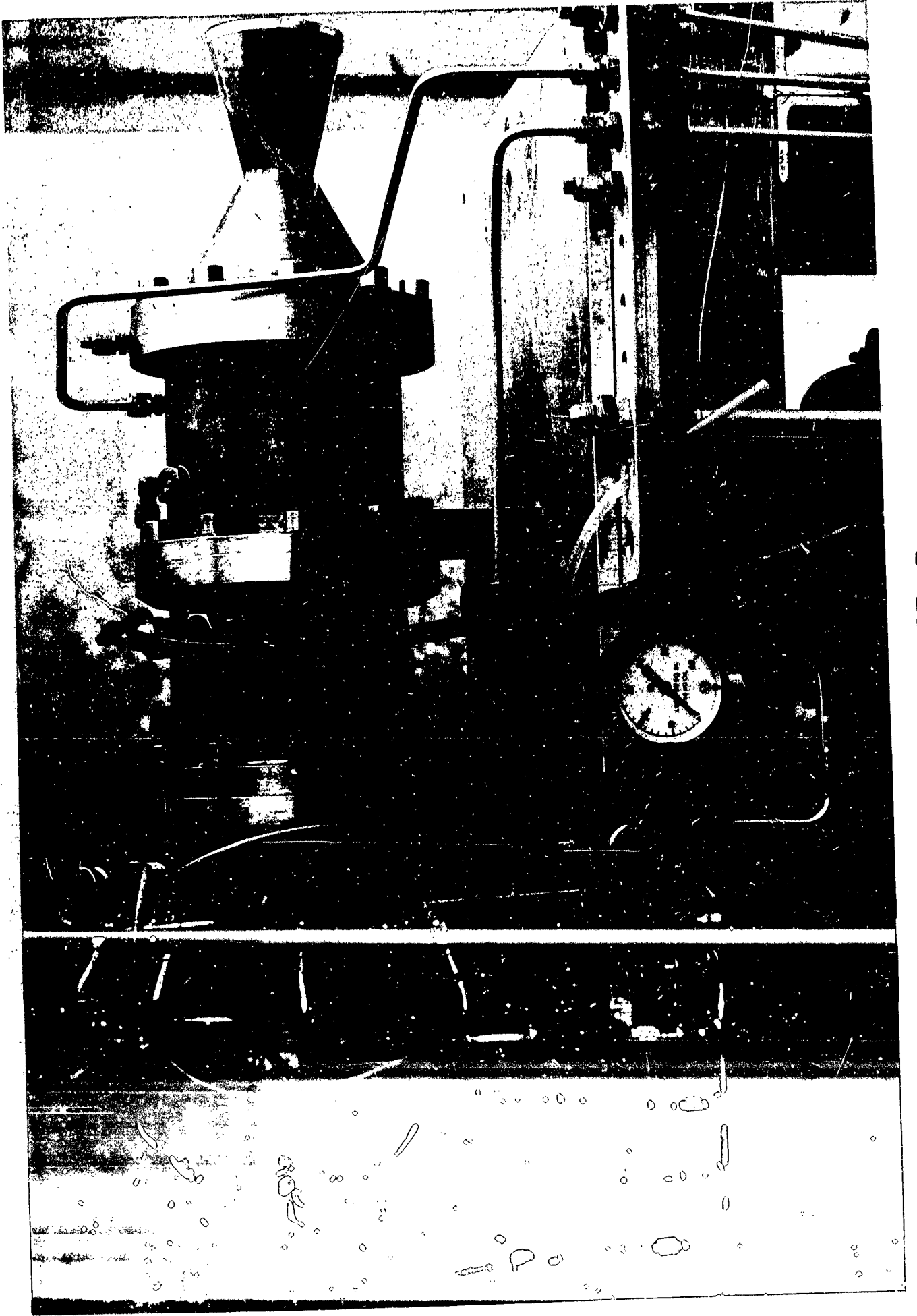


FIGURE 3
MONOPROPELLANT ROCKET MOTOR

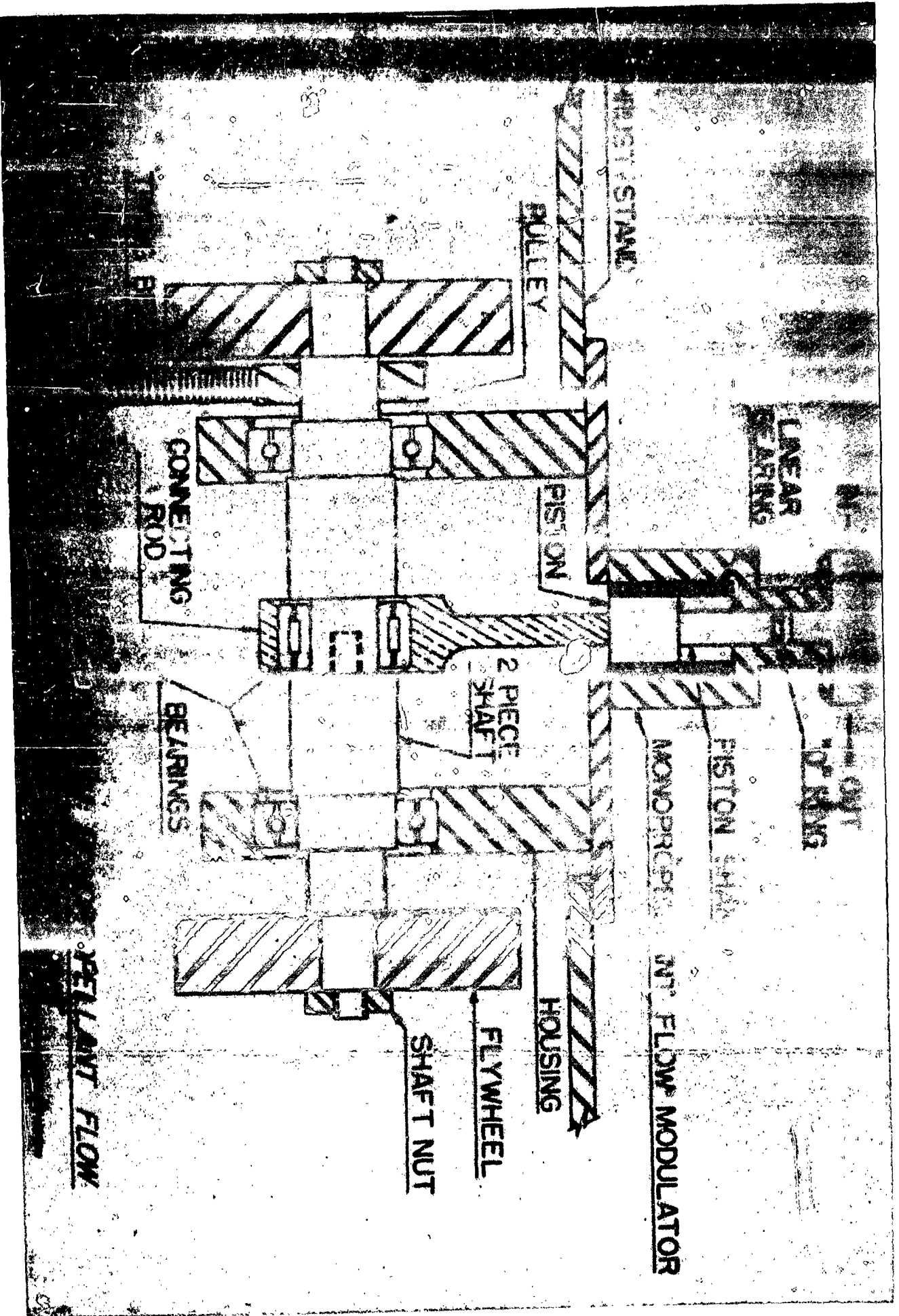


FIGURE 4

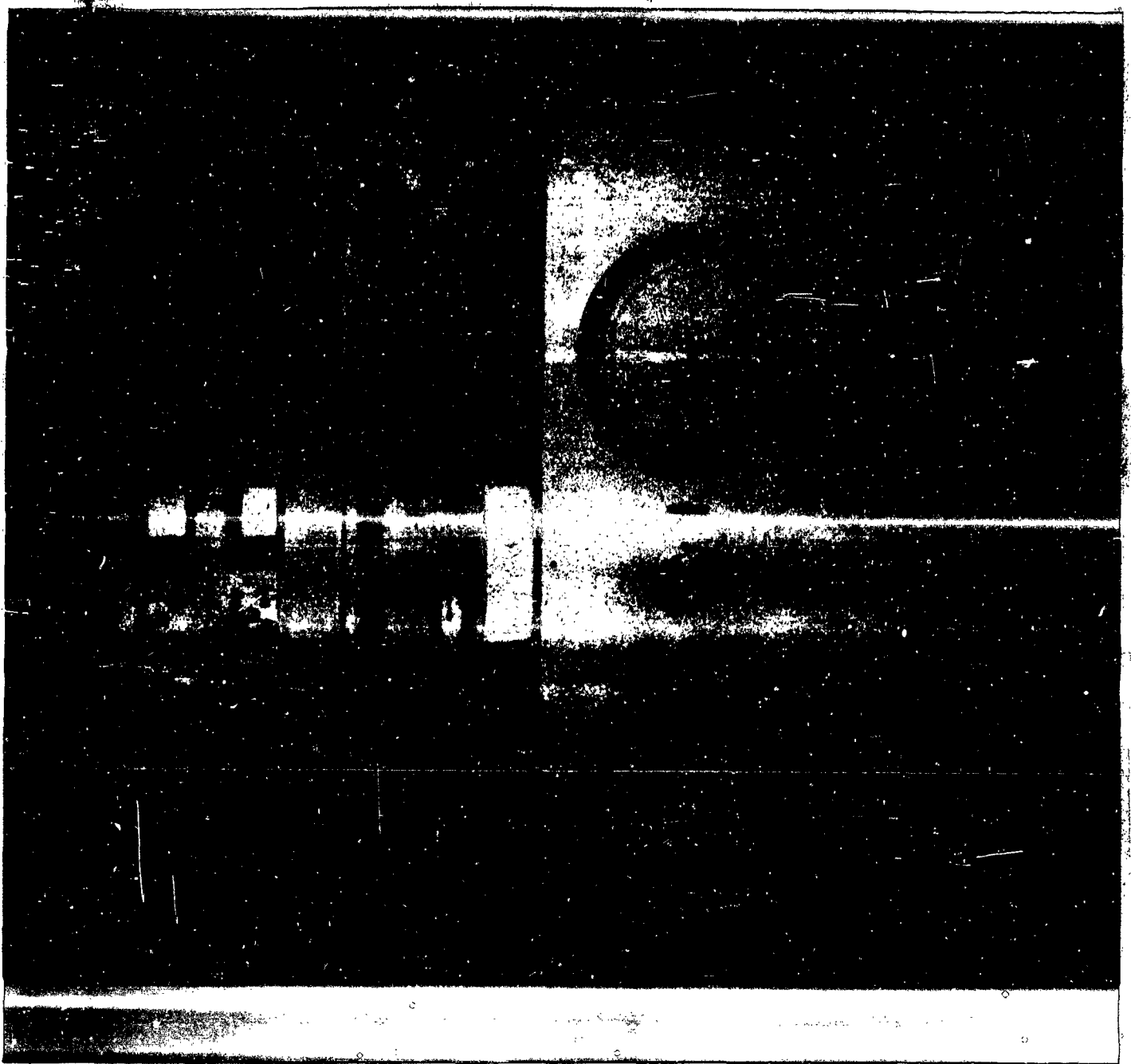
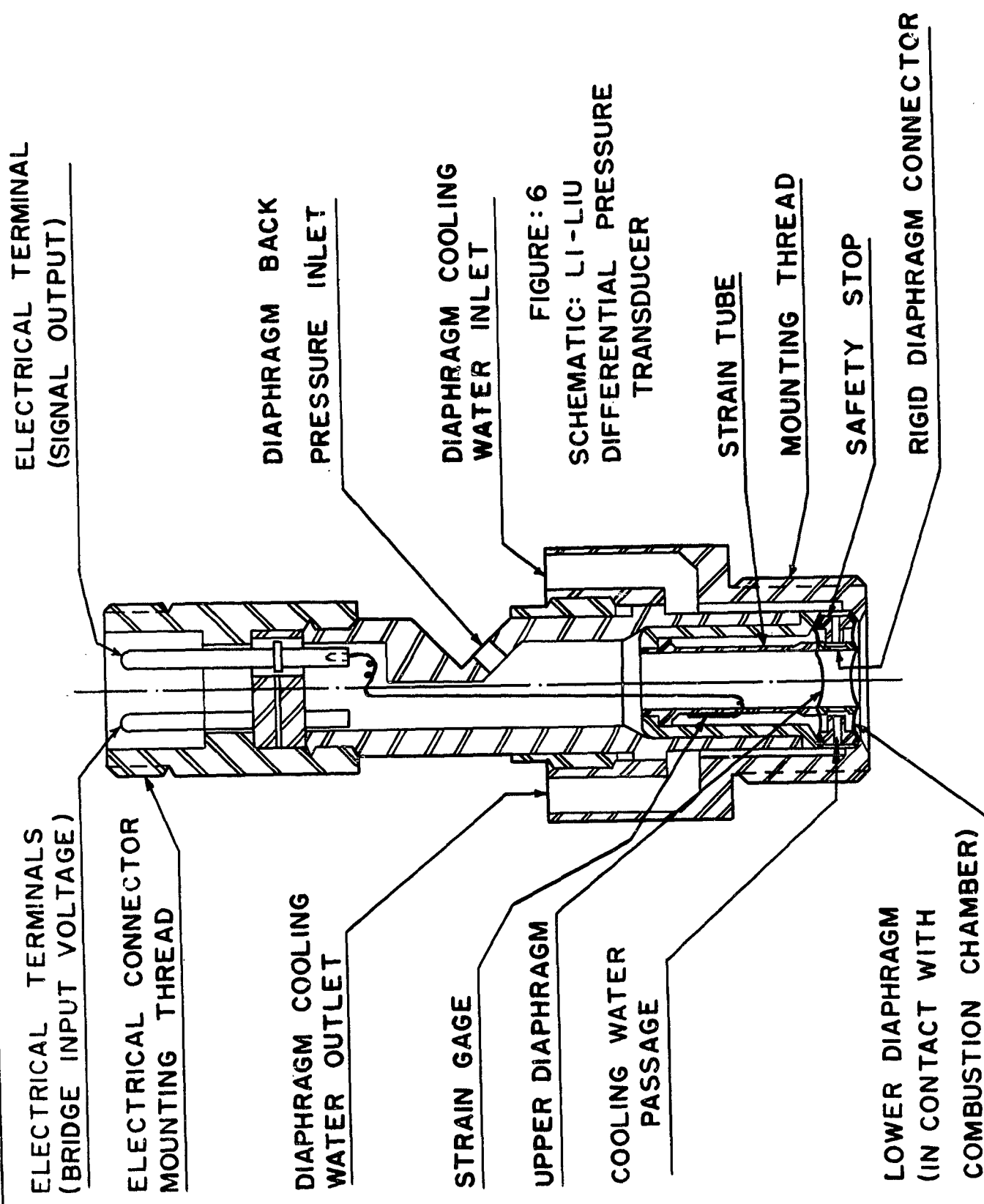


FIGURE 5
MONOPROPELLANT ROCKET CONTROL
PANELS



ELECTRICAL TERMINAL
(SIGNAL OUTPUT)

DIAPHRAGM BACK
PRESSURE INLET

DIAPHRAGM COOLING
WATER INLET

FIGURE: 6
SCHEMATIC: LI-LIU
DIFFERENTIAL PRESSURE
TRANSDUCER

STRAIN TUBE

MOUNTING THREAD

SAFETY STOP

RIGID DIAPHRAGM CONNECTOR

ELECTRICAL TERMINALS
(BRIDGE INPUT VOLTAGE)

ELECTRICAL CONNECTOR
MOUNTING THREAD

DIAPHRAGM COOLING
WATER OUTLET

STRAIN GAGE

UPPER DIAPHRAGM

COOLING WATER
PASSAGE

LOWER DIAPHRAGM
(IN CONTACT WITH
COMBUSTION CHAMBER)

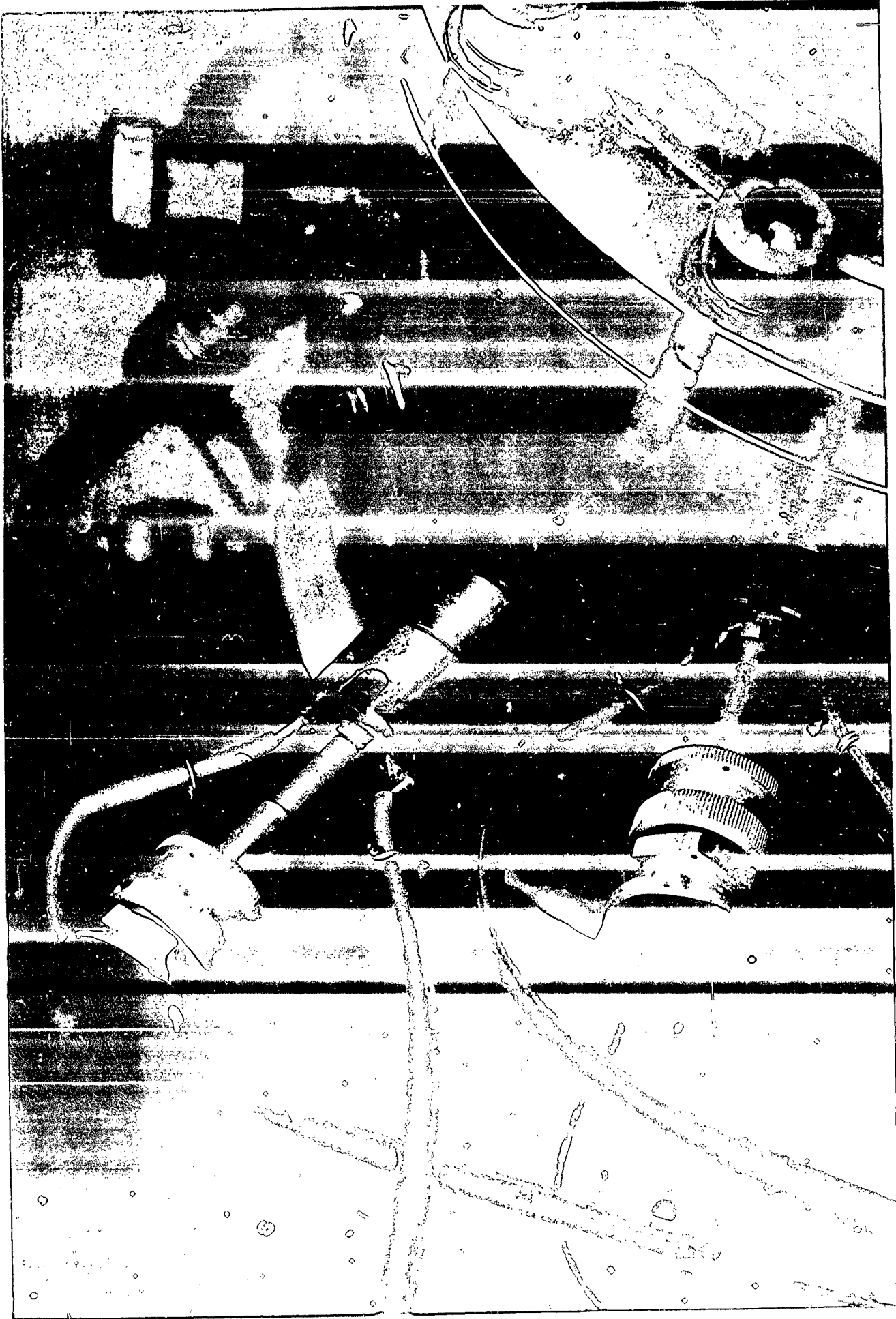


FIGURE 7
INSTALLATION OF TWO LI-LIU PICKUPS ON THE MONOPRO-
PELLANT ROCKET MOTOR

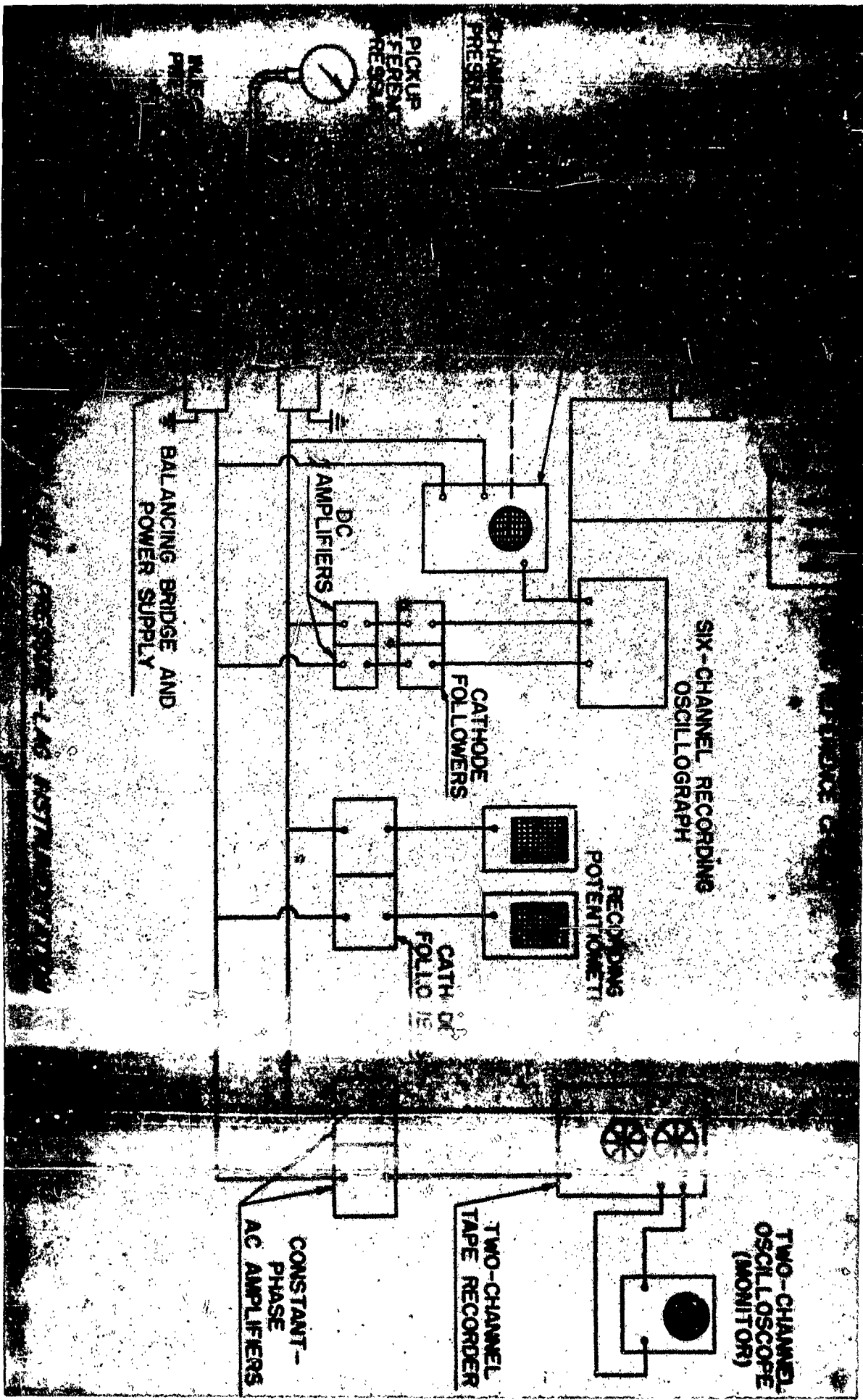


FIGURE 8 PRESSURE-LAG MEASURING SYSTEM

FIGURE 8

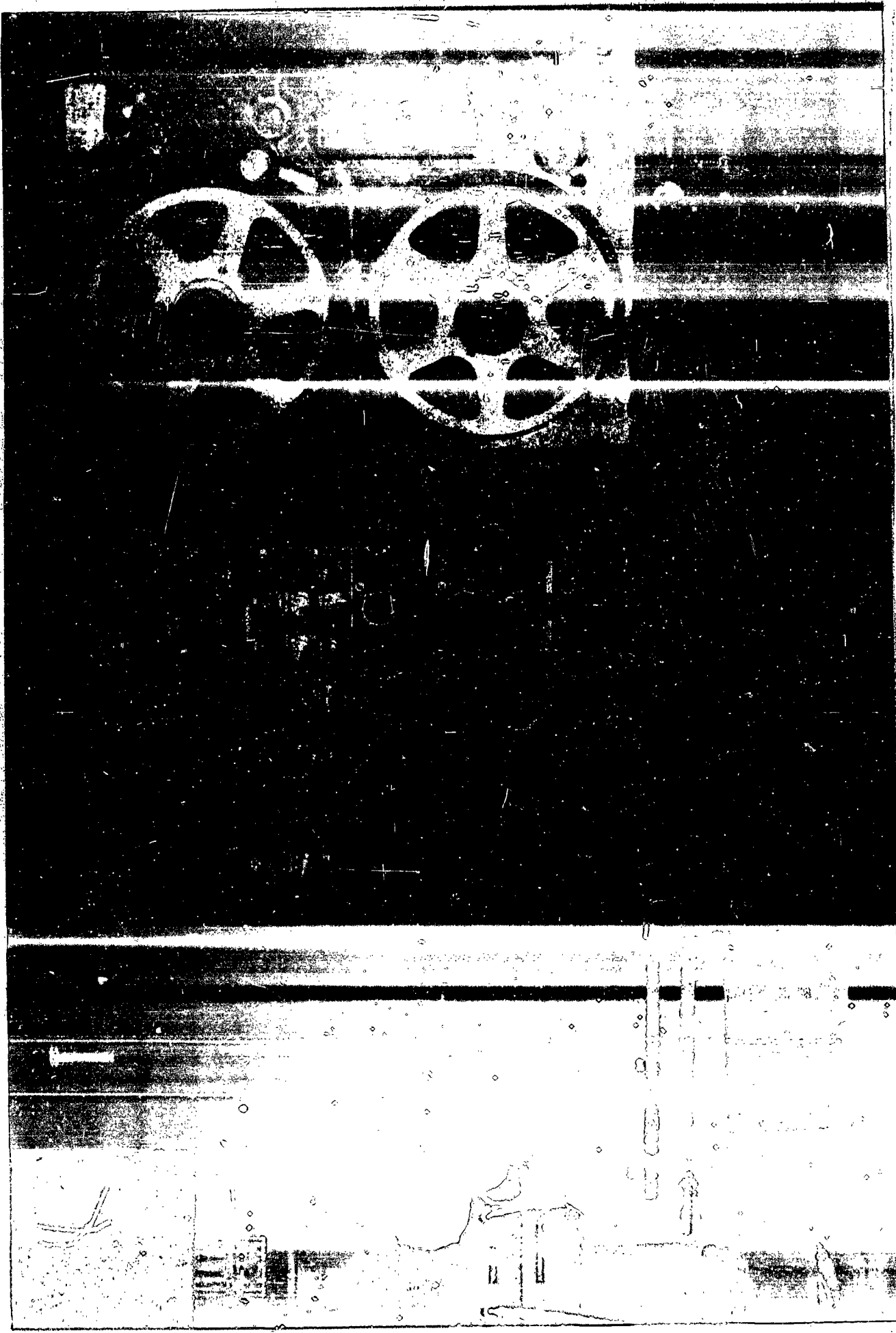


FIGURE 9
INSTRUMENT INSTALLATION

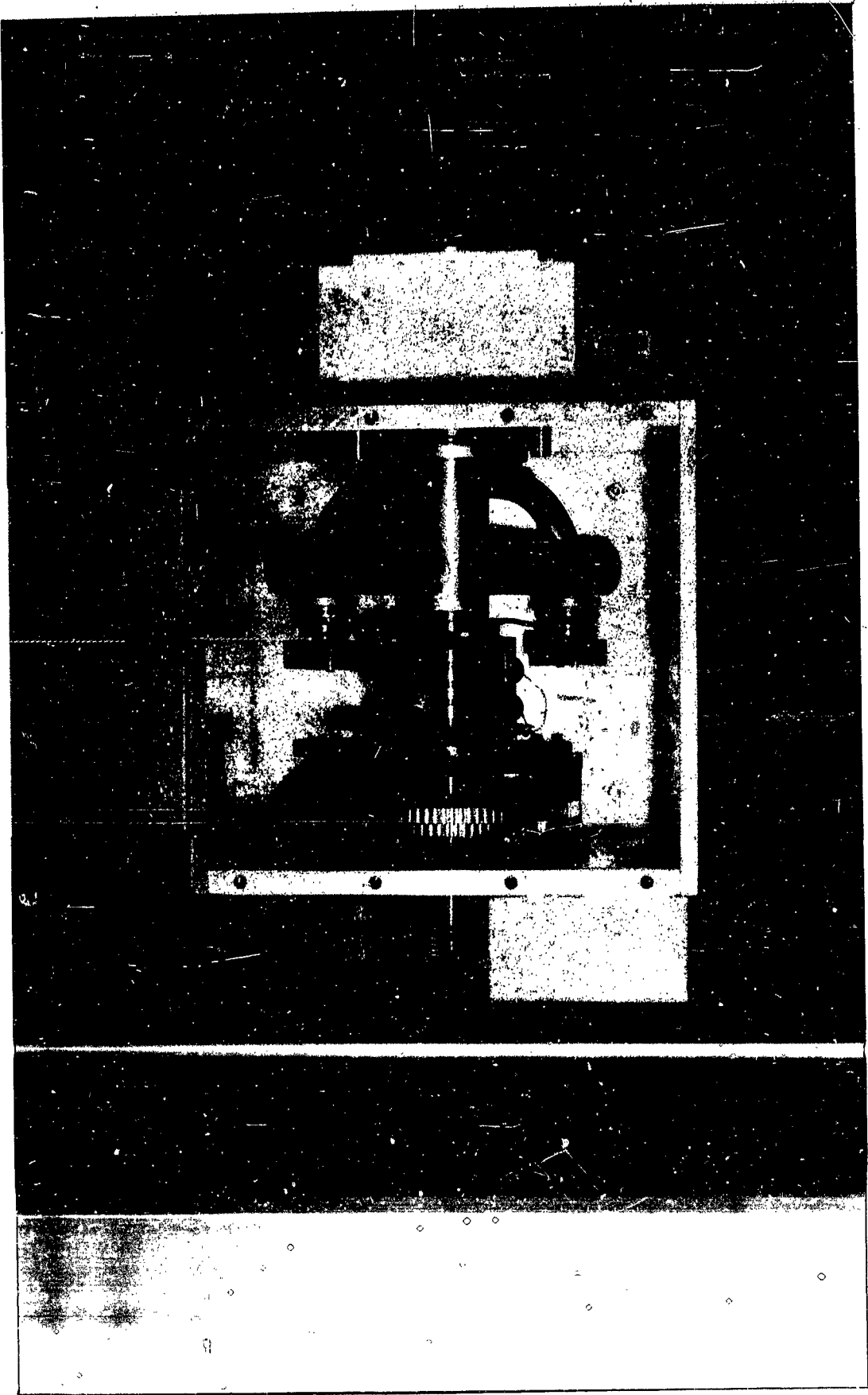


FIGURE 10
LI MASS FLOWMETER

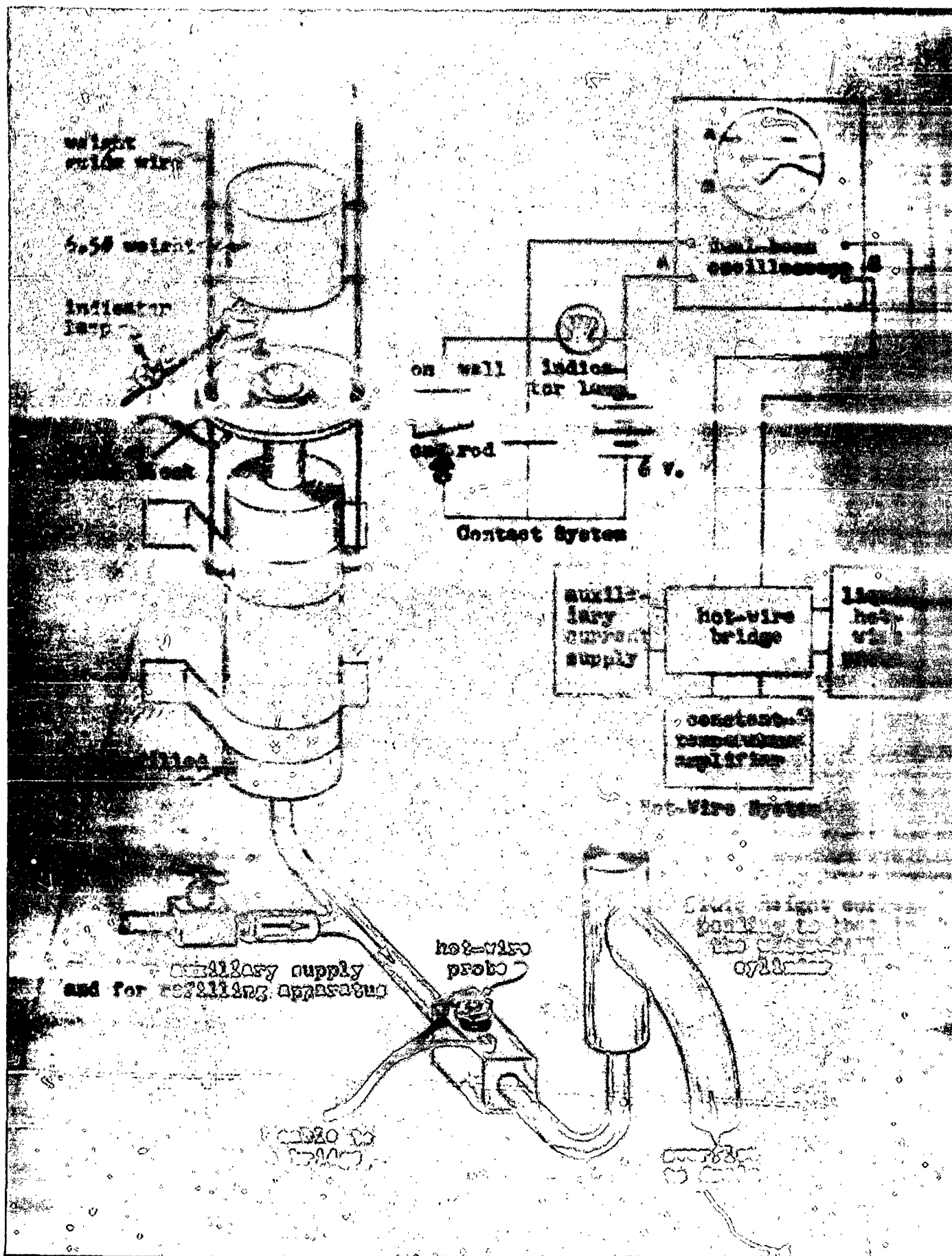


FIGURE 11
SCHEMATIC: HOT-WIRE PISTON-IMPULSE SYSTEM

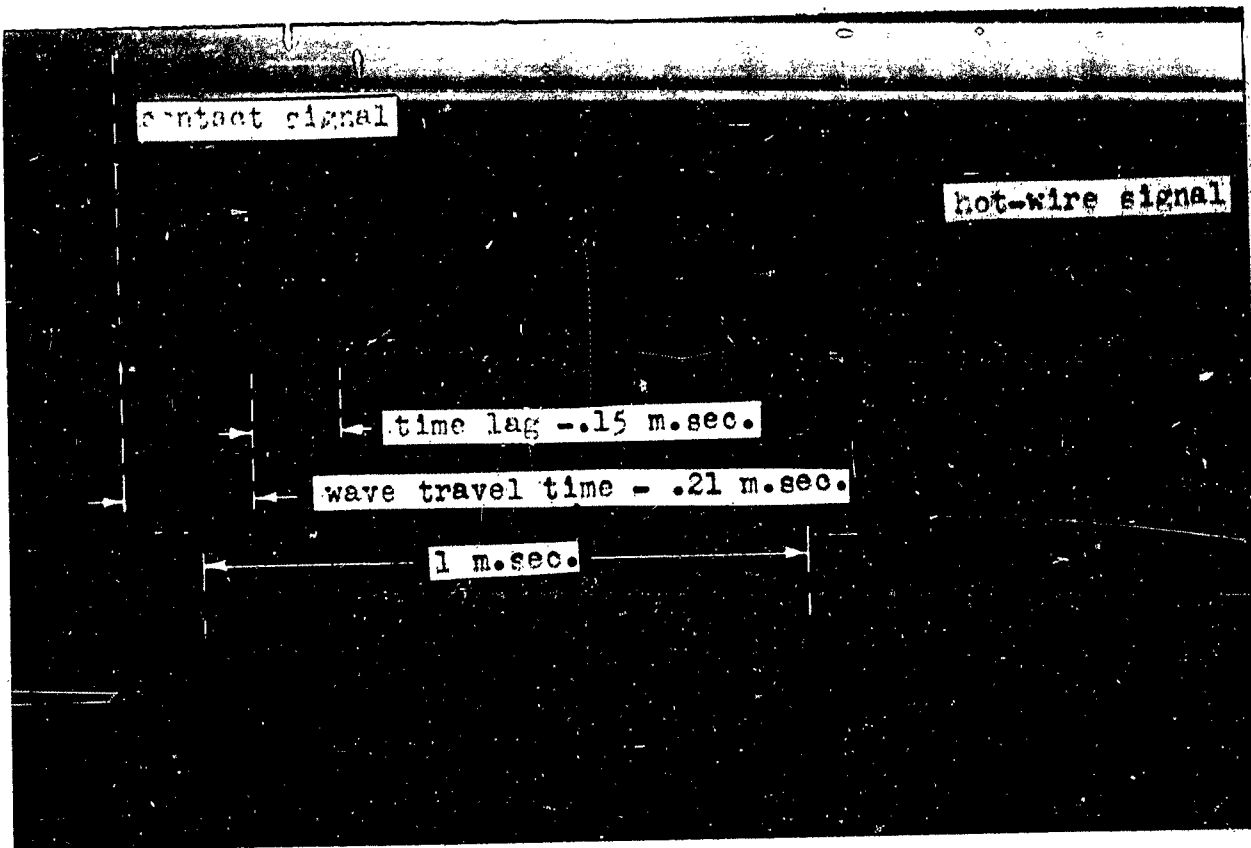


FIGURE 12A
HOT WIRE PISTON-IMPULSE TEST-STILL WATER

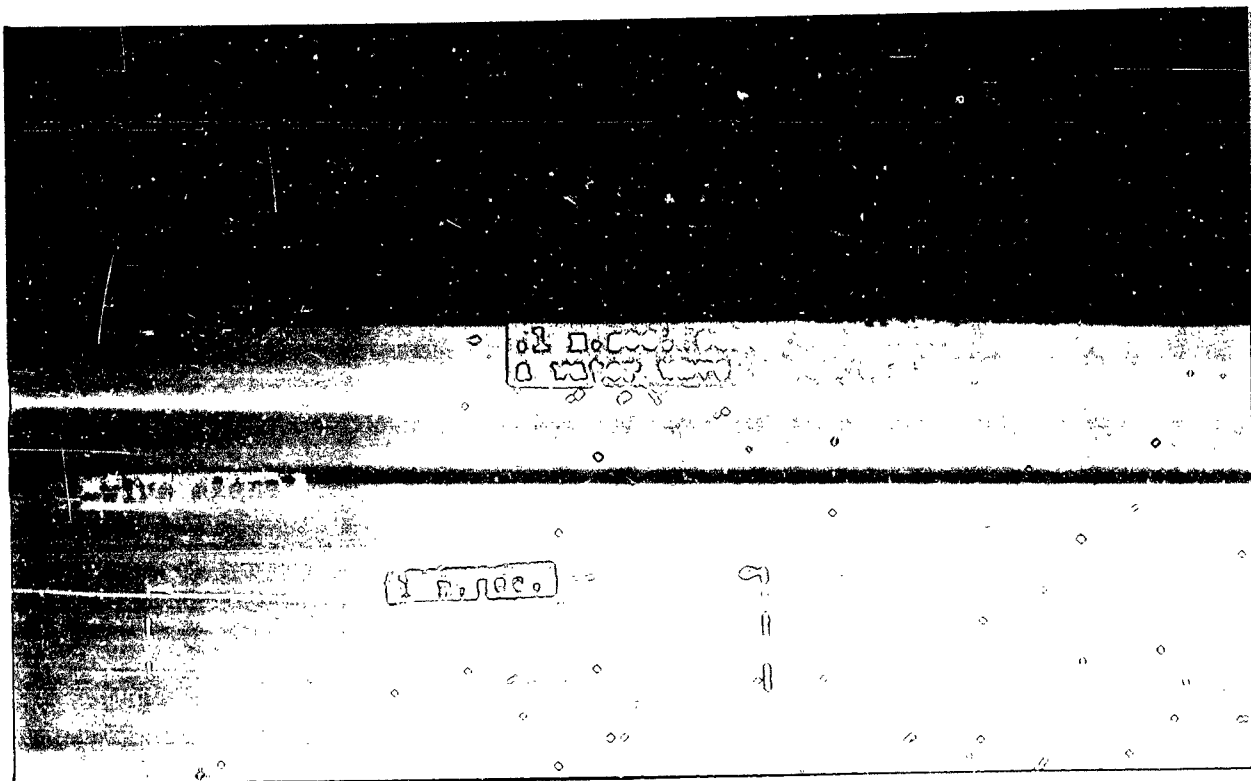


FIGURE 12B
HIGH AMPLITUDE HOT-WIRE TRACE SHOWING FINE DETAIL

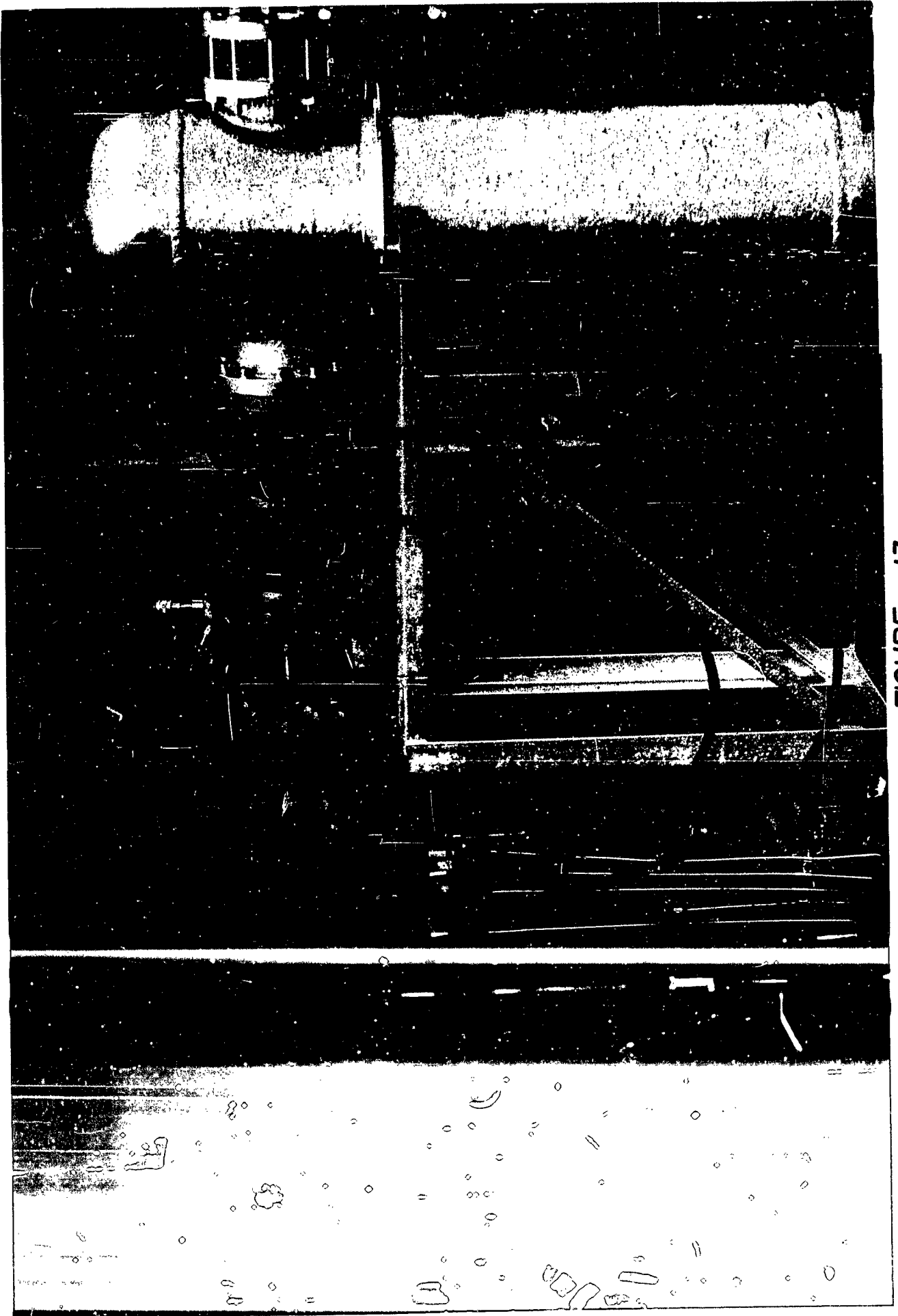


FIGURE 13
DYNAMIC FLOW CALIBRATION TEST RIG



FIGURE 14 A
TYPICAL OSCILLOSCOPE PRESSURE DATA WITH MONOPROPELLANT
FLOW MODULATION

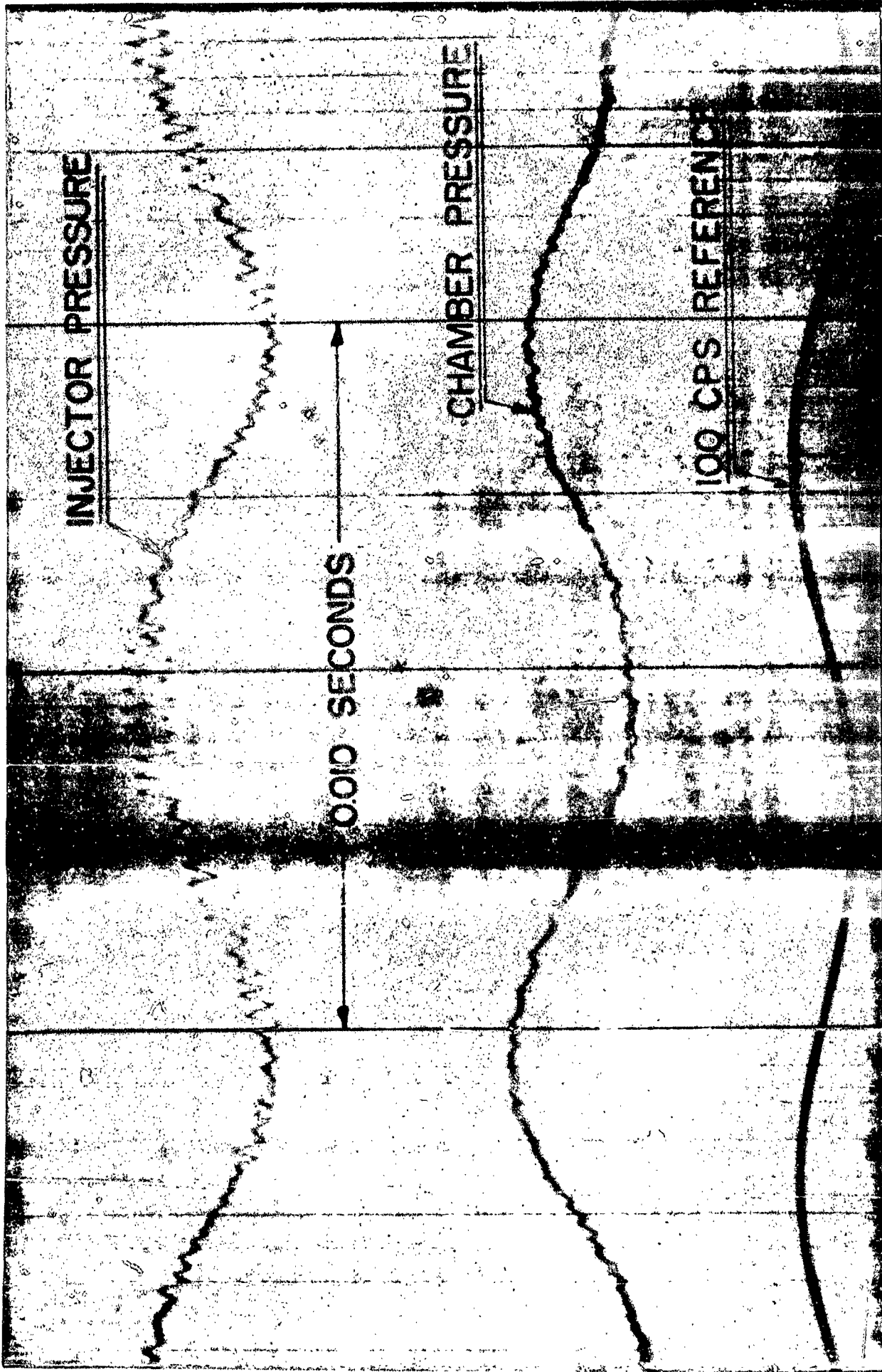
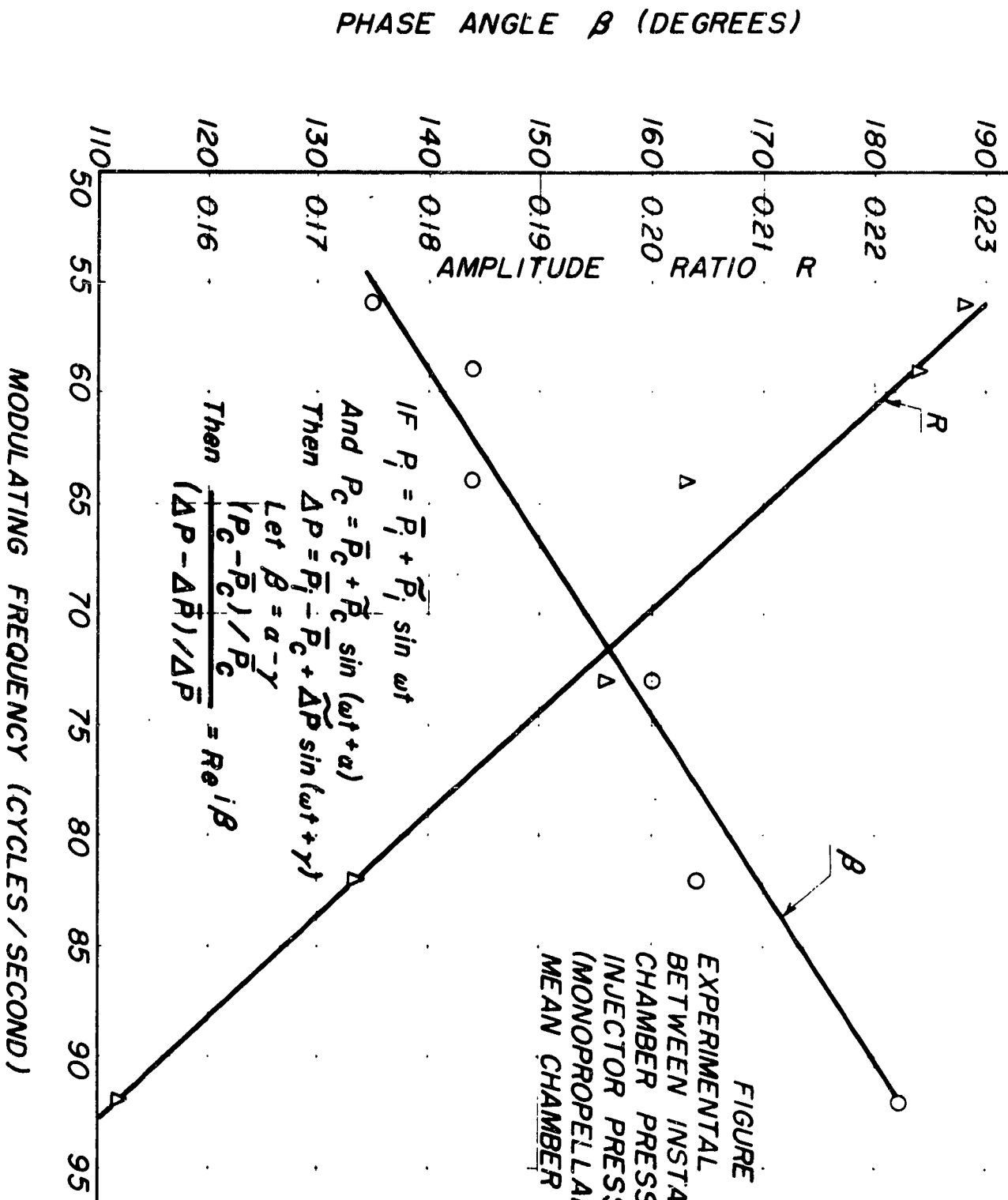


FIGURE 14 B
TYPICAL TAPE-RECORDED PRESSURE DATA WITH MONOPROPELLANT
FLOW MODULATION



IF $P_i = \bar{P}_i + \tilde{P}_i \sin \omega t$

And $P_c = \bar{P}_c + \tilde{P}_c \sin (\omega t + \alpha)$

Then $\Delta P = \bar{P}_i - \bar{P}_c + \Delta \tilde{P} \sin (\omega t + \gamma)$

Let $\beta = \alpha - \gamma$

Then $\frac{(P_c - \bar{P}_c) / \bar{P}_c}{(\Delta P - \Delta \bar{P}) / \Delta \bar{P}} = R e^{i\beta}$

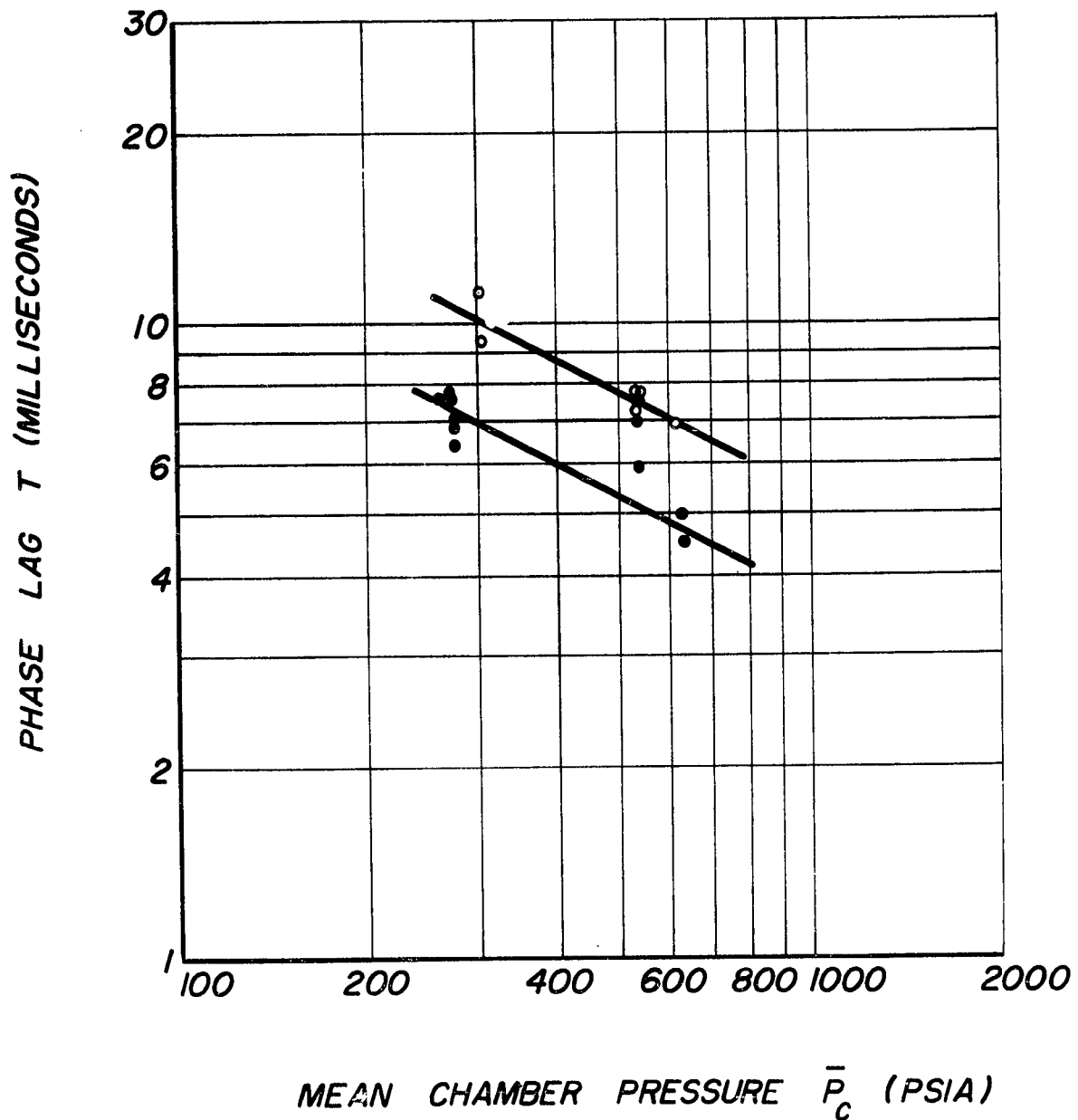
FIGURE 15:
 EXPERIMENTAL RELATION
 BETWEEN INSTANTANEOUS
 CHAMBER PRESSURE AND
 INJECTOR PRESSURE DROP
 (MONOPROPELLANT-CONSTANT
 MEAN CHAMBER PRESSURE)

FIGURE 16

EXPERIMENTAL PHASE DIFFERENCE BETWEEN INJECTOR
AND CHAMBER PRESSURE VS MEAN CHAMBER PRESSURE

● Frequency = approximately 100 cps

○ Frequency = approximately 50 cps



AD No. 36 005-C

ASTIA FILE COPY

APPENDIX C

DEVELOPMENT OF THE LI-LIU PRESSURE PICKUP

Development of the Li-Liu Pressure Pickup

INTRODUCTION

Experimental investigators are continually searching for new sensing devices to measure the elusive parameters of combustion processes. One of the most important of these variables is pressure, and a great number of pressure-sensing instruments have been developed especially for rocket testing.

Reliable pressure measurements are of particular importance in the study of unstable combustion, in which the phenomenon itself is identified by regular, generally extreme, fluctuations in combustion chamber pressure. Observation and recording of these oscillations requires a true dynamic response of the pressure-receiving element. This requirement involves several essential features which must be present in any pickup and implies other desirable qualities of such an instrument. The first requirement is that of an undistorted wave shape. That is, both amplitude and phase of the input pressure must be faithfully reproduced by the output signal. This, of course, calls for a high natural frequency of the pickup and suggests an output proportional to the applied pressure rather than to any of its time derivatives. The undesirability of distortion of the true signal immediately prohibits the use of any connecting tubes from the pressure source to the pickup or pressure receiver. The possible inaccuracies introduced by even very short connecting passages are thoroughly demonstrated by McCullough (1)¹ for the case of internal combustion engine cylinders. Hence, we may draw the logical conclusion

that an accurate pickup must be flush-mounted into the pressure source. For high temperature combustion research, flush-mounting demands the presence of some cooling facilities if the pickup is to be employed for any period of operation longer than a few seconds. In addition it is desirable that the pickup be of small size for convenience of installation and that it be of sufficiently rugged construction to withstand the severe vibrations of unstable rocket motor operation.

A short comparison of the interesting properties of several types of pickups was drawn up by Grey and is reproduced in Fig. 1 from a forthcoming article on pressure instruments (2). Of course, each of the types mentioned has its own advantages, and there may be individual situations where one style is clearly superior to all others. However, on the basis of existing information, the strain-gauge type pressure transducer was chosen as probably the most promising for all-around use in rocket engine research.

The particular model of this pickup herein discussed is the result of a cooperative design-development program between Y. T. Li of Massachusetts Institute of Technology and F. F. Liu of Princeton University. The pickup was intended for use at Princeton University as a primary sensing element in a study of liquid rocket combustion instability, directed by L. Crocco and sponsored by the U. S. Navy Bureau of Aeronautics. This pickup is the outgrowth of the early Li-Draper models (produced by Control Engineering Corporation) which featured a catenary-section diaphragm and air cooling. The advantages of the catenary diaphragm shape

1. Numbers in parentheses refer to references at the end of the manuscript.

over the flat diaphragm or the piston-spring type pressure indicators are clearly pointed out in a paper by Li and Draper (3). The successful performance of these pickups led to the design of a new model with increased sensitivity, improved cooling facilities, and integral safety features which has been named the Li-Liu pressure pickup. In addition to the discussion of this instrument which follows, a detailed analysis of its construction and method of operation appears in a recent paper by Li (4).

DESCRIPTION OF PICKUP

A photograph of the first of the Li-Liu pickups is shown in Fig. 2. Note the small size, simple electrical and pressure connections and rugged exterior construction. The threads for mounting the pickup are standard spark plug size, i.e., 18 mm. The construction details are better visualized in the cross-sectional drawing shown in Fig. 3. Pressure acts on the outer diaphragm, which is of catenary cross-section, and is transmitted through a spacer ring to the inner diaphragm. A strain-generating tube of .003-inch wall thickness presses upon this inner diaphragm; and this tube generates an output signal by changing the resistance of the strain gauge wires bonded to its surface. Since the tube is rigidly mounted to the body of the pickup at one end, the strain produced is proportional to the applied pressure. The electrical signal is led through a pressure-tight seal to three output terminals in the pickup cap, which is of the "Cannon plug" type.

As described in Reference 4, the strain gauges actually consist of two separate sets of windings. One set is wrapped circumferentially, while the others are longitudinal. This configuration performs two

useful functions. First, an application of pressure compresses the strain tube and increases its diameter slightly. This action increases the cross-section of the longitudinal windings and decreases that of the circumferential windings. The two resistance values are changed in opposite directions, doubling the unbalance between them and hence doubling the sensitivity of the pickup. Second, any change in temperature, or the existence of any slight temperature gradients, will change the dimensions of both sets of windings in the same direction, will act over approximately the same length of wire (if the spacing of the wires is carefully controlled), and will thus minimize the thermal sensitivity of the pickup.

In addition, each set of windings is double-wrapped to eliminate induction effects. That is, for each longitudinal strand wound from top to bottom, there is an adjacent one wound from bottom to top; and for each clockwise circumferential winding there is a neighboring counterclockwise one.

Provision has been made for applying a reference pressure to the inner diaphragm, producing an unbalance on the strain tube equal to the difference between absolute and reference pressures. Since this quantity can be made considerably smaller than the absolute pressure, the differential pickup sensitivity may be increased appreciably over that of the absolute pickup. An additional feature in the construction is the existence of a double-acting safety stop. This takes the form of a solid ring attached to the body of the pickup which floats freely between the edges of a notch machined in the periphery of the spacer ring. When either the applied pressure or the reference pressure reaches a value close to the elastic limit of operation of the strain tube or the diaphragms, the safety notch

presses against the safety-stop ring, and further deformation is possible only through bending of the ring-shaped cantilever beam thus formed. The details of this safety ring and of the force-transmitting spacer are more clearly shown in Fig. 13.

The cooling water inlet and outlet tubes are indicated in Fig. 3, but the description of the flow path and the cooling passage details will be left until later when some heat transfer performance data is presented.

Several troublesome mechanical problems arose during testing of the original models of the pickup. Reference pressure tubes were very fragile and repeatedly snapped during connection and disconnection of the back pressure supply. Also, the seal on the electrical output terminals was unsatisfactory. Although it performed the task of insulating the output from the pickup body, it failed to seal the terminals effectively from the high reference pressures employed. Hence a revised model of the pickup was manufactured with heavier reference pressure connections and Kovar-to-glass seals on the terminals. These modifications satisfactorily solved the difficulties, and the revised model is shown in Fig. 4.

One of the major advantages of strain gauge type pickups is the simple electrical circuit required to energize the sensing element as well as to transmit, interpret, and record the output signal. A schematic diagram of the circuit components appears in Fig. 5. Either AC or DC power source may be used to supply current to a simple 2-arm resistance bridge and to two of the terminals on the pressure pickup, whose strain gauges form the other two bridge arms. The output consists merely of an unbalance in the bridge and is therefore measured as the difference in potential between the center points of opposite sides of the bridge. In a DC system, this EMF may be recorded directly on a potentiometer or

observed on an oscilloscope as shown in the diagram. Of course, a variety of other recording and indicating instruments may be used, but the essential elements necessary for obtaining and transmitting a signal consists of batteries, precision resistors, and shielded two- and three-wire cables. The AC output circuit requires a carrier current whose amplitude or frequency may be modulated by the pickup output. The DC system is simpler to construct, but the AC output is considerably easier to amplify for recorders which demand a large driving signal.

EXPERIMENTAL INVESTIGATIONS

The tests conducted on the Li-Liu pickup were intended to evaluate its properties as well as to suggest additional developments. Consequently, the results will be grouped according to the particular properties they demonstrate rather than in the sequence in which they were conducted. As a guide for this presentation, the discussion will follow the approximate order appearing in the pickup comparison chart of Fig. 1.

First among these characteristics is frequency response. A high natural frequency is essential for any pickup designed to respond to the oscillations encountered in rocket motor combustion. Fig. 6 is a photographic record showing the natural frequency and damping ratio of the Li-Liu pickup. This is the result of a test performed at the Massachusetts Institute of Technology in which the pickup was flush-mounted in the wall of a shock tube. A shock wave was generated in the tube and allowed to pass over the exposed pickup diaphragm, approximating a step-function increase in pressure. The resulting change in output

was played onto an oscilloscope screen and photographed with a continuous strip camera having a film speed of 400 inches per second. For the case in which cooling water was flowing through the pickup (Fig. 6), the natural frequency was found to be approximately 20,000 cycles per second. A similar test without cooling water indicated a natural frequency of 28,000 cycles per second. The damping ratio observed is 0.10; hence the water-cooled pickup is capable of measuring pressure oscillations of frequencies up to about 5000 cycles per second with a dynamic error of less than 7 per cent.

A second property of obvious importance is output sensitivity. Here a strain-tube transducing element has distinct advantages; for the sensitivity can be controlled over a wide range by varying the length and cross-section of the strain wire or the length, diameter, and wall thickness of the strain tube. Of course, an increase in sensitivity can generally be obtained only at a sacrifice of some other desirable property. For example, if the strain tube is lengthened to allow for additional windings, the natural frequency of the pickup is correspondingly reduced. Or if the tube wall thickness is decreased, the allowable maximum load will be decreased. The final design chosen must therefore be a compromise of all these factors.

An output curve for a Li-Liu absolute pressure pickup is shown in Fig. 7. This pickup has a working pressure of 1200 p.s.i. and a rupture pressure of 3000 to 3500 p.s.i. without provision for the application of any reference pressure. Because of its relatively high working range, its sensitivity is lower than that of the differential pressure pickups tested. As exhibited by the curve, however, the output signal is still sufficiently large for easy recording, being approx-

imately 0.07 millivolts per p.s.i. The sensitivity of a differential pickup is observed from the output curve of Fig. 9 to be approximately 0.21 millivolts per p.s.i. In all the tests shown, the output was observed on a hand-balanced potentiometer with a combined resolution and reading error of ± 0.05 millivolts, while the applied pressure was indicated on a Heise gauge with a calibrated accuracy of ± 1 p.s.i. The standard input current chosen was 19.0 milliamperes which was produced by a DC battery source of approximately 70 volts. Note also on Fig. 7 the excellent linearity of output and the absence of noticeable hysteresis, two properties to be examined later.

A third very desirable characteristic of a pickup is thermal stability, that is, relative insensitivity to temperature changes in the medium surrounding the pickup. Three possible effects arise in consideration of this thermal drift problem. First of these is the expansion of the diaphragms and the consequent change of applied load on the strain tube, second is the change in strain wire resistance from increasing temperature and the consequent unbalance in the Wheatstone bridge circuit, and third is the change in output sensitivity as a result of the resistance change and the change in elastic modulus of the strain tube and wires with temperature. The relative freedom of a catenary diaphragm from thermal distortion at temperatures probably encountered in the presence of cooling water is pointed out in Reference 3, and the compensation of the strain tube windings for temperature unbalance has previously been discussed. In order to minimize the variation of output sensitivity the strain tube has been constructed of a stainless steel alloy with very little change in Young's modulus with temperature, and the strain wire material has been chosen on the basis of

the lowest possible thermal coefficient of resistivity consistent with acceptable elastic changes. The thermal drift tests performed thus far have given an indication of the combined effects of these three phenomena.

In these preliminary experiments, which were conducted at the Lewis Flight Propulsion Laboratory of the NACA at the request of Princeton University and the Bureau of Aeronautics, the pickup was mounted on a pressurizable adapter which was then inserted in the wall of an electric furnace. The furnace temperature was measured by an iron-constantan thermocouple recording on a Brown potentiometer, as was the temperature at a point on the boss into which the pickup was threaded. Applied pressure was observed on a commercial quality gauge with an estimated accuracy of ± 20 p.s.i., and pickup output was recorded on a precision Brown recording potentiometer with a reliable accuracy of approximately $\pm .25$ millivolts. Equilibrium temperatures were established in the furnace in all cases before pickup output was recorded, representing an elapsed time of ten to fifteen minutes exposure to elevated temperature at each point.

The results of these tests are exhibited in Fig. 8, where the variation of output with temperature is shown at several applied pressures.

The drift over a range of 500°F is approximately $2\frac{1}{2}\%$ in the curves shown, but the pressure inaccuracies are great enough to make this quantity somewhat unreliable. It is interesting to note the action of the pickup with 400 p.s.i. applied pressure at furnace temperatures above 500°F . There was a steady drop in output to a final value of 970°F , where it fell sharply to zero. Following this, the pickup was removed and checked for electrical continuity, whereupon it was found that one arm of the strain gauge bridge was broken. The boss temperature (with thermocouple about one inch from the pickup) indicated a temperature

increase from 76°F at start to 123°F when the furnace temperature reached 500°F. Above this, the boss temperature rose to a maximum of 184°F at a point where the rapid drop in output occurred. The actual pickup body temperature may have been appreciably higher than this value and may have melted a soft-soldered electrical connection.

Cooling water was flowing through the pickup during the entire test, and heat transfer rates of the order of 0.1 BTU per square inch per second were noted. Thus, the diaphragm temperature during the run probably varied only slightly; and the test constitutes primarily an examination of the output drift under long-time heating of the pickup body and strain tube. Thermal gradients undoubtedly existed within the pickup, particularly along the strain tube, in spite of the relatively long times involved; and these are practically impossible to oppose by compensating windings.

The next property investigated was linearity of output. Fig. 9 shows the results of a calibration test on an original model of the pickup with a linear range of slightly less than 200 p.s.i. This test was conducted with a differential pickup without applying a reference pressure. The action of the safety stops is clearly indicated at both ends of the linear range. However, there is no sharp change in curvature at these points to completely invalidate the signal if the applied pressure slightly exceeds the linear load. Although the output sensitivity of 0.21 millivolts per p.s.i. was more than adequate for the particular installation desired in the rocket test cell at Princeton, a linear range of 200 p.s.i. was considered insufficient; so later models of the pickup were constructed to extend this as much as possible. This was accomplished at the cost of a reduction of sensitivity, as may be seen in the calibration

curve of Fig. 10. Here the output signal is approximately 0.13 millivolts per p.s.i., which is still appreciably greater than that of the absolute pickup previously discussed. Note the excellent linearity of response exhibited over a much wider range of differential pressure, in this case slightly over 600 p.s.i. Again the test was conducted without applying reference pressure to the inner diaphragm.

The cycling of pressure in the calibration tests shown thus far illustrate the next important property to be discussed, namely hysteresis. A late model differential pressure pickup was tested by applying 400 p.s.i. steady reference pressure and varying the pressure on the outer diaphragm through two complete increasing-decreasing cycles. The results appear in Fig. 11, where an obvious hysteresis effect is seen. The maximum variation between rising and falling pressure curves was about 20 p.s.i., definitely an unacceptable amount in an average reading of 200 to 400 p.s.i. This inelastic behavior was thought to be the result of inaccurate forming of the diaphragms over the force-transmitting spacer ring connecting them, and Li suggested the application of an over-pressure of about 2500 p.s.i. to both diaphragms simultaneously to stretch them into a closer fit at the points of tangency to the spacer ring. This was done and was followed by an application of a slight over-pressure (1650 p.s.i.) to the outer diaphragm alone to re-seat the diaphragm assembly onto the strain tube. The resulting calibration test is shown in Fig. 12. Here three complete cycles of increasing and decreasing pressure were applied (again with 400 p.s.i. steady reference pressure) without observing any hysteresis effects within the experimental accuracy previously indicated. Comparison of the curves of Figs. 11 and 12 indicates that the application of overpressure

shifted the zero output point slightly but did not change the strain tube sensitivity, hence the treatment was considered satisfactory.

Of considerable significance in rocket applications is the response of a pressure pickup to noise, vibration, and acceleration. The errors introduced by such response are thoroughly discussed by Li and Draper in Reference 3, where the advantages of catenary-shaped diaphragms are treated analytically. The preliminary tests conducted to date to evaluate this relative insensitivity to non-pressure perturbations are purely qualitative, but they give evidence of excellent performance in this respect.

A perfunctory check of these effects consisted of mounting a pickup firmly to the exterior of a rocket motor where it would be exposed to the complete spectrum of small vibrations, non-linear and irregular accelerations, and the wide range of acoustical disturbances usually associated with rocket combustion. An oscillograph record of the output under these conditions showed a response of the order of that produced by a pressure of 1 to 2 p.s.i.

Additional checks on vibration, noise, and acceleration effects were conducted at the request of Princeton University at Bell Aircraft Corporation, where in one test acoustic disturbances of unknown amplitude up to frequencies of 20,000 cycles per second were produced by a high-powered speaker and directed against the pickup body without noticeable change in output. Following this, the pickup (with cooling water flowing through it) was mounted on a vibration table where harmonic oscillations of sufficient amplitude to produce 10 g's acceleration were applied to it at frequencies ranging up to 2,000 cycles per second. Again no response was observable on the instrument used to indicate output. Two such tests

were performed with the axis of the pickup both parallel and perpendicular to the vibration direction. A third check was carried out by placing the pickup on a centrifuge with its axis in the radial direction. Here steady accelerations were produced up to a maximum of 28 g's, and again no noticeable output changes occurred. During these centrifugal tests, however, no cooling water was flowed through the pickup, suggesting additional checks that would be desirable.

Perhaps the greatest single advantage of the double-diaphragm configuration is the ease with which the pressure-sensing element may be cooled. The space between the two diaphragms offers an ideal passage for water or other coolants. The details of this construction are shown in Fig. 13, where arrows indicate the path of cooling water from inlet to outlet tubes. The water flows down a milled slot in the inlet side of the pickup body, expands into a semi-annular cavity, passes through holes in the safety stop and spacer ring, flows between the diaphragms, and exits by a similar course on the outlet side. Note that there are actually two possible paths for the water through this space between the diaphragms, since the safety stop has two separate sets of holes cut in it. One set of three radial holes leads the water directly into the interior area surrounded by the spacer ring, and similar holes in the diametrically-opposite side of the spacer ring-safety stop assembly lead the water out. The second set of holes (appearing as hidden lines in Fig. 13) directs the water through the safety stop and downward at a slight angle into the annular region between the diaphragms and outside the periphery of the spacer ring, furnishing cooling water for this exterior area. Again similar holes appear as exit passages on the opposite side of the pickup.

The actual effectiveness of this design is illustrated by the experimental heat transfer performance curves in Figs. 14 and 15. The first of these represents a stable test run on a small scale uncooled acid-hydrocarbon rocket motor and the second an unstable, or "screaming" run on the same motor. These tests were conducted at the Lewis Flight Propulsion Laboratory of the NACA at the request of Princeton University, and a "dummy" pickup, i.e., a pickup with all components present except the actual wire-wound strain tube, was mounted at the nozzle end of the combustion chamber. The pickup was undamaged in both tests, although the motor wall burned out under screaming conditions. Since the runs ended at the point where all three quantities change abruptly, one may conclude that steady-state heat transfer conditions were never reached. The figures show some interesting factors. The water temperature rise increases throughout the running time, and the water flow rate for a constant pressure drop decreases during this same time. The decrease in flow rate suggests a decrease in liquid coolant passage cross-section, possibly due to surface boiling on the outer diaphragm. The very sharp drop in flow observed in the screaming run bears out this conclusion, since the heat transfer rate also increases sharply without an appreciable change in flame temperature, a characteristic of the incidence of boiling heat transfer.

The maximum values of heat transfer rate in each case are significant. For the normal run, this value is 2.3 BTU per square inch per second, while for the screaming run it is 3.4 BTU per square inch per second. These two figures are based on the total exposed area of the face of the pickup, including the annular area of the support and threads. If the calculations are based on the area of the 7/16 inch diameter diaphragm alone, the heat transfer rates for non-screaming and screaming become 5.2 and 7.6 BTU per

square inch per second respectively. The true rates undoubtedly lie somewhere between these two pairs of values. It is noteworthy that the 0.004-inch thick diaphragm withstood the temperatures and pressures existing under such conditions without apparant damage, since these heat transfer rates are above those normally encountered in existing motors. Some later tests indicate that the pickup will respond without difficulty to oscillations in pressure up to 5000 cycles per second even at screaming motor conditions. However, the effects of thermal shock and fluctuating temperatures on the output must be carefully checked before the pickup can be used for accurate quantitative measurements.

CONCLUSIONS

The investigations reported herein were carried out as one phase of a study of liquid rocket combustion instability under the sponsorship of the U.S. Navy Bureau of Aeronautics. A development and test program was conducted by Princeton University in cooperation with the Massachusetts Institute of Technology, the National Advisory Committee for Aeronautics, and the Bell Aircraft Corporation. Although a great deal of information about the performance of the Li-Liu pickup has been obtained, the evaluation tests are not yet complete. Before the instrument becomes commercially available, it is necessary to continue the test program to determine such factors as response to high-amplitude vibrations, acceleration sensitivity with static and flowing cooling water, effects of oscillating temperatures on heat transfer rates and pickup output, and reliability and repeatability of calibrations.

However, on the basis of results obtained to date the pickup appears quite promising. Frequency response is acceptably high; cooling facilities are adequate; hysteresis, noise sensitivity, and steady-state thermal drift are insignificant; and sensitivity and range of linear output are more than sufficient. These properties, plus the small size, rugged construction, and simple electrical circuit, make the Li-Liu pickup an excellent instrument for the measurement of pressures in rockets, ramjets, turbojets, internal combustion engines, or any other application involving high rates of energy release.

References

1. McCullough, J. D., "Engine Cylinder-Pressure Measurement", Presented at the Annual Meeting of the Society for Automotive Engineers, Detroit, Michigan, January 12-16, 1953 - Reproduced by the Ethyl Corporation Research & Engineering Department, Detroit, Michigan.
2. Grey, J., "Pressure Transducers", unpublished article soon to appear in "Product Engineering" magazine, (McGraw-Hill Publishing Co.)
3. Li, Y. T. and Draper, C. S., "A New High-Performance Engine Indicator of the Strain-Gauge Type", Journal of the Aeronautical Sciences, Vol. 16, No. 10, October, 1949.
4. Li, Y. T., "Dynamic Pressure Measuring Systems for Jet Propulsion Research", Journal of the American Rocket Society, Vol. 23, No. 3, May-June, 1953.

List of Figures

1. Comparison of Pickup Characteristics
2. Li-Liu Differential Pressure Pickup (Original Model)
3. Sectional View of a Water-Cooled Differential Pressure Indicator
4. Li-Liu Differential Pressure Pickup (Revised Model)◊
5. Schematic Diagram of Pressure Measuring System
6. Pickup Frequency Response
7. Calibration Test of Absolute Pressure Pickup No. 4
8. Thermal Drift of Li-Liu Pickup No. 9
9. Calibration Test of Pressure Pickup No. 3
10. Calibration Test of Li-Liu Differential Pressure Pickup No. 11
11. Cycling Check of Li-Liu Differential Pickup No. 12
(Before Application of Overpressure)
12. Cycling Hysteresis Check of Li-Liu Differential Pressure Pickup No. 12
(After Application of Overpressure)
13. Schematic Diagram of a Catenary Diaphragm Water-Cooled Pressure
Receiving Element
14. Heat Transfer to Li-Liu Dummy Pressure Pickup (Non-Screaming)
15. Heat Transfer to Li-Liu Dummy Pressure Pickup (Screaming)

COMPARISON OF PICKUP CHARACTERISTICS

	STRAIN GAGE	CAPACITANCE	CRYSTAL	RELUCTANCE
FREQUENCY RESPONSE	Up to 40,000 cps.	Some claims up to 500,000 cps. Author's experience: up to 20,000 cps.	Up to 1,000,000 cps.	Approx. 1,000 cps.
SENSITIVITY	About 1/2% of full-scale.	Less than 1% of full-scale.	Less than 1/2% of full-scale.	Less than 1% of full-scale.
THERMAL STABILITY	Excellent for compensated bridge winding.	Temperature drift: approx. .025% per °F.	Poor; temperature drift up to 50% per °F.	Approx. .02% per °F.
LINEARITY	Less than 1%.	About 1%.	Less than 1/2%.	About 1%.
RESPONSE TO VIBRATION, NOISE, ACCELERATION	Negligible for light-diaphragm and fully-rigid types.	Low, but noticeable.	Appreciable, also highly sensitive to electrical "noise".	Low, but noticeable about 1% per 100 G.
HYSTERESIS	Approx. 0.2%.	Low (less than 1%).	Negligible.	Less than 0.5%.
COOLING	Some designs have air or water cooling (special types have heat-transfer rates up to about 7 Btu/in ² /sec.)	Some designs water-cooled. (Special types have heat-transfer rates up to about 4 Btu/in ² /sec.)	Generally none possible.	Generally none possible.

Figure 1

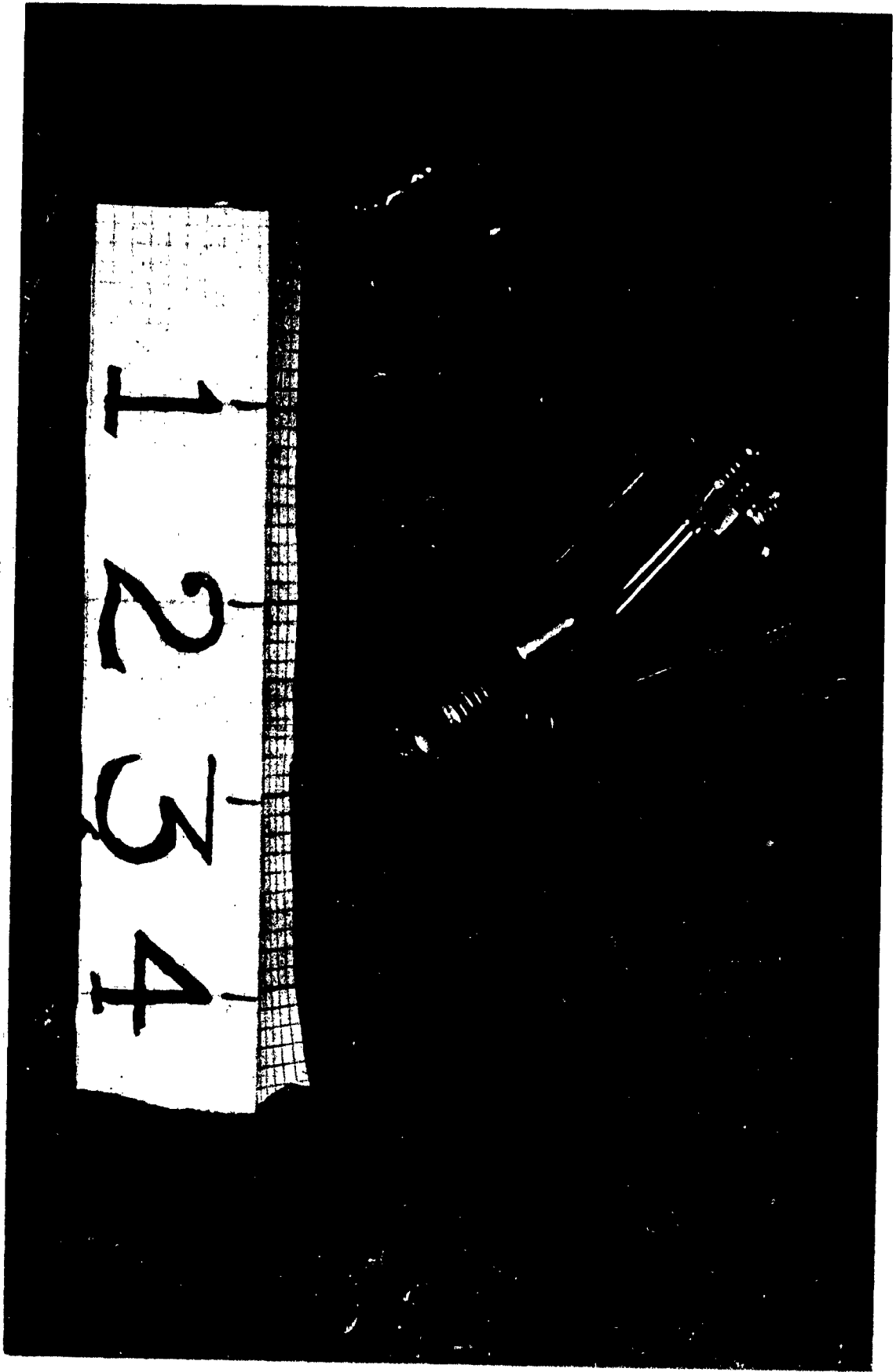


Figure 2

ELECTRICAL TERMINAL
(SIGNAL OUTPUT)

ELECTRICAL TERMINALS
(BRIDGE INPUT VOLTAGE)

ELECTRICAL CONNECTOR
MOUNTING THREAD

DIAPHRAGM BACK
PRESSURE INLET

DIAPHRAGM COOLING
WATER OUTLET

STRAIN GAGE

DIAPHRAGM COOLING
WATER INLET

UPPER DIAPHRAGM

COOLING WATER
PASSAGE

FIGURE:3
SCHEMATIC: LI-LIU
DIFFERENTIAL PRESSURE
TRANSDUCER

STRAIN TUBE

MOUNTING THREAD

SAFETY STOP

LOWER DIAPHRAGM
(IN CONTACT WITH
COMBUSTION CHAMBER)

RIGID DIAPHRAGM CONNECTOR

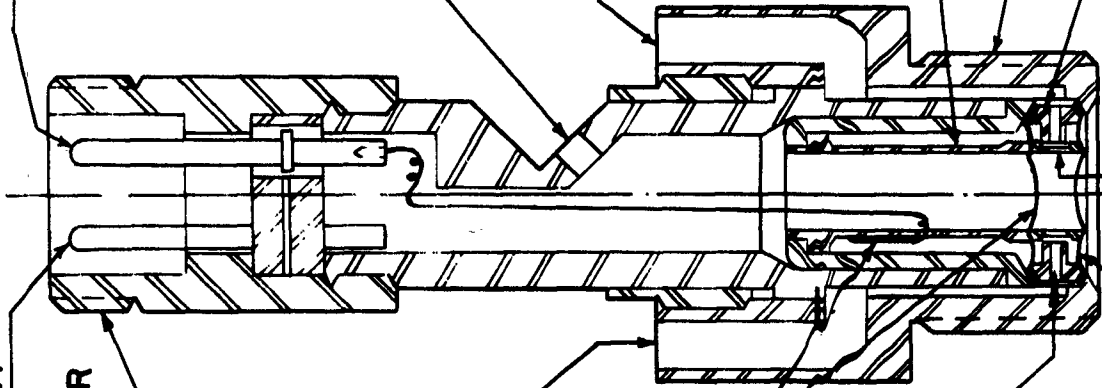
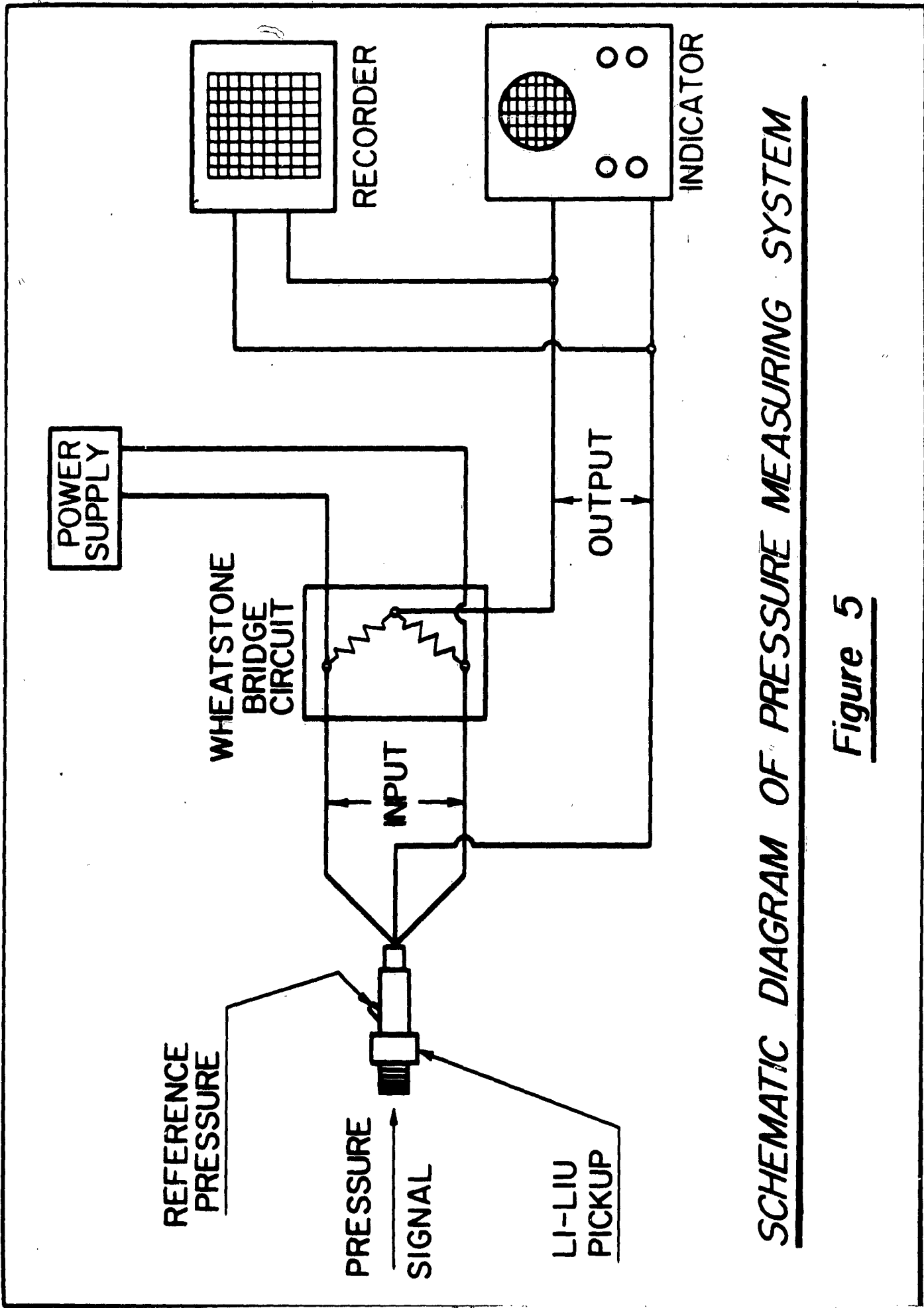




Figure 4



SCHEMATIC DIAGRAM OF PRESSURE MEASURING SYSTEM

Figure 5

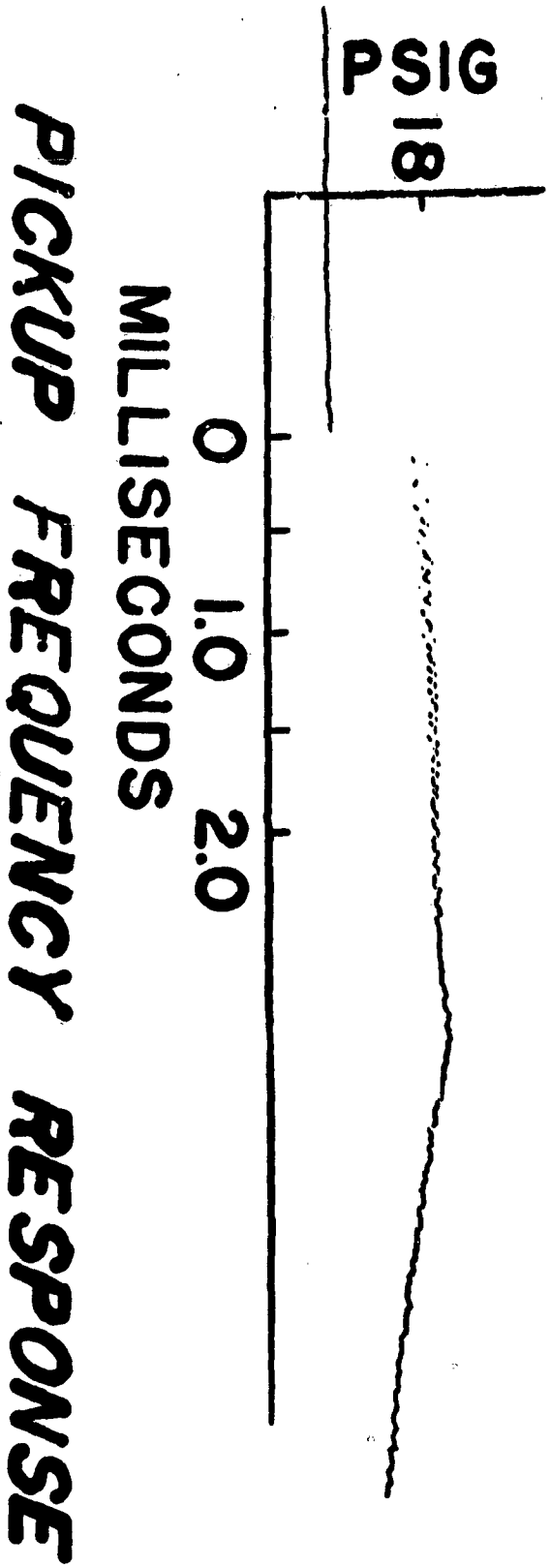


Figure 6

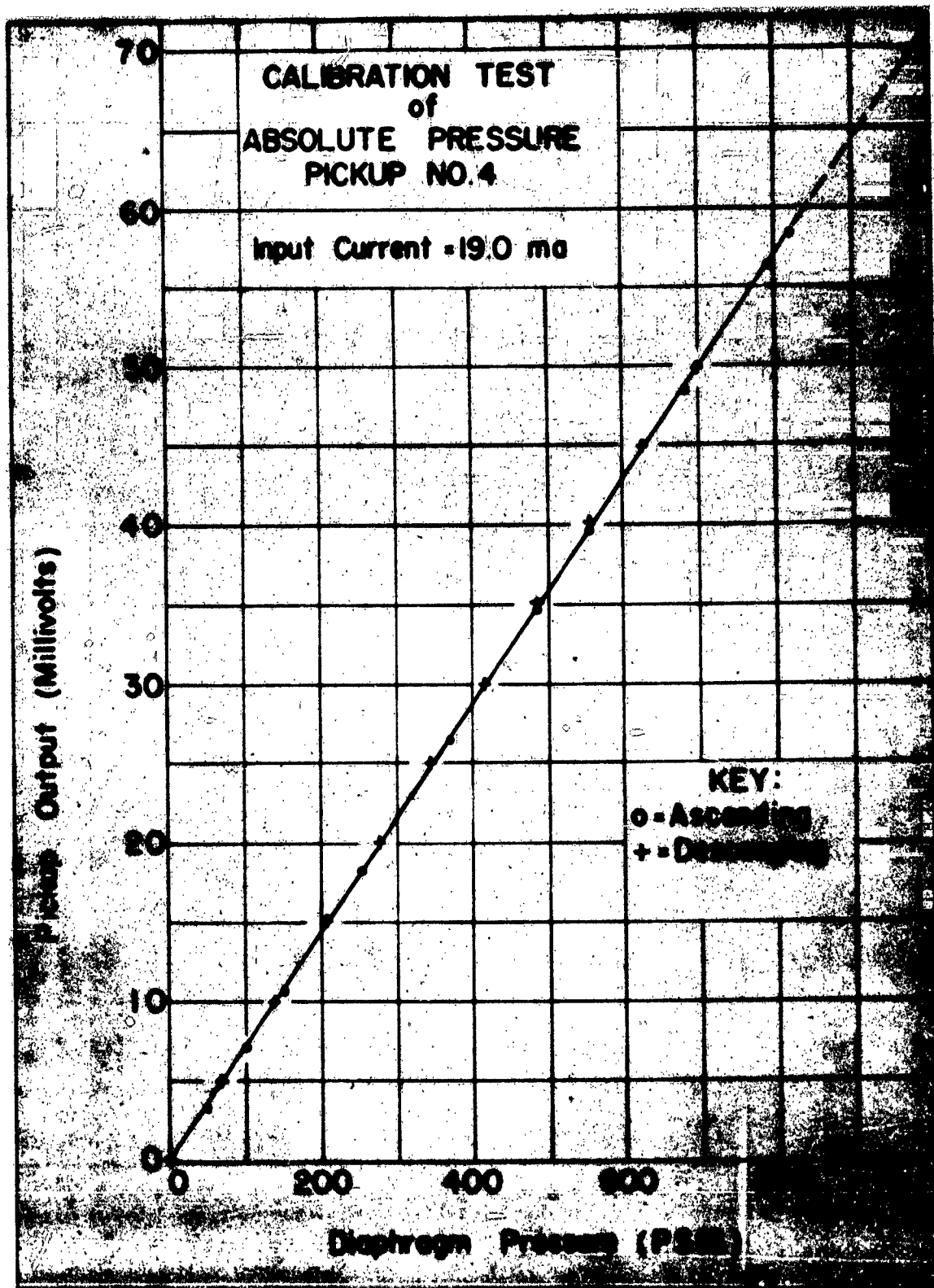
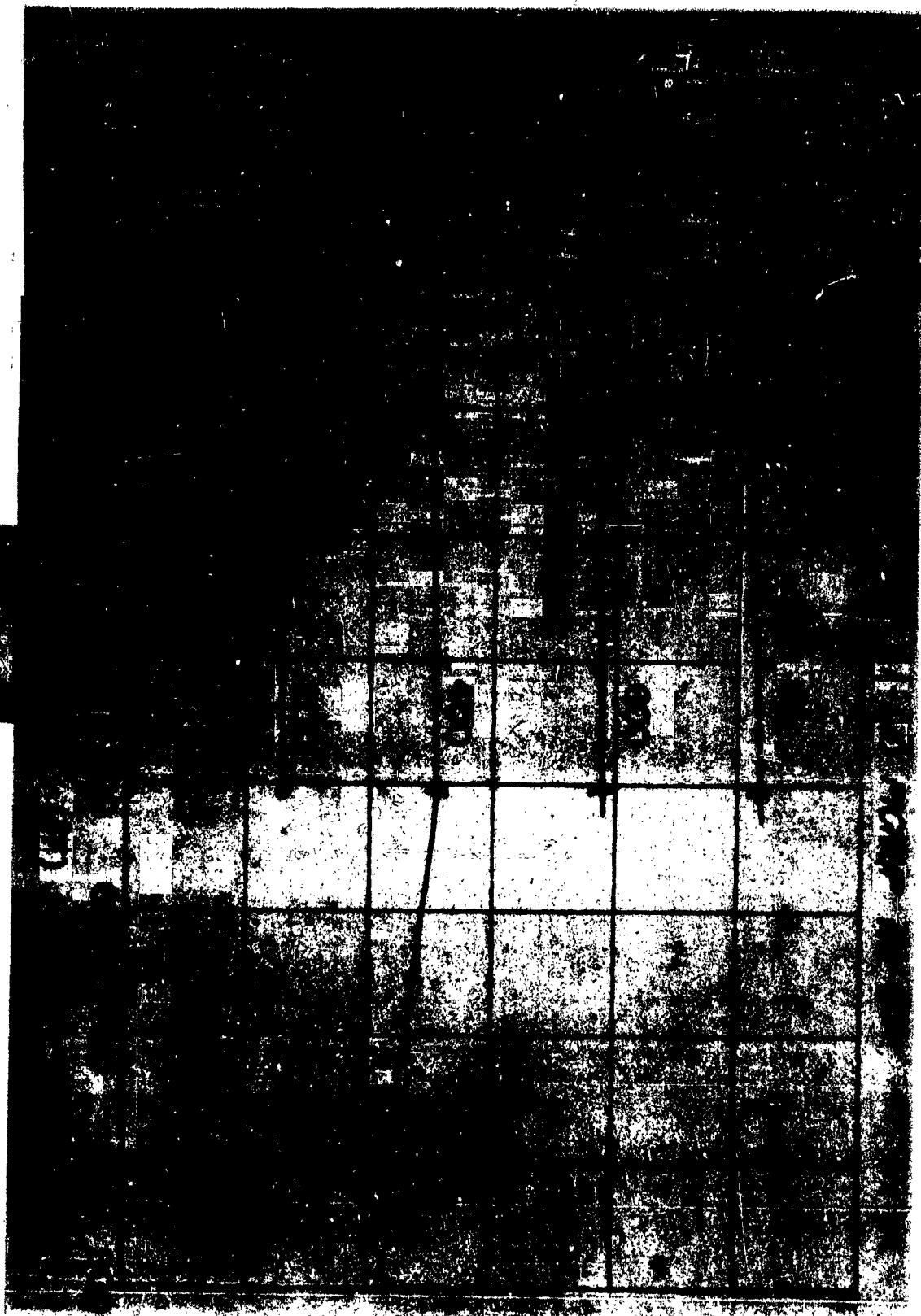


Figure 7



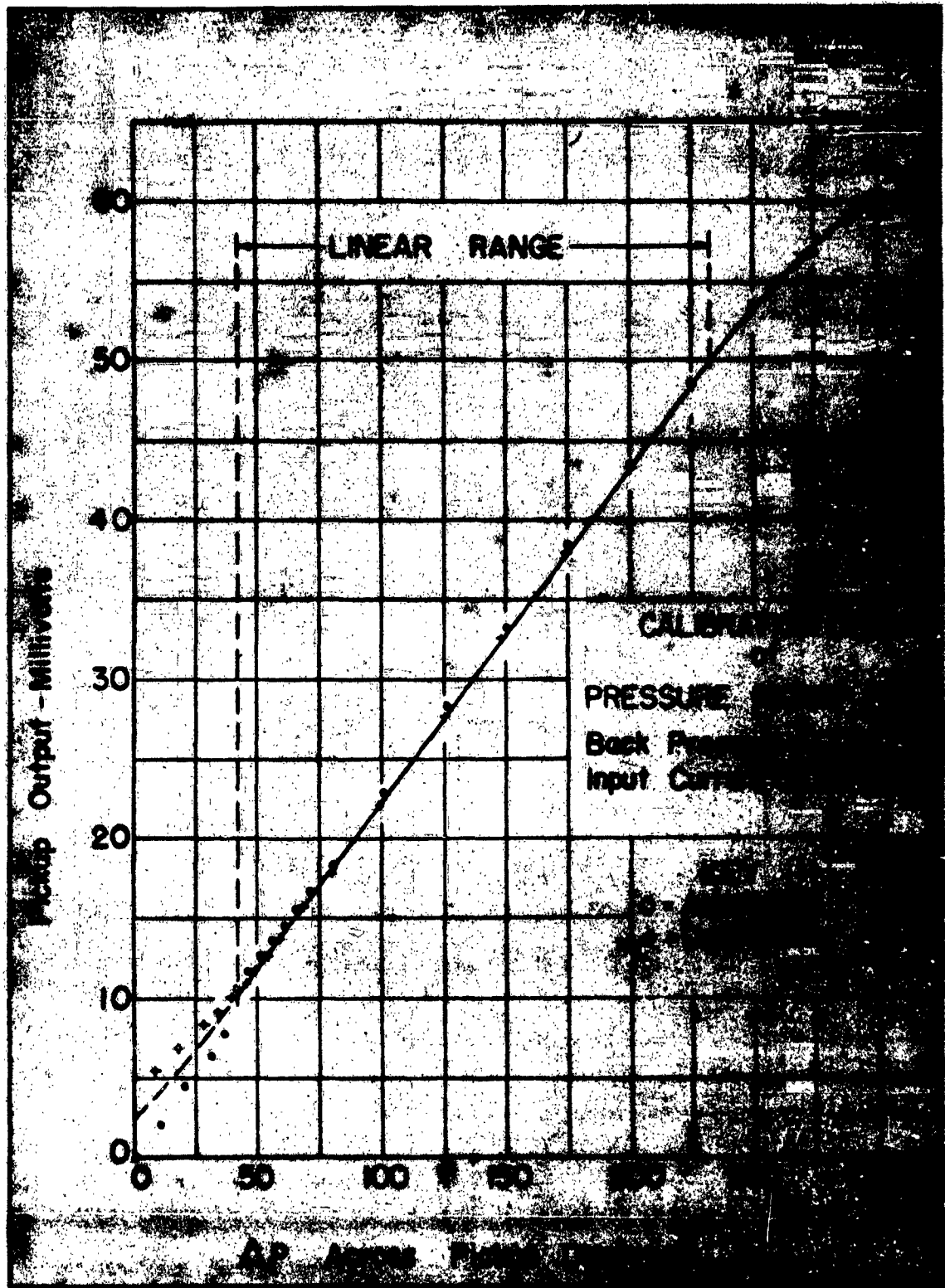
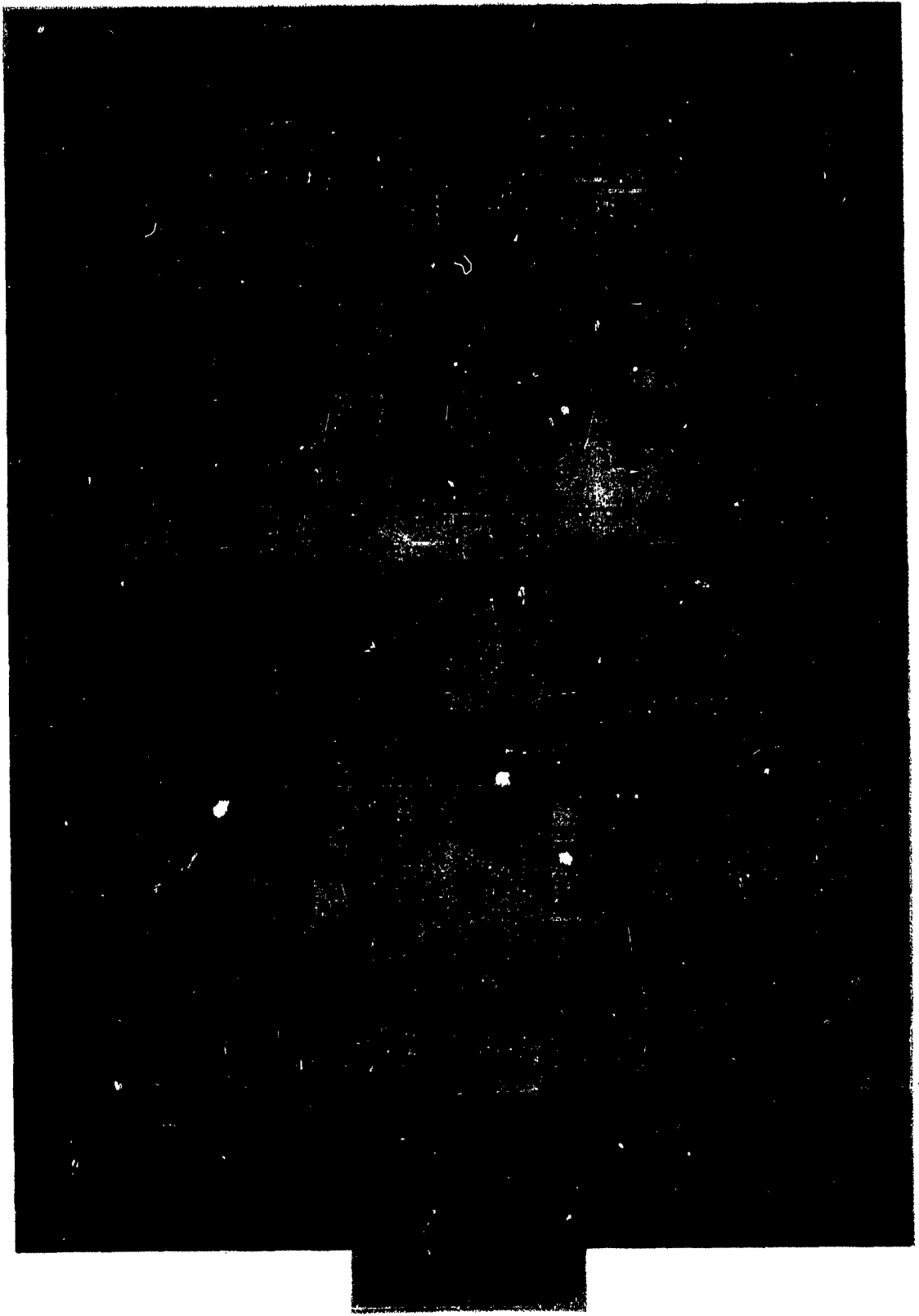


Figure 3



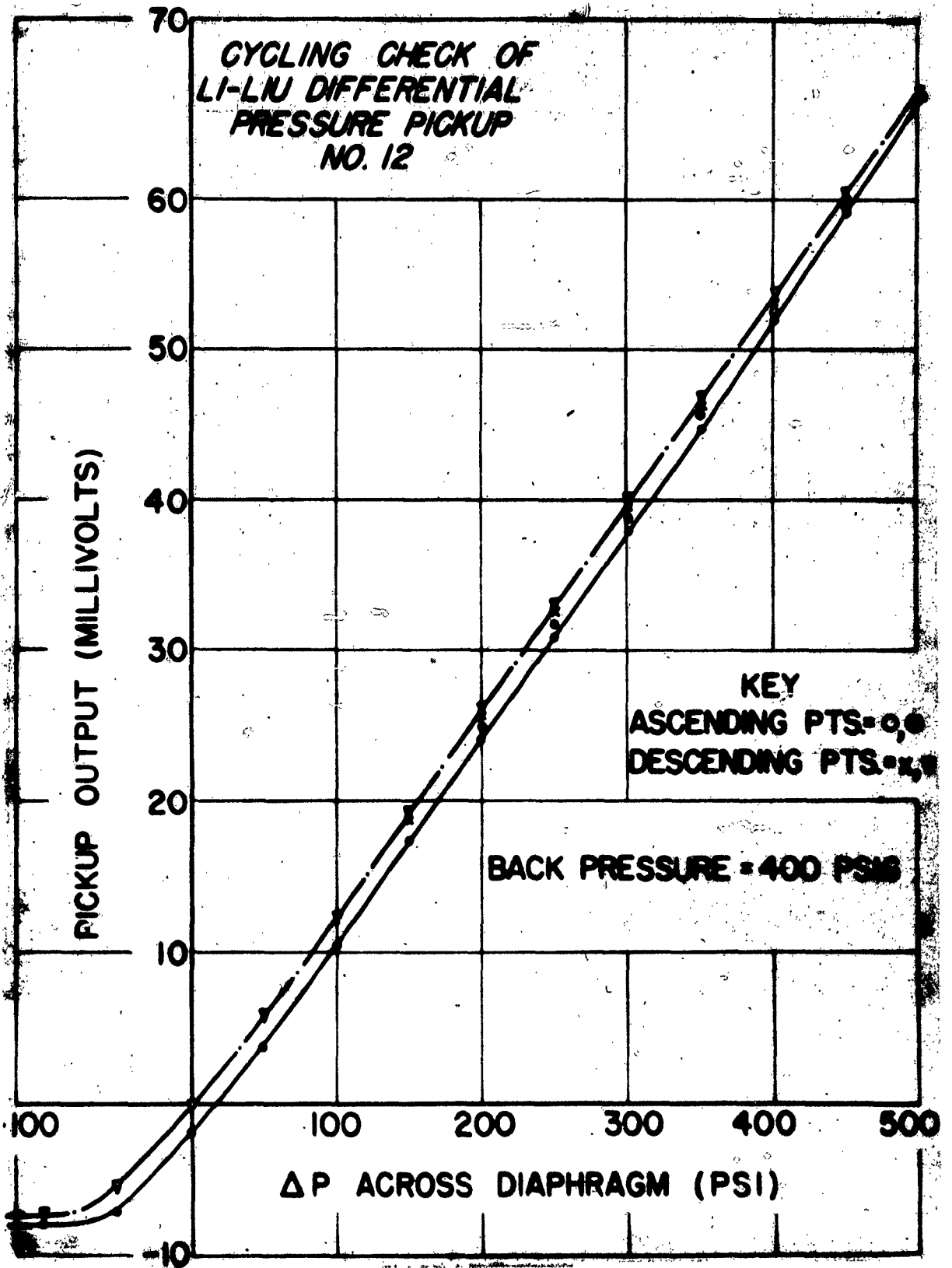


Figure 11

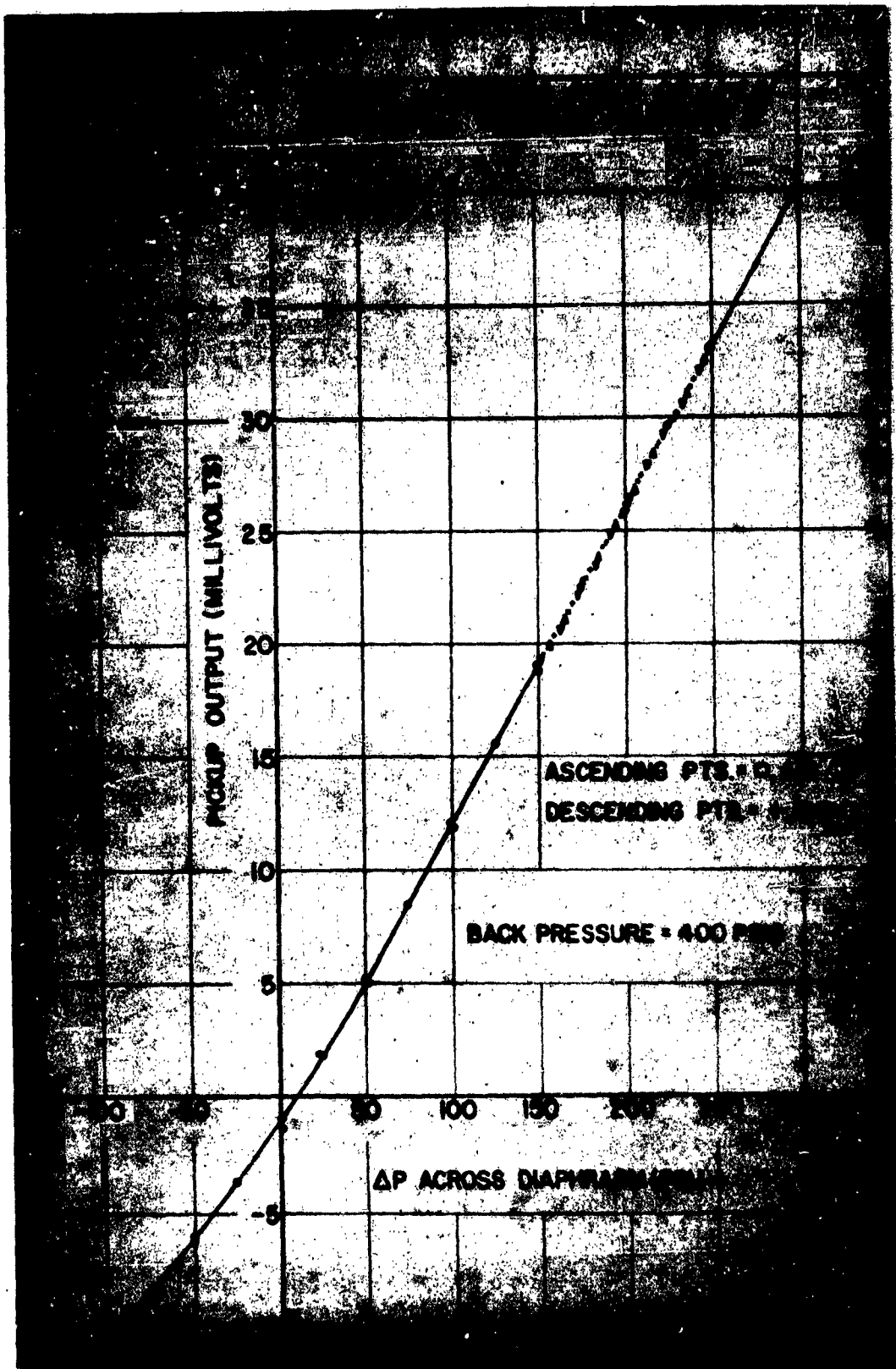


Figure 12

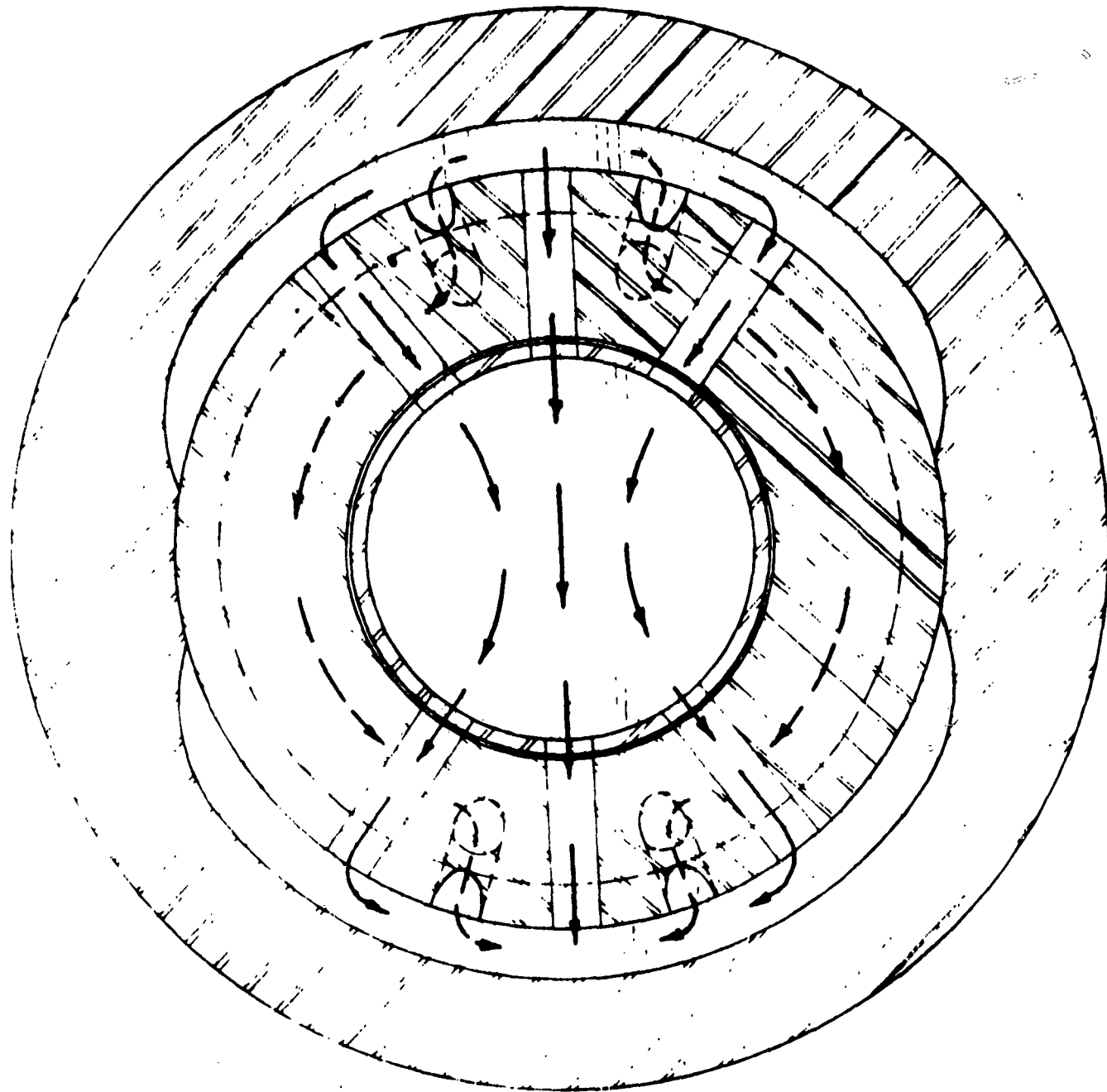


Figure 13A

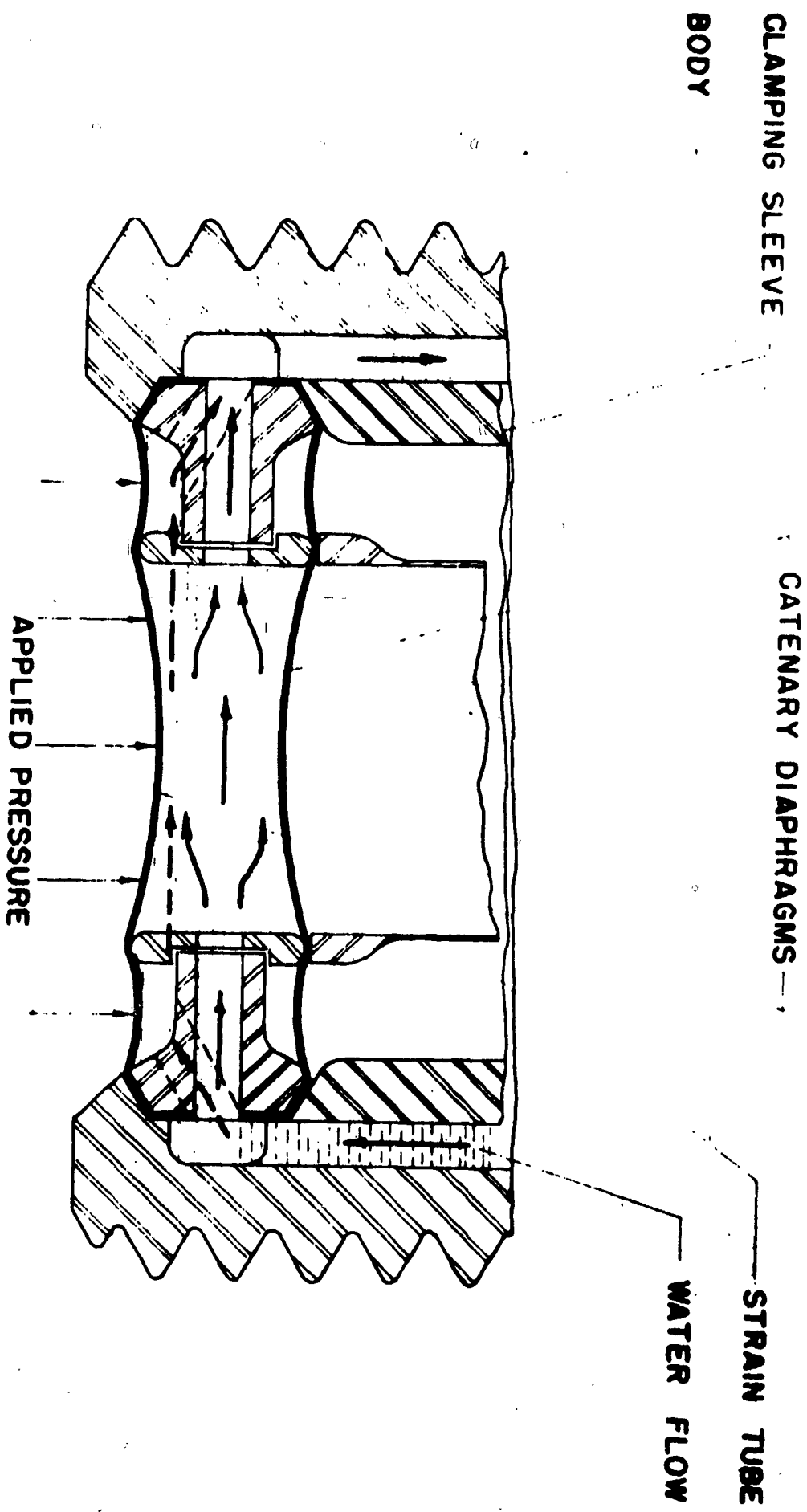


FIG. 3 SCHEMATIC DIAGRAM OF A CATENARY DIAPHRAGM-WATER-COOLED PRESSURE RECEIVING ELEMENT

Figure 13B

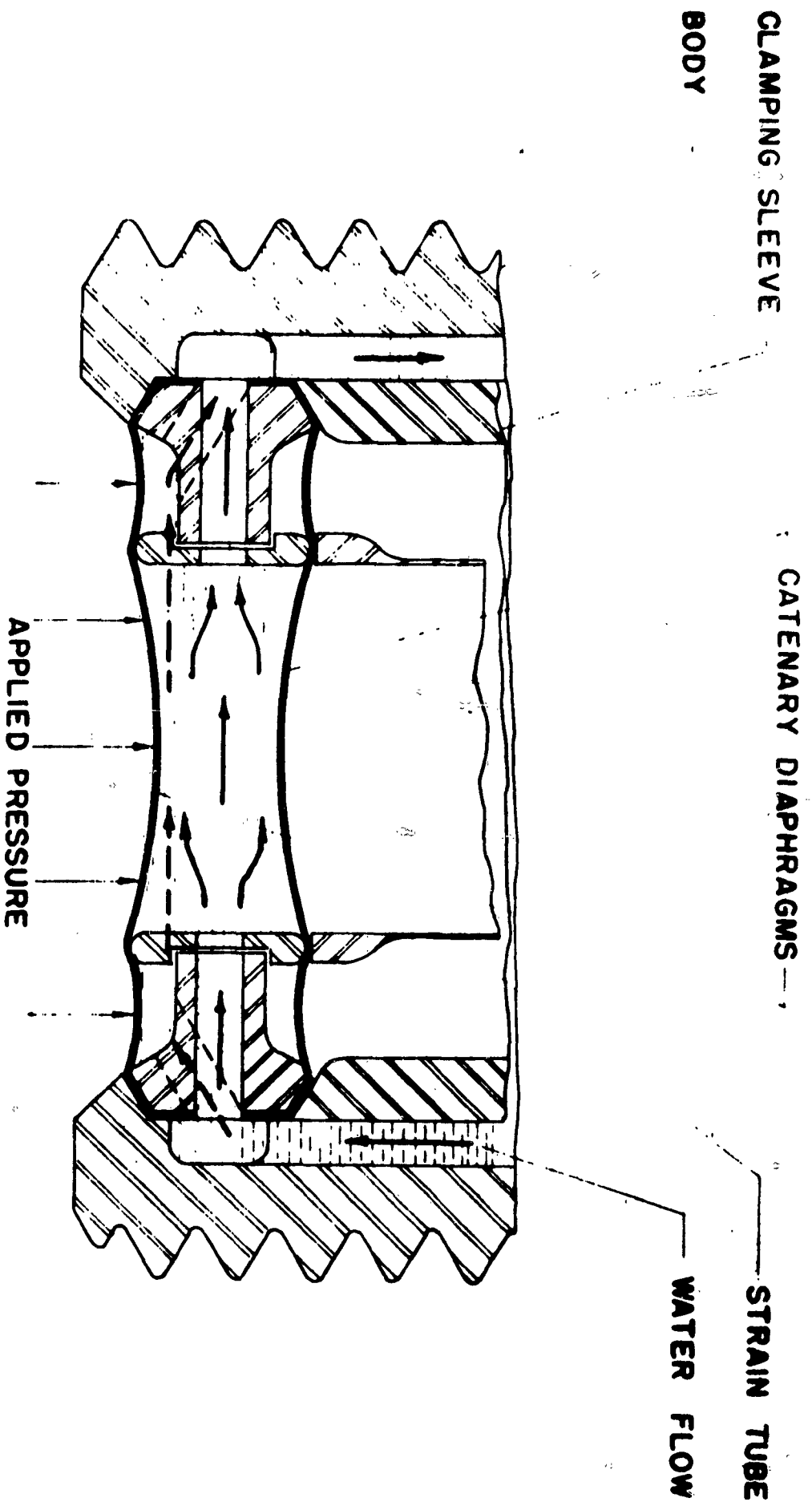


FIG. 3 SCHEMATIC DIAGRAM OF A CATENARY DIAPHRAGM WATER-COOLED PRESSURE RECEIVING ELEMENT

Figure 13B

**HEAT TRANSFER TO LI-LIU DUMMY
PRESSURE PICKUP (NON-SCREAMING)**

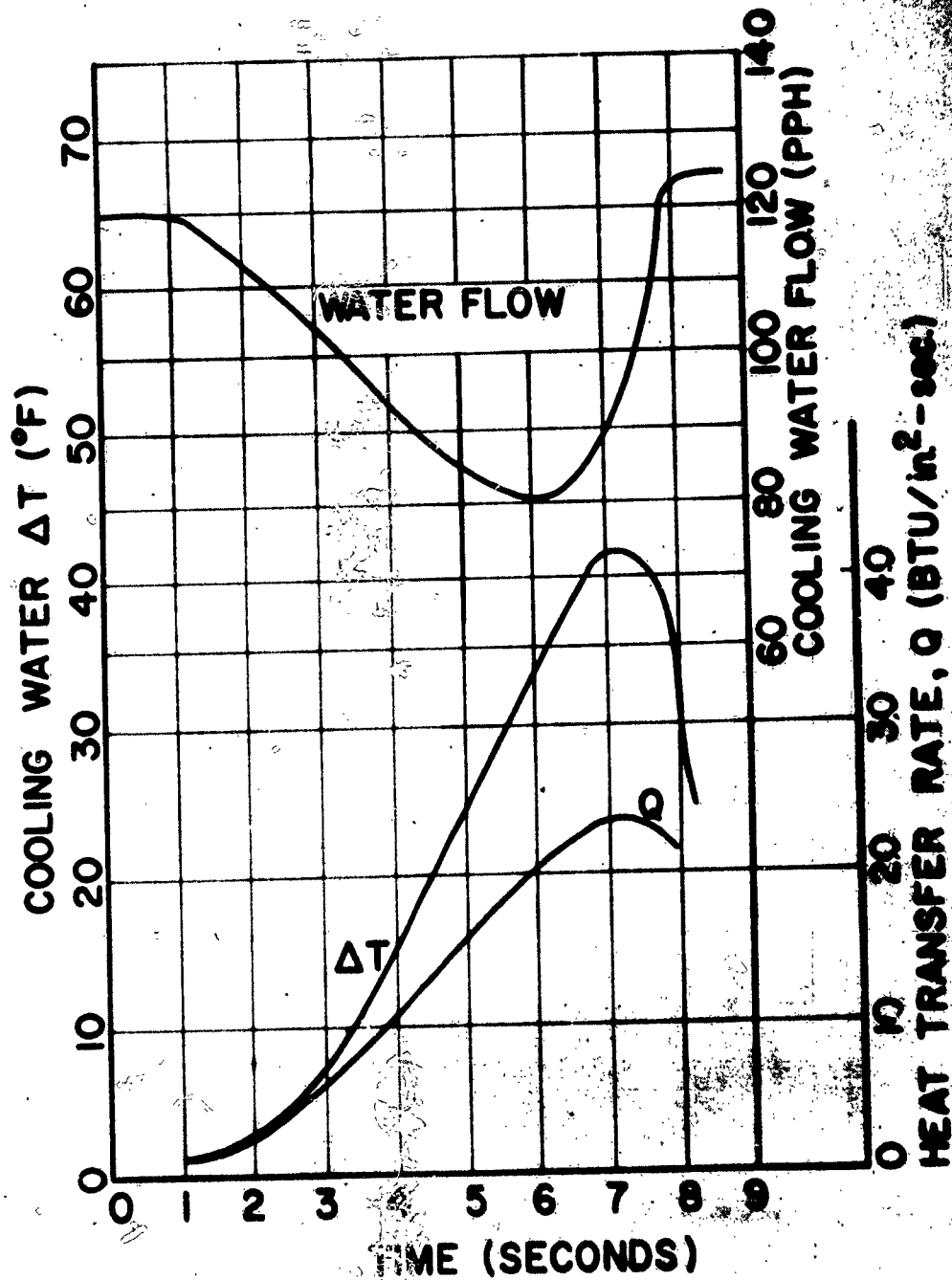


Figure 14

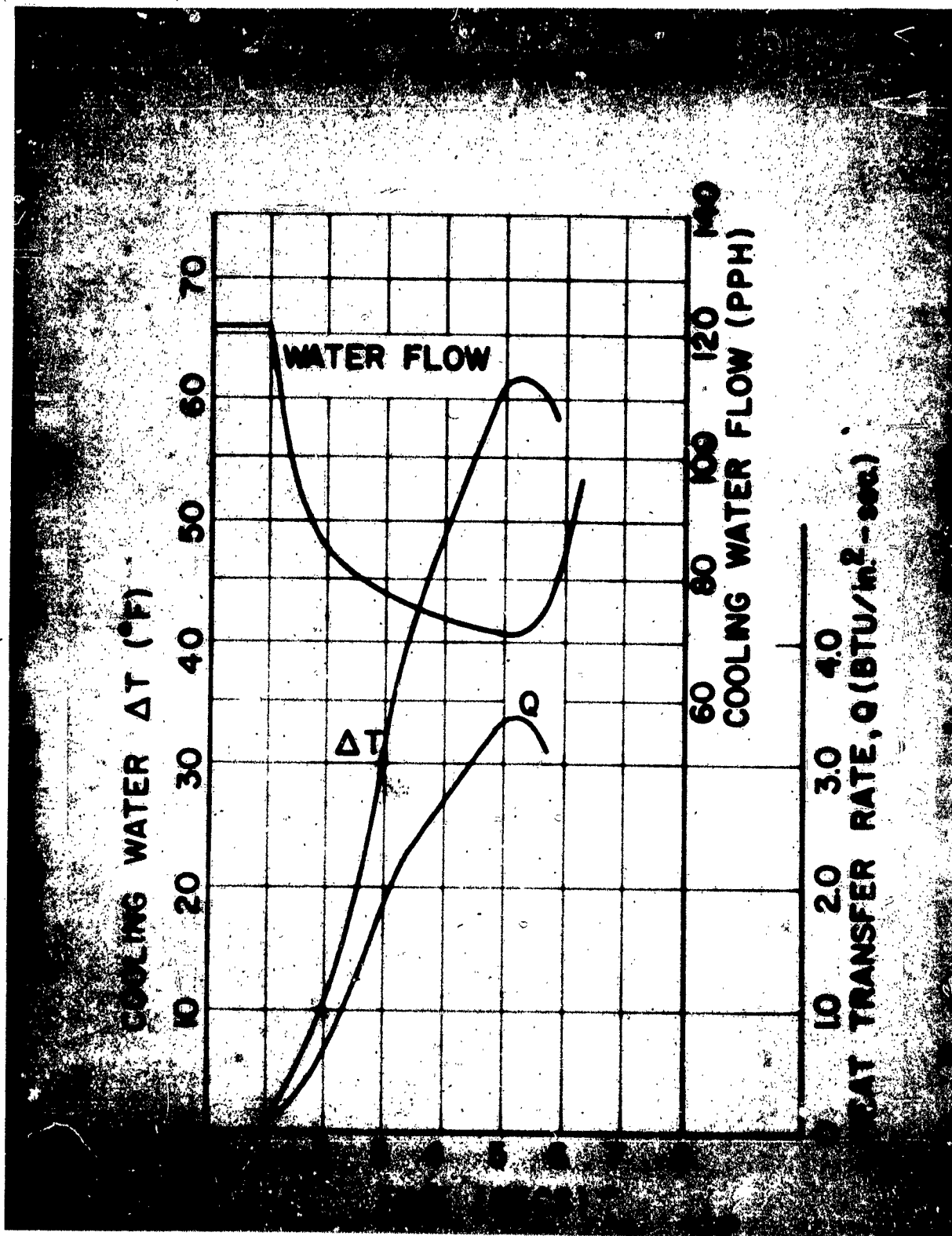


Figure 15